



Norwegian University of  
Science and Technology

# Numerical simulations for lift-off operation of an offshore wind turbine monopile

**Shi Deng**

Marine Technology

Submission date: June 2016

Supervisor: Zhen Gao, IMT

Norwegian University of Science and Technology  
Department of Marine Technology



## **Preface**

This master thesis is on offshore wind turbine monopile construction. Upending process of monopile on crane vessel and transport barge is considered. Characters of different upending methods are cleared to find a suitable one. And some suggestions about lifting velocity and lifting force will be given to limit maximum lift wire force in process. Moreover, different sea states are also concerned to find the critical load condition which will not challenge safety. Distance between crane vessel and transport barge will also be analysed to clear its effect on relative position between the barge and crane vessel. In addition, maximum thruster force of barge and minimum changing time from maximum force to minimum force are also taken into account. At last, ballast water in the crane vessel is cleared to maintain roll stability in different cases of distances between barge and crane vessel.

Trondheim, 10-06-2016

Shi Demg







## **MSC THESIS IN MARINE TECHNOLOGY**

**SPRING 2016**

**FOR**

**STUD. TECHN. Shi Deng**

### **Analysis of Lift-off Operation of an Offshore Wind Turbine Monopile**

#### **Background:**

Transportation and installation of offshore wind turbine components and systems are important aspects for reducing the life-cycle cost of offshore wind farms. Most of the offshore wind farms today are based on monopile foundations, which are usually deployed in relatively shallow waters (10-30 m of water depths).

Installation of monopile at the offshore sites are based on crane operations mostly using a jack-up installation vessel, which can provide a stable platform for lift-off, lowering and hammering operations to install the monopile foundations. Purpose-built floating installation vessels are now being developed for ‘mass’ installation of offshore wind turbine foundations due to an easy deployment. However, under the wave loads, the moored floating installation vessel will experience both wave-frequency and low-frequency motions, which will also lead the lifted monopile to move and potentially cause an impact between the monopile and the vessel. This is in particular the case when the monopile is lifted off from the deck of the installation vessel. If the monopile is originally located on a barge, the contact between them will be of a concern. It is therefore important to quantify the dynamic responses of the monopile motions and the lift wire tension during such lift-off operations.

The purpose of this study is to numerically model the coupled system of the monopile, the floating installation vessel, (the barge if used) and the lift wire during the lift-off process and to study their dynamic responses in stochastic waves.

The student will be provided the design and the numerical model of the floating installation vessel in SIMO, as well as the design data of the OC3 monopile.

#### **Assignment:**

The following tasks should be addressed in the thesis work:

1. Literature review on crane operations for installation of offshore equipment with focus on lift-off operations. Two scenarios might be envisaged, one with the monopile originally placed on the same installation vessel, and the other with the monopile placed on another barge. Literature review on numerical modeling and dynamic analysis of lifting operations.
2. Investigate the detailed procedure for lift-off of the monopile from the same floating installation vessel or from a barge. Model the possible contacts between the monopile and the deck of the installation vessel, which will be used later in the numerical model.
3. Considering a jack-up installation vessel, study a few cases with predefined motions of the crane and the winch speed and investigate the corresponding monopile motions and lift wire tension. Establish a numerical model in Simo considering the same scenarios, compare the results of the numerical simulations and the analytical results.

4. Extend the work in Section 3 to include the harmonic motions of a floating installation vessel, and compare the results with the jack-up case.

5. Establish a coupled numerical model of the monopile and the floating installation vessel in Simo, considering the wire coupling and the contact between the monopile and the vessel deck. Perform dynamic analysis of the lift-off operation for given sea states. Perform the analysis for the second case considering a barge in addition. Compare the results of the two scenarios.

6. Report and conclude on the investigation.

In the thesis the candidate shall present his personal contribution to the resolution of problem within the scope of the thesis work.

Theories and conclusions should be based on mathematical derivations and/or logic reasoning identifying the various steps in the deduction.

The candidate should utilize the existing possibilities for obtaining relevant literature.

The thesis should be organized in a rational manner to give a clear exposition of results, assessments, and conclusions. The text should be brief and to the point, with a clear language. Telegraphic language should be avoided.

The thesis shall contain the following elements: A text defining the scope, preface, list of contents, summary, main body of thesis, conclusions with recommendations for further work, list of symbols and acronyms, reference and (optional) appendices. All figures, tables and equations shall be numerated.

The supervisor may require that the candidate, in an early stage of the work, present a written plan for the completion of the work. The plan should include a budget for the use of computer and laboratory resources that will be charged to the department. Overruns shall be reported to the supervisor.

The original contribution of the candidate and material taken from other sources shall be clearly defined. Work from other sources shall be properly referenced using an acknowledged referencing system.

The thesis shall be submitted electronically in DAIM:

- Signed by the candidate
- The text defining the scope included
- In bound volume(s)
- Drawings and/or computer prints which cannot be bound should be organized in a separate folder.

Zhen Gao  
Shixiao Fu  
Supervisors

Deadline: 10.6.2016

## **Acknowledgment**

My supervisors Prof. Zhen Gao and Prof. Shixiao Fu have provided me much guidance during whole semester of thesis. I would like to express my deepest thanks for their guidance and supervision. I am grateful for Zhen Gao's generous support. I gained a lot from Shixiao Fu's deepest knowledge, experience and great enthusiasm and discipline in scientific research. It was a great pleasure and experience to work with them.

I would like to thank Dr. Xiaopeng Wu and Dr. Lin Li for patient guidance of software and accuracy checking. Panel model of crane vessel and its hydrodynamic factors using in time domain analysis and multi-body analysis were got from Dr.Lin Li.

Finally, my warmest thank goes to my family in China for their support.

Shi Deng

June 2016

Trondheim, Norway



## Summary and Conclusions

From this study, lift-off process of monopile in single crane vessel scenario and two vessels scenario are all considered. Challenges from environmental conditions and upending process are all cleared. In the single crane vessel scenario, the vessel was assumed as jack-up and floating structures respectively. Different lifting methods were concerned under former assumption, such as constant angular velocity, vertical lifting velocity, vertical lifting forces, fixed crane tip and horizontal moving crane tip. Some suggestions about lift wire force and lifting velocity were listed from these analysis. Regular translation and rotation motions of crane vessel were concerned under latter assumptions. Results of time series of three concerned forces (lift wire, horizontal and vertical support force) were studied with heave and roll motions of crane vessel. Based on this analysis, vessel motion had little effects to concerned forces compared with upending process.

In order to minimize maximum value of three concerned forces, different sea states and upending process were considered. High sea state (means large  $H_s$  and  $T_p$ ) just leded large standard deviation, which means environmental load was not very important. Then smaller lifting velocity was used to minimize challenge to safety.

When the two vessels scenario concerned, distance between transport barge and crane vessel was the main factor. Effects to hydrodynamic factors and ballast due to such distance were cleared. Moreover, time series of lift wire force in this scenario was also got to show critical step.



## Nomenclature

$\omega$  Angular Velocity

$\varepsilon$  Angular Acceleration

$I$  Inertia Moment

$F_l, F_{line}$  Lift Wire Force

$F_{linetau}, F_l^t$  Lift Wire Force in Tangential Direction

$F_{linen}, F_l^n$  Lift Wire Force in Radial Direction

$F_{supporttau}, F_\tau^S$  Support Force in Tangential Direction

$F_{supportn}, F_n^S$  Support Force in Radial Direction

$F_x^S, F_{Supportx}$  Horizontal Support Force

$F_y^S, F_{Supporty}$  Vertical Support Force

$F_N^i$  Radial Inertial Force

$F_\tau^i$  Tangential Inertial Force

$\theta$  Inclination Angle of Monopile

$v_a$  Absolute Velocity

$v_e$  Convected Velocity

$v_r$  Relative Velocity

$v_c$  Second Order Velocity

$a_a$  Absolute Acceleration

$a_e$  Convected Acceleration

$a_r$  Relative Acceleration

$a_c$  Second Order Acceleration

$a$  Acceleration

$v$  Velocity

$\zeta_A$  Amplitude of Incident Wave

$\beta$  Incident Angle of Incident Wave

$\phi$  Velocity Potential

$G$  Gravity of Monopile

$M^I$  Inertial Moment on COG of Monopile



## **Acronyms**

**FFT** Fast Fourier transform

**SWL** Safe Working Load

**COG** Center of Gravity

**H<sub>s</sub>** Significant Wave Height

**T<sub>p</sub>** Peak Period

**DP** Dynamic Positioning

**JONSWAP** Joint North Sea Wave Project



# Contents

Preface . . . . .	i
Acknowledgment . . . . .	v
Summary . . . . .	vii
Nomenclature . . . . .	ix
Acronyms . . . . .	xi
List of Figures . . . . .	xvii
List of Tables . . . . .	xxi
<b>1 Introduction</b>	<b>1</b>
1.1 Background . . . . .	2
1.2 Objectives . . . . .	5
1.3 Limitations . . . . .	6
1.4 Approach . . . . .	6
<b>2 Theoretical Background</b>	<b>9</b>
2.1 Theoretical Mechanics . . . . .	9
2.1.1 Lift-off Using Jack-up Installation Vessel . . . . .	9
2.1.2 Lift-off Using Floating Installation Vessel . . . . .	10
2.2 Hydrodynamic Analysis . . . . .	12
2.3 Coupled Motion Analysis . . . . .	13
2.4 Numerical Model in SIMA . . . . .	16
2.5 Theories Used in Two Vessels Scenario . . . . .	17
2.5.1 Panel Model . . . . .	18
2.5.2 Coefficients of Hydrodynamic Load . . . . .	19

2.5.3	Sensitive of Distance Between Barge and Crane Vessel . . . . .	20
<b>3</b>	<b>Analytical Result</b>	<b>23</b>
3.1	Upending on Fixed Crane Vessel . . . . .	23
3.1.1	Description of Monopile Upending . . . . .	23
3.1.2	Concentrated Mass Assumption of Monopile . . . . .	24
3.1.3	Distributed Mass Assumption of Monopile . . . . .	36
3.2	Results Based on Constant Lifting Velocity and Lift Wire Force . . . . .	39
3.2.1	Results Based on Constant Lifting Velocity . . . . .	39
3.2.2	Results Based on Constant Lifting Force . . . . .	41
3.3	Regular Heave Motion of Crane Vessel . . . . .	43
3.3.1	Theory Analysis of Coupled Motion . . . . .	43
3.3.2	Effects Based on Heave Amplitude . . . . .	44
3.3.3	Effects Based on Heave Frequency . . . . .	45
3.4	Regular Roll Motion of Crane Vessel . . . . .	46
3.4.1	Mechanism Analysis of Coupled Motion . . . . .	47
3.4.2	Weight of Different Part . . . . .	49
3.4.3	Effects Based on Roll Frequency . . . . .	50
3.4.4	Effects Based on Roll Amplitude . . . . .	51
<b>4</b>	<b>Numerical Model and Analysis</b>	<b>55</b>
4.1	Model Discription . . . . .	55
4.1.1	Vessel . . . . .	55
4.1.2	Crane . . . . .	56
4.1.3	Monopile . . . . .	57
4.1.4	Connection between Monopile and Vessel . . . . .	59
4.2	Motion Setting of Crane Bottom and Inclination Column . . . . .	61
4.3	Decrease Maximum Value of Concerned Forces in Numerical Simulation . . . . .	63
4.3.1	Environmental Load Factor . . . . .	63
4.3.2	Upend Motion . . . . .	66
4.4	Effects From Different State . . . . .	67

4.4.1	Location of Selected Sea and Its Representative Value	67
4.4.2	Result of Different Sea States Effect	67
4.5	Two Vessels Scenario	69
4.5.1	Panel Model in HydroD	69
4.5.2	Model in SIMA	71
4.5.3	Numerical Result of Two Vessels Scenario	73
<b>5</b>	<b>Comparative Study</b>	<b>77</b>
5.1	Basic Assumption of Numerical Simulation	77
5.1.1	Mass Distribution	77
5.1.2	Geometrical Relation	78
5.1.3	Motion of Crane	79
5.1.4	Motion of Crane Vessel	79
5.2	Result Comparison	79
5.2.1	Jack-up Vessel Assumption	79
5.2.2	Regular Heave Motion	80
5.2.3	Regular Roll Motion	81
5.3	Comparison Between Different Freedom Setting of Vessel	81
<b>6</b>	<b>Summary and Recommendations for Future Work</b>	<b>85</b>
6.1	Summary and Conclusions	85
6.2	Discussion	86
6.3	Recommendations for Further Work	86
	<b>Bibliography</b>	<b>87</b>
<b>A</b>	<b>Appendix A-ROA of Crane Vessel Motion</b>	<b>89</b>
<b>B</b>	<b>Appendix B-Result of Concerned Forces in Different Case</b>	<b>90</b>
B.1	Result in Different Lifting Velocities	90
B.2	Result in Different Lifting Forces	92
B.3	Result under Different Heave Amplitude	92
B.4	Result under Different Heave Frequency	93

B.5	Different Terms Under Roll Motion . . . . .	93
B.6	Result under Different Roll Frequency . . . . .	95
B.7	Result in Different Hs and Tp . . . . .	95
<b>C</b>	<b>Appendix C-Matlab Code in Theoretical Analysis</b>	<b>97</b>
C.1	Code for Crane Bottom Velocity-First Part . . . . .	97
C.2	Code for Crane Bottom Velocity-Second Part . . . . .	98
C.3	Code for Concerned Forces under Different Frequencies Roll Motion of Crane Vessel	99
C.4	Code for Concerned Forces under Different Lifting Velocities . . . . .	103
<b>D</b>	<b>Appendix D-SIMA Code</b>	<b>107</b>

# List of Figures

1.1	Wind Farms over 100 MW Online and Under Construction - October 2010 . . . . .	3
2.1	Relation Between Frequency Domain and Time Domain Analysis . . . . .	14
2.2	SWL vs. Radius, and Hook Height vs. Radius . . . . .	21
3.1	Upending Process in Practical . . . . .	24
3.2	description of upending process . . . . .	25
3.3	Forces on Monopile in Static Condition . . . . .	26
3.4	Static Result of All Concerned Forces . . . . .	27
3.5	Forces on Monopile in Dynamic Condition . . . . .	27
3.6	Forces in Constant Angular Velocity Condition . . . . .	28
3.7	Force versus Theta in Constant Angular Velocity Condition . . . . .	29
3.8	Vertical Support Force Versus Theta in Constant Angular Velocity Vondition . . . . .	30
3.9	Mechanism Analysis Based on Constant Vertical Lifting Velocity Condition . . . . .	31
3.10	Time Series of Concerned Forces . . . . .	32
3.11	Concerned Forces Versus Theta . . . . .	32
3.12	Concerned Forces Versus Theta(88-90) . . . . .	33
3.13	Fixed Crane Tip Position . . . . .	34
3.14	Mechanism Analysis for Fixed Crane Tip Condition . . . . .	34
3.15	Time Series of Concerned Forces in Fixed Crane Tip Condition . . . . .	35
3.16	Time Series of All Forces Under Constant Vertical Lifting Velocity Assumption . . . . .	37
3.17	Theta Series of All Forces Under Constant Vertical Lifting Velocity Assumption . . . . .	37
3.18	Time Series of All Forces under Linear Moving Crane Tip Assumption(1m/s) . . . . .	38

3.19 Time Series of All Forces under Linear Moving Crane Tip Assumption(0.5m/s) . . .	39
3.20 Theta Series of Vertical Support Force for Different Lifting Velocity . . . . .	40
3.21 Theta Series(0-60) of Vertical Support Force for Different Lifting Velocity . . . . .	40
3.22 Theta Series of Vertical Support Force for Different Lifting Forces . . . . .	42
3.23 Theta Series of Lifting Velocity for Different Lifting Forces . . . . .	42
3.24 Time Series of Wire Line Force with Different Heave Amplitude . . . . .	45
3.25 Time Series of Horizontal Support Force with Different Heave Amplitude . . . . .	45
3.26 Time Series of Wire Line Force with Different Heave Frequency . . . . .	46
3.27 Mechanism Analysis of Relation Between Roll and Upending Process . . . . .	48
3.28 Extra Forces under Regular Roll Assumption . . . . .	48
3.29 Different Parts in Horizontal Support Force due to Roll Motion . . . . .	50
3.30 Different Parts in Vertical Support Force due to Roll Motion . . . . .	51
3.31 Time Series of Horizontal Support Force With Different Roll Frequency . . . . .	52
3.32 Time Series of Wire Line Force With Different Roll Frequency . . . . .	52
3.33 Time Series of Horizontal Support Force With Different Roll Amplitude . . . . .	53
3.34 Time Series of Wire Line Force With Different Roll Amplitude . . . . .	54
4.1 Crane Vessel Model Got From Senior Student . . . . .	56
4.2 Model for Crane . . . . .	57
4.3 Whole Model Outlook . . . . .	58
4.4 Theory of Docking Cone . . . . .	59
4.5 Theory of Point Fender . . . . .	60
4.6 Arrangement of Docking Cone and Point Fender . . . . .	60
4.7 Theory of Two Part Motion . . . . .	62
4.8 Numerical Result of Constant Lift Velocity . . . . .	62
4.9 Wire Line Force with Different Hs . . . . .	64
4.10 Horizontal Support Force with Different Hs . . . . .	64
4.11 Wire Line Force with Different Tp . . . . .	65
4.12 Horizontal Support Force with Different Tp . . . . .	65
4.13 Result after Modification . . . . .	66



4.14	Location of 18 Potential European Offshore Sites . . . . .	68
4.15	Result of Mean Vertical Support Force in Different Sea States . . . . .	69
4.16	Result of Vertical Support Force Standard Deviation in Different Sea States . . . . .	70
4.17	Result of Lift Wire Force Standard Deviation in Different Sea States . . . . .	70
4.18	Panel Model of Two Vessels . . . . .	71
4.19	Two Vessels Model in SIMA . . . . .	72
4.20	(a)Step1 in Two Vessels Scenario. (b)Step2 in Two Vessels Scenario. (c)Step3 in Two Vessels Scenario.(d)Step4 in Two Vessels Scenario. . . . .	72
4.21	Time Series of Lift Wire Force . . . . .	74
5.1	Comparison Between SIMA and Theoretical Result with Fixed Vessel . . . . .	80
5.2	Comparison Between SIMA and Theoretical Result with Regular Heave Motion . . . . .	81
5.3	Comparison Between SIMA and Theoretical Result with Regular Roll Motion . . . . .	82
5.4	Comparison Between SIMA and Theoretical Result of Horizontal Support Force . . . . .	82
5.5	Time Series of Concerned Forces with Irregular Heave Motion . . . . .	83
5.6	Time Series of Concerned Forces with Irregular Roll Motion . . . . .	83
5.7	Time Series of Concerned Forces with Irregular Total Motion . . . . .	84
A.1	ROA of Heave Motion . . . . .	89
A.2	ROA of Roll Motion . . . . .	89
B.1	Theta Series of Horizontal Support Force for Different Lifting Velocity . . . . .	90
B.2	Theta Series of Lift Wire Force for Different Lifting Velocity . . . . .	91
B.3	Theta Series of Horizontal Support Force for Different Lifting Velocity(60) . . . . .	91
B.4	Theta Series of Lift Wire Force for Different Lifting Velocity(60) . . . . .	92
B.5	Theta Series of Horizontal Support Force for Different Lift Force . . . . .	92
B.6	Time Series of Vertical Support Force under Different Heave Amplitude . . . . .	93
B.7	Time Series of Horizontal Support Force under Different Heave Frequency . . . . .	93
B.8	Time Series of Vertical Support Force under Different Heave Frequency . . . . .	94
B.9	Time Series of Vertical Support Force under Different Heave Frequency . . . . .	94
B.10	Time Series of Vertical Support Force under Different Roll Frequency . . . . .	95
B.11	Time Series of Vertical Support Force with Different Significant Wave Height . . . . .	95

B.12 Time Series of Vertical Support Force with Different Peak Period . . . . . 96

# List of Tables

- 4.1 Main parameters of the crane vessel . . . . . 56
- 4.2 Main Parameters of the Monopile . . . . . 58
- 4.3 Result of Two Vessels Scenario with Different Gap Values . . . . . 73
- 4.4 Ballast Water for Different Gaps . . . . . 74



# Chapter 1

## Introduction

For the reason of renewable energy targets around the world, wind power investment have gained large acceleration at the end of last century including the application in offshore field. Many advantages of wind energy in offshore field such as high potential, less disturbance and large area make offshore wind zone highly attractive. This situation is obvious for the countries with long coastal line near North Sea and Baltic Sea. Such countries are highly interested in developing offshore wind farm. Admittedly, cost of wind turbine park in offshore is much higher than onshore, the benefit and convenient of offshore wind park make engineers focus on it. The main reasons for the high cost of offshore wind park were electrical grid connections, complex foundation, challenge in offshore operation such as weather, wind and sea state and limited number of purpose built installation vessels.

Many factors should be concerned carefully before making a choice of foundation and turbine for offshore wind farms. While seabed properties, sea depth, tides currents and wave height will decide the foundation type, wind profile and other characters of wind determine the type of wind turbine. Special designed vessel would be used in offshore wind turbine installation and transportation. These kinds of special vessels are usually with jacket-up legs, mooring or other kinds of dynamic position system to create a considerable steady working platform in the offshore site which is chosen. In order to lift heavy pieces, a large crane always set on on the deck of special vessels. Position and geometry size of crane could affect the safe of operation.

Generally speaking, offshore installation of wind turbine structure could be divided into two process. The foundation and wind turbine are installed separately. The installation of wind

turbine should be followed by foundation installation.

For the different size of turbine and foundation, the character of operation is slightly different. In this thesis, monopile structure which is commonly used for water depth up to 40 meters [Li et al. \(2014\)](#), will be focused on. In installation strategy, the lift-off process could increase dangerous possibility. Capacity of lift wire, connection between monopile and crane vessel and many other factors challenge lift-off operation. Talked factors would be discussed in this thesis.

## 1.1 Background

Offshore wind-farms have been widely installed since the beginning of 1990s. [Uraz \(2011\)](#) According to figure 1.1, many Europe countries adopt this kind of eco-friendly energy. And usage of it has been sharply increasing in recent years. In order to maintain wind turbines in offshore working condition, various support structures have been introduced to offshore wind turbines (OWTs) for different seabed condition and water depth. There are four kinds of popular bottom-fixed support structures in industry, in details they are monopile, jacket, tripod and gravity-based. [Thomsen \(2014\)](#) Among them monopile is the most widely used one. From the research published in 2008, more than 75 percent offshore wind turbines were supported by monopile foundation. [Moller \(2005\)](#) The structure of typical monopile is very simple only consist of a large tube, with generally 4 to 6 metres diameter, which driven into seabed through hydraulic hammer. However, size of such tube lead to various kinds of the transportation and lifting process. Installation of monopile generally includes the following steps:

1. Tube should be upended from horizontal position by crane, which may on the transporting vessel or on another operation vessel.
2. Monopile should be lowed down cross sea surface to seabed. In the process, hydrodynamic load may lead unexpected motion of tube.
3. A hydraulic hammer could be used in the last step to drive the monopile into seabed soil.

The first and second steps challenge operation severely due to the unexpected response motion of the crane vessel and upend motion of monopile. This study will focus on the above

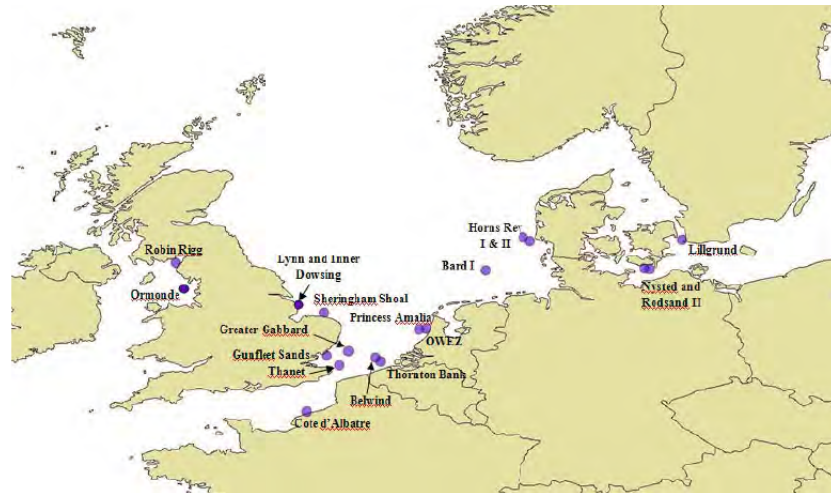


Figure 1.1: Wind Farms over 100 MW Online and Under Construction - October 2010

motions and their coupled motion to analysis critical . Generally speaking, lifting operation means the installment of monopile or other kinds of offshore structures. In the analysis process, numerical studies should be introduced to estimate the response characters of offshore lifting operations, including sub-sea template installation, [Aarset et al. \(2011\)](#) suction anchors, [Gordon et al. \(2013\)](#) topsides and foundations of platforms, wind turbine components etc. [Graczyk and Sandvik \(2012\)](#) In order to guarantee the accuracy of calculation, hydrodynamic coefficients should be decided at first, such as the hydrodynamic mass and damping of monopile, [Perry et al. \(2005\)](#) to tune the critical parameters for numerical models, e.g., the damping or stiffness level of important support structures in the lifting system. [Van der Wal et al. \(2008\)](#)

## Problem Formulation

There are two kinds of lift-off operation in the monopile installation. Crane vessel transport monopile to working station by itself could be seen as one of methods. [Li et al. \(2013\)](#) In another method, a barge is introduced to transport monopile. Lift-off operation will be done by the crane vessel talked in former method. In such upending process, monopile will be lifted at one tip and the whole monopile rotate along a hinge connection, which connect monopile and crane vessel, until it lifted vertically. In this period, lift wire, horizontal and vertical support forces challenge safety of operation and personnel. Lift velocity and lift wire force should be controlled carefully to prevent slack and overloading of lift wire. Moreover this control will be

used to protect hinge connection from fracture. In addition, rotational velocity of crane bottom would also be considered, which affects direction of lift wire. This direction also challenge safety of operation. Furthermore, motions of crane vessel could provide extra inertia forces and moments to monopile during whole process. So every type of crane vessel motion will be considered.

When the second scenario is chosen, interaction between barge and crane vessel becomes the key factor to challenge safety. Because lift capacity of crane is much larger than weight of monopile and one extra barge help monopile keeping static during whole process. When the gap between crane vessel and barge larger than the width of crane vessel, hydrodynamic interaction between barge and vessel could be neglected. However, such big gap challenge lift capacity of on-board crane and stability of crane vessel. Reason of former phenomenon is the lifting limit decreasing a lot when the cantilever length increasing. Extra bending moment due to large gap and weight of monopile lead latter problem. When the gap decreasing, second order effect for water in gap will be emphasized. Standing wave may appear and cause water resonance to challenge the safety. So the distance between crane vessel and barge should be concerned carefully.

## Literature Review

Details for process of talked two scenarios were got from 'construction report' and 'construction video'. From those, distribution of crane and monopile on vessel were cleared. And how did the monopile be upended. From this knowledge, basic assumptions of monopile and crane bottom could be drawn. Different types of transportation was cleared in the master thesis of [Uraz \(2011\)](#). Moreover, some papers about this topic would also be read. [Crol \(2015\)](#) studied similar topic under static assumption, which means inertia moment and forces due to upending process was neglected and even vessel motions. That was an ideal situation, that the upending of monopile and sea state had no effects to whole system. From this thesis, a more practical condition will be cleared with vessel motions and different coupling motions of crane tip and monopile.

From point of [Li et al. \(2015\)](#), different sea states assumptions which were suitable for Norwegian North Sea were got. These data could be used to check whether the suggested operation is suitable in Norwegian North Sea [Gao and Moan \(2009\)](#). From her result, two-parameter JON-



SWAP spectrum was chosen with  $H_s$  and  $T_p$  correspond to ranges of 1.5m to 2.5m and 5s to 12s. These two ranges would be discussed in the following part.

In order to clear crane vessel motion in single vessel scenario and interaction motion in two vessels scenario, hydrodynamic analysis of these two systems should be clearly done. From knowledge of [Faltinsen \(1993\)](#), panel model was used to get concerned factors such as mass, damping, restoring and transfer function. However, panel model could just be concerned in HydroD, this means changing of draft and shape of under water part in upending process cannot be concerned. Because the weight of monopile was much smaller than crane vessel. The talked draft changing could be neglected in practical.

SIMA as a time domain simulation tool was used in this case to clear time series of motion and concerned forces. SIMA manual [Pre'Consultants \(1997\)](#) was used to clear characters of each body type and motion setting.

## 1.2 Objectives

From study in this thesis, different lift-off cases were learned with various crane vessel assumptions in single vessel scenario. Lift wire, horizontal and vertical support forces were considered to get the critical condition of whole process. Lifting capacity and strength of the hinge connection were the key factors in single vessel scenario. From this study, a suitable lifting velocity series could be got to ensure safety. Moreover, the corresponding rotation speed of crane bottom was also achieved. These velocities were used to guarantee safety for most sea state.

Various sea states were introduced to clear environmental limit for safety of operation. In this part, variance, max, and mean values of three concerned forces in different sea states would be entirely considered. Through this analysis, slack and overloading of lift wire and fracture of connection hinge would be prevented.

Distance between transport barge and crane vessel would be considered and some suggestions about this value would also be shown. Time series of lift wire force in two vessels scenario would also be concerned to clear critical part in whole lift-off process. From this analysis, suitable velocity of lifting and crane bottom rotation would be concerned to make a reasonable choice. Moreover, thruster on barge should also be cleared to keep relative position between

crane vessel and barge in two vessels scenario.

### 1.3 Limitations

Theories used in this the simulation provide some limitations of result. Firstly, hydrodynamic coefficients from panel model were got from a fixed draft and constant underwater shape. But this was not practical in whole process. Upending motion of monopile, irregular incident wave could change the draft of crane vessel in single vessel scenario. Then draft of both barge and crane vessel were all changed during whole process. This effect was also neglected when using hydrodynamic coefficients from panel model.

Prescribed motion of crane setting in SIMA was not reasonable. Rotational velocity of crane bottom could not be set as a function of time, which made upending process in numerical simulation not similar as in theoretical analysis. This might provide some extra difference between numerical and theoretical analysis.

For limited storage of computer, only 64 sea states with 20 realizations of each sea state could be considered. This was not enough to show effects from environmental load. Mean and variance values from such simulation could only be as part of truth.

For two vessels scenario, direction of barge and crane vessel should also be discussed detail, which affected hydrodynamic factors very much. Furthermore, longitudinal distance between barge and crane vessel should also be discussed. Water depth in this study was only 25 meters, so the condition of seabed might affect vessel motion severely when large wave period was used. This kind of effect was neglected in the whole simulation, which limited accuracy of result.

### 1.4 Approach

Character of vessel motion would be discussed in this thesis through frequency domain analysis. This simulation was done in HydroD with panel model. In order to clear time series of three concerned forces, time domain analysis would be introduced. So SIMA was used in this part.

When the effects due to different sea states were concerned, Gumbel Distribution was used to find 90 percent maximum. From this distribution, reasonable representative of maximum

value of lift wire, horizontal and vertical support forces could be got to find acceptable environmental condition for lift-off operation.

Except numerical simulation, theoretical analysis would also be used to find theory result and checking accuracy of numerical simulation. Basic assumption of crane vessel such as jack-up and floating were considered respectively in theoretical analysis. Six degrees of vessel motions were divided into two parts as translation and rotation. Heave and roll motions were taken as examples to clear their effects on concerned forces.



# Chapter 2

## Theoretical Background

All theories used in this thesis would be discussed in this chapter, including theoretical mechanics, hydrodynamic analysis, frequency domain, time domain analysis and basic theories in SIMA for single vessel scenario. And potential theory for two vessels analysis.

### 2.1 Theoretical Mechanics

Theoretical mechanics would be used in theoretical analysis of single vessel scenario. In this case, lift wire, horizontal and vertical support forces would be considered when crane vessel assumed as jack-up structure and floating structure respectively.

#### 2.1.1 Lift-off Using Jack-up Installation Vessel

Crane vessel was assumed as jack-up structure without any motion. All three concerned forces depended on upending process. Forces on monopile were gravity and inertia forces due to rotation along hinge support on crane vessel. Two inertia forces which relied on angular velocity and acceleration would be considered when mass of monopile assumed as point mass on the COG. Equations 2.1 show these two forces, where 'r' means distance from COG to rotation centre, ' $\omega$ ' and ' $\varepsilon$ ' means angular velocity and acceleration of monopile respectively.

$$\begin{aligned} F_I^t &= \varepsilon r m \\ F_I^n &= \omega^2 r m \end{aligned} \tag{2.1}$$

When mass of monopile was assumed as evenly distributed along its length, talked forces would be got through integration along monopile which shown in equations 2.2 (where  $\rho$  means mass per unit length of monopile). Moreover, distributed mass of monopile led an inertia moment because distance from each mass point to centre of rotation. Equations 2.3 show the inertia moment on COG. However, equilibrium equation often built on center of rotation rather than COG, which led an additional inertia moment due to this change. Equation 2.4 shows this additional inertia moment where  $l_1$  means distance from center of rotation to COG.

$$\begin{aligned} F_I^t &= \int_l \varepsilon r \rho \cdot dl \\ F_I^n &= \int_l \omega^2 r \rho \cdot dl \end{aligned} \quad (2.2)$$

$$\begin{aligned} M_I &= I \varepsilon \\ I &= \frac{1}{12} m l^2 \end{aligned} \quad (2.3)$$

$$I_1 = I_0 + m l_1^2 \quad (2.4)$$

### 2.1.2 Lift-off Using Floating Installation Vessel

Crane vessel was assumed as floating structure in this part. Its motions were divided into two parts correspond to translation and rotation. Coupled motion between upending and vessel based on different theories.

When translation of crane vessel concerned, equation 2.5 show the absolute velocity and acceleration. The relative motion to global coordinate system was a translation. So the only first order relative term included.

$$\begin{aligned} v_a &= v_e + v_r \\ a_a &= \frac{dv_a}{dt} = a_e + a_r \end{aligned} \quad (2.5)$$

where,

- $v_a$  means absolute velocity
- $v_e$  means convected velocity

- $v_r$  means relative velocity
- $a_a$  means absolute acceleration
- $a_e$  means convected acceleration
- $a_r$  means relative acceleration

When rotation motion of crane vessel considered, a rotational coordinate system( $o' x' y' z'$ ) was introduced. Assumed its rotation could be described by angular velocity( $\omega$ ) and acceleration( $\varepsilon$ ). Absolute velocity and acceleration were shown in equation 2.6 with additional term due to rotation. First term of acceleration could be written as equation 2.7. Then the second term could be written as equation 2.8. At last, absolute acceleration could be written as equation 2.9. From above discussion, both first and second order terms would be considered when rotation motion was assumed.

$$\begin{aligned} v_a &= \omega \times r + \frac{dx}{dt} i' + \frac{dy}{dt} j' + \frac{dz}{dt} k' \\ a_a &= \frac{dv_a}{dt} = \left( \frac{d\omega}{dt} \times r \right) + \left( \omega \times \frac{dr}{dt} \right) + \left( \frac{d^2x}{dt^2} i' + \frac{d^2y}{dt^2} j' + \frac{d^2z}{dt^2} k' \right) \end{aligned} \quad (2.6)$$

$$\frac{d\omega}{dt} \times r = \varepsilon \times r \quad (2.7)$$

$$\begin{aligned} \omega \times \frac{dr}{dt} &= \omega \times \frac{d}{dt} (x' i' + y' j' + z' k') \\ &= \omega \times \left( \frac{dx}{dt} i' + \frac{dy}{dt} j' + \frac{dz}{dt} k' \right) + \omega \times \left( x' \frac{di'}{dt} + y' \frac{dj'}{dt} + z' \frac{dk'}{dt} \right) \\ &= \omega \times v_r + \omega \times (\omega \times r) \end{aligned} \quad (2.8)$$

$$a_a = \varepsilon \times r + \omega \times (\omega \times r) + a_r + 2\omega \times v_r = a_e + a_r + a_c \quad (2.9)$$

where,

- $v_c$  means second order velocity
- $a_c$  means second order acceleration

## 2.2 Hydrodynamic Analysis

Hydrodynamic coefficients of crane vessel would be calculated then induced into SIMA for coupled motion analysis. So a practical numerical tools based on three-dimensional analysis would be used to predict linear wave-induced motions and loads on large-volume structures at zero Froude Number. Panel methods are the most common techniques used to analyse the linear steady state response of large-volume structures in regular waves. There are different panel methods. One way is to distribute sources (and sinks) over the mean wetted body surface. Another way is to use a mixed distribution of both sources, sinks and normal dipoles distributed over the mean wetted body surface.

The talked panel method is used in HydroD software to find hydrodynamic response. Panel methods are based on potential theory. Basic assumption of that is oscillation amplitudes of the fluid and the body are small relative to cross-sectional dimensions of the body. Flow separation effect is neglected. The method can only predict damping due to radiation of surface waves. In other words, panel method cannot predict rolling motion of a ship close to the roll resonance period because the wave radiation damping moment due to roll may be small and viscous damping effects due to flow separation are important. In this offshore lift-off operation, roll motion of crane vessel is far away from resonance. So hydrodynamic response calculated through panel method could be seen as correct.

Panel method used to get hydrodynamic coefficients for crane vessel in single vessel scenario and both crane vessel and transport barge in two vessels scenario. For the talked reasons, roll motion of crane vessel and barge in these two scenarios cannot be very large in time domain analysis for coupled motion. Because constant hydrodynamic coefficients would be used in each time domain simulation.

## Frequency Domain Analysis

Frequency domain analysis were mainly focus on motions in irregular wave condition. From a hydrodynamical point of view it was sufficient to analyse a structure in incident sinusoidal waves of small steepness, since it was possible to obtain results in irregular sea states by linearly superposing results from regular wave components. A rigid body in 3-dimensional coordinate



system had 6 degrees of freedom but only heave and roll motion were important in this study. Study of motion transfer function have been done in project of last semester. ROA of single crane vessel with all motions and different incident wave directions would be shown in appendix.

In order to consider irregular wave, wave energy density spectrum was used with specific formulation of JONSWAP. It was suitable for Norwegian North Sea. Two parameters JONSWAP spectrum used here with  $H_s$  and  $T_p$ . Former metocean report would also introduced to find reasonable value of two parameters.

## 2.3 Coupled Motion Analysis

Lift-off process would be discussed in this thesis for both single vessel and two vessels scenarios. Crane vessel and barge were assumed to experience irregular wave with response follow transfer function calculated through panel method. And the monopile had its own rotation or translation motion. In order to clear character of coupled motion and concerned lift wire, horizontal and vertical support forces due to coupled motion, time series of motion and forces should be got. So time domain analysis would be used. Theory of time domain analysis would be discussed in this part. Details of analysis in SIMA would discussed in next part.

## Time Domain Analysis

When assuming linear and steady-state conditions response could be calculated based on frequency domain analysis. In order to manage nonlinear and transient conditions, time domain analysis had to be introduced. Then the principle of superposition was omitted. SIMO(simulation of complex marine operations) was a program developed by MARINTEK suitable for upending and lift-off operations. In time domain analysis, motion equations could be written as follows 2.10.

$$[m + A(\omega)] \ddot{x} + C\dot{x} + D_1\dot{x} + D_2f(\dot{x}) + K(x)x = q(t, x, \dot{x}) \quad (2.10)$$

where

- $m$  means body mass matrix

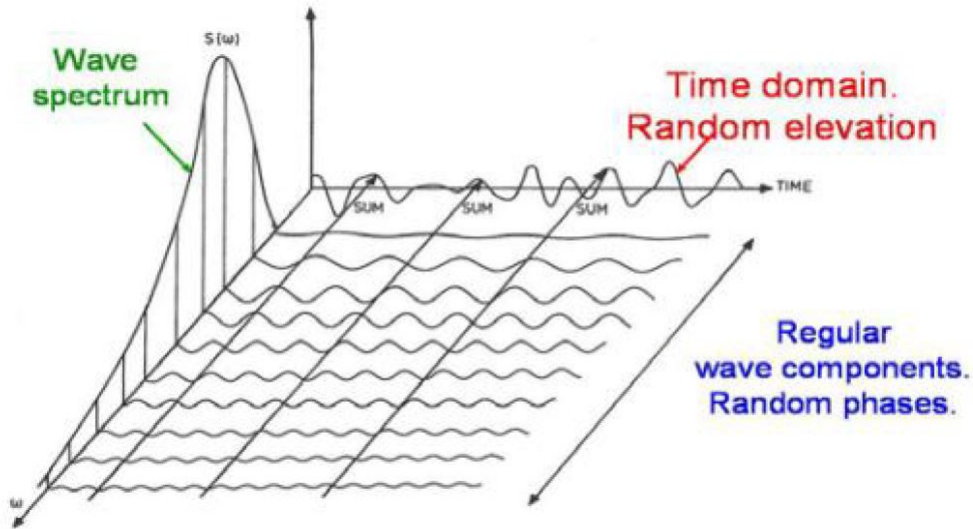


Figure 2.1: Relation Between Frequency Domain and Time Domain Analysis

- $A(\omega)$  means frequency-dependent added mass
- $C$  means frequency-dependent potential damping matrix
- $D_1(\omega)$  means linear damping matrix
- $D_2$  means quadratic damping matrix
- $f$  means vector function where each element is give by  
 $f_i = \dot{x}_i |\dot{x}_i|$
- $K(\omega)$  means (position-dependent) hydrostatic stiffness matrix
- $x$  means position vector
- $q$  means exciting force vector

Exciting forces,  $q(t, x, \dot{x})$  in this formula could be expressed as the follows

$$q(t, x, \dot{x}) = q_{w1} + q_{WA}^1 + q_{WA}^2 + q_{CU} + q_{EXT} \quad (2.11)$$

where

- $q_{w1}$  means wind drag force

- $q_{WA}^1$  means first order wave excitation force
- $q_{WA}^2$  means second order wave excitation force
- $q_{CU}$  means current drag force
- $q_{EXT}$  means other forces as wave drift damping, specified forces and forces from station-keeping and coupling elements

Above motions could be solved by integral or separation of motions. Retardation function was used in solving whole differential equation 2.10 when separation of motions was chosen. Moreover, motions were separated into two parts corresponding to high-frequency part and low-frequency part. Latter part could be solved by frequency domain analysis. This method required the motions linear to wave amplitude. Low-frequency part must be solved by time domain analysis.

Former method was used in SIMO. Through convolution integral frequency-dependent equation of motion would be expressed as a dynamic equilibrium where the frequency dependent parts were set equal to a force that varies sinusoidally at one single frequency. Furthermore, inverse Fourier transform was used to transform the frequency-dependent equation into a function of time.

Time-dependent equation of motion could be written as following equation 2.12

$$(m + A_{\infty}) \ddot{x} + D_1 \dot{x} + D_2 f(\dot{x}) + Kx + \int_0^t h(t - \tau) \dot{x}(\tau) d\tau = q(t, x, \dot{x}) \quad (2.12)$$

$\int_0^t h(t - \tau) \dot{x}(\tau) d\tau$  in above equation was the convolution integral which was forces due to frequency-dependent added-mass and damping. Furthermore,  $h(\tau)$  was the retardation function and could be expressed, for  $\tau > 0$  as in equation 2.13. Retardation function was computed by a transform of the frequency-dependent damping in SIMO. At last, added mass value was required in the calculation. Other parameters appeared in equation 2.12 were the same as those outlined in the explanation of equation 2.10.

$$h(\tau) = \frac{2}{\pi} \int_{-\infty}^0 \cos(\omega t) d\omega = -\frac{2}{\pi} \int_0^{\infty} \omega a \sin(\omega t) d\omega \quad (2.13)$$

## 2.4 Numerical Model in SIMA

Large body assumption of crane vessel and monopile was used in this case. Because motions of them were depended on environmental load and upending process. Moreover, heavy lift assumption in marine operation was used based on weight of monopile and displacement of crane vessel. Motion of crane vessel and monopile could be considered separately and then coupled together in heavy lift case.

Articulated structure was used to simulate crane on vessel due to its prescribed rotation motion. There were three types methods to describe rotation motion of crane. Second one was chosen in order to maintain constant rotation speed during whole process. However, there was a limitation about velocity setting. Acceleration, velocity and retardation were setting constant respectively in each interval. Following equation 2.14 gave relation between velocity and acceleration in each interval. It was obviously seen that velocity would be accelerated from '0' to defined value base constant acceleration and then decreased to '0' with the same acceleration. Based on such setting, velocity would be increased or decreased quickly at beginning and end of each interval. In order to have constant velocity, acceleration was assumed as very large value.

- 1. By giving start time, distance to move, velocity at steady state and ramp-up acceleration
- 2. By giving start time, stop time, velocity at steady state and ramp-up acceleration
- 3. By giving start time, stop time, distance to move and ramp-up acceleration

$$\Delta x = \Delta t_a^2 a + \Delta t_v v \quad (2.14)$$

Lift wire was assumed in vertical direction in whole upending process. So the rotation speed of crane bottom would keep changing in the process. From description in former paragraph, time series of rotation velocity cannot be set as a function of time. Large acceleration of each interval was induced by this reason. This shortcoming of SIMA made the whole process divided into more than 1,000 parts. Velocity was assumed as constant in every part. Code to get velocity of each part would be shown in appendix.

Multi-body model was used in SIMA to account for couple motion. From theory manual of SIMA, motion of body was concerned in each body fixed coordinate system then transferred to

global coordinate system. However, the motion was decided by prescribed forces and environmental load. In order to simplify calculation, current and wave load were neglected in this study. Only wave load was concerned with first and second order terms. First order wave responses such as first order excitations, first order wave-induced motions or first order diffracted wave kinematics. Second order wave responses such as full or simplified second order wave forces (and third order ringing forces) are all considered. Time series were generated by superposition of harmonic components with uniformly distributed phases by means of pre-generation by the Fast Fourier transform (FFT), by time domain summation of the harmonic components. For the reason of neglect of wind load, state-space model driven by white noise was not used in this study.

Basic theories of superposition of FFT would not be discussed in detail in this thesis. However, the setting of 'requested time series length' and 'time increment' were limited by FFT method, which requires equal frequency spacing and a number of frequencies (or number of time samples) to be  $N = 2^r$  'r' is an integer number. Largest value of 'r' was set as 20 to limit complexity of calculation. For this reason, time increment could not be set as very small value in order to guarantee the enough simulation time length. So forces of each time interval should be controlled to prevent very large acceleration.

Freedom of every body could be defined in SIMA when did time domain analysis. It helped to do the simulation based on jack-up assumption and regular motion assumption of crane vessel. Such analysis were done to check the accuracy of numerical method through comparison with theoretical result.

## 2.5 Theories Used in Two Vessels Scenario

Except the scenario, monopile transported by crane vessel itself monopile could also be transported to the working station by another barge. There were two vessels in lift-off operation process. So hydrodynamic effects in multi-body system would be discussed here.

Firstly, Laplace equation, water surface dynamic, kinematic boundary condition, seabed boundary condition, body surface boundary condition and infinite fluid boundary condition were introduced. Then the velocity potential would be divided into three parts (incident, diffrac-

tion and radiation) based on linear assumption as equation 2.15 shown.

$$\phi(x, y, z, t) = \phi_I(x, y, z, t) + \phi_D(x, y, z, t) + \phi_R(x, y, z, t) \quad (2.15)$$

Incident wave potential could be written as equation 2.16 through Airy theory.

$$\phi_I = \frac{ig\zeta_A}{\omega} \frac{\cosh(z+H)}{\cosh kH} e^{-ik(x\cos\beta+y\sin\beta)} \quad (2.16)$$

$\zeta_A$  and  $\beta$  mean amplitude and incident angle of incident wave. For complicated structure, diffraction and radiation potential could not get directly from Laplace Equation and boundary condition. From panel model each potential could be got.

### 2.5.1 Panel Model

Diffraction potential and radiation potential of body  $m$  in  $j$  mode could be written as source distribution on surface of body shown as equation 2.17. Where  $Q$  means source and  $\sigma(Q)$  means strength of source. Based on shown 3-dimensional Green equation 2.18 and body surface boundary condition, integral of source strength could be got as function 2.19. In panel model, wet surface was divided into several elements. Source strength of each element was assumed as constant. Based on above equations, diffraction and radiation velocity potential could be got.

$$\phi_D(P) = \iint_S \sigma(Q)G(P,Q)dS \quad (2.17)$$

$$G(P,Q) = \frac{1}{r} + \frac{1}{r_2} + 2PV \int_0^\infty \frac{(\mu+v)e^{-\mu H} \cosh[\mu(\xi+H)] \cosh[\mu(z+H)]}{\mu \sinh(\mu H) - v \cosh(\mu H)} J_0(\mu R) d\mu - \quad (2.18)$$

$$2\pi i \frac{k^2 - v^2}{H(k^2 - v^2) + v} \cosh[k(\xi+H)] \cosh[k(z+H)] J_0(kR)$$

$$\iint_S \sigma(Q) \frac{\partial G(P,Q)}{\partial n} dS = \frac{\partial \phi_D(P)}{\partial n} = -\frac{\partial \phi_I(P)}{\partial n}, P \in S^{(m)} \quad (2.19)$$

## 2.5.2 Coefficients of Hydrodynamic Load

After getting potential, linear Bernoulli equation was introduced to get pressure as equation 2.20 shown. And the fluid force could be divided into three parts as equation 2.21 shown. Then the radiation force on body number 'm' in 'i' mode could be written as equation 2.22. Then the first and second order response could be got from integration of pressure. In order to clear effects from gap between two vessels when its value was very small. Six parts of second order force were listed in equation 2.23 which corresponding to relative wave height, second order velocity term, first order pressure gradient coupled with motion, rotation motion of first order force, first order motion coupling and second order potential effect. Relative wave height effect could lead sum-frequency, difference-frequency effects when irregular wave considered.

$$P = -\rho \frac{\partial \phi}{\partial t} = i\omega\rho\phi e^{-i\omega t} = i\omega\rho(\phi_I + \phi_D + \phi_R) e^{-i\omega t} \quad (2.20)$$

$$F_w = F_w^k + F_w^d = - \iint_{S^{(m)}} i\omega\rho(\phi_I + \phi_D) e^{-i\omega t} n^{(m)} dS^{(m)} \quad (2.21)$$

$$F_R = \omega^2 e^{-i\omega t} \sum_{l=1}^M \left[ \sum_{j=1}^6 \zeta_j^{(1)} \left( \mu_{ij}^{ml} + \frac{\lambda_{ij}^{ml}}{i\omega} \right) \right] \quad (2.22)$$

$$\mu_{ij}^{ml} + \frac{\lambda_{ij}^{ml}}{i\omega} = \rho \iint_{S^{(m)}} \phi_j^{(l)} n_l^{(m)} dS^{(m)}$$

$$\begin{aligned}
& \int_{wl} \frac{1}{2} \rho g (\eta_r^{(1)})^2 n^{(0)} dl \\
& \iint_{S_0} \frac{1}{2} \rho |\nabla \phi^{(1)}| n^{(0)} dS \\
& - \iint_{S_0} \rho \left( X^{(1)} \cdot \nabla \frac{\partial \phi^{(1)}}{\partial t} \right) n^{(0)} dS \\
& \frac{1}{\varepsilon} \alpha^{(1)} \times F^{(i)} \\
& - \iint_{S_0} \left( \rho g X_2^{(2)} n^{(0)} + \rho g X_2^{(0)} n^{(2)} \right) dS \\
& - \iint_{S_0} \rho \frac{\partial \phi^2}{\partial t} n^{(0)} dS
\end{aligned} \tag{2.23}$$

### 2.5.3 Sensitive of Distance Between Barge and Crane Vessel

Firstly, vessel in downstream experienced smaller motion and wave force under beam sea assumption. However, some incident wave with special frequency couple with wave reflected by downstream vessel became standing wave. This phenomenon may lead resonance of water in the gap area. For very large or small frequency of incident wave, two separate vessels had almost same motion as a single one. From study of [Zhang et al. \(2014\)](#), when distance between two vessels was very large interaction between each other could be neglected. Once value of distance decreased from value of vessel width, interaction between each other could be serious. In this case, vertical relative motion between barge and crane vessel might effect lift wire force. And horizontal relative motion might challenge mooring system of crane vessel and also might lead collision. Mean drift force was heavily effected when the value of gap less than half width of vessel. Former study showed that mean drift force could be increased to around 10 times compared with single vessel, especially in yaw direction. So there would be a high probability for collision when the two vessels close to each other. Also from result of [Zhang et al. \(2014\)](#), the wave length which lead to water resonance would increase when the gap became larger, in other words low frequency wave was easier to make resonance in large gap condition.

Relative heave motion was enforced when the gap value around the width of crane vessel similar as relative horizontal motion. From above discussion, various values of distances be-



tween crane vessel and barge would be considered in the simulation part.

Except influence to hydrodynamic factors, gap value between crane vessel and transport barge also effected the capacity on-board crane. Safe working load (SWL) of a crane was always defined at a certain radius since SWL was a function a the radius. As it was clearly seen in figure 2.2, the SWL capacity gradually decreased as the radius increasing. Radius means distance from crane vessel to transport barge in this case. Based on this phenomenon, the value of distance should be carefully selected. Large one leaded small capacity of on-board crane, while small one leaded serious interaction between two floating structures.

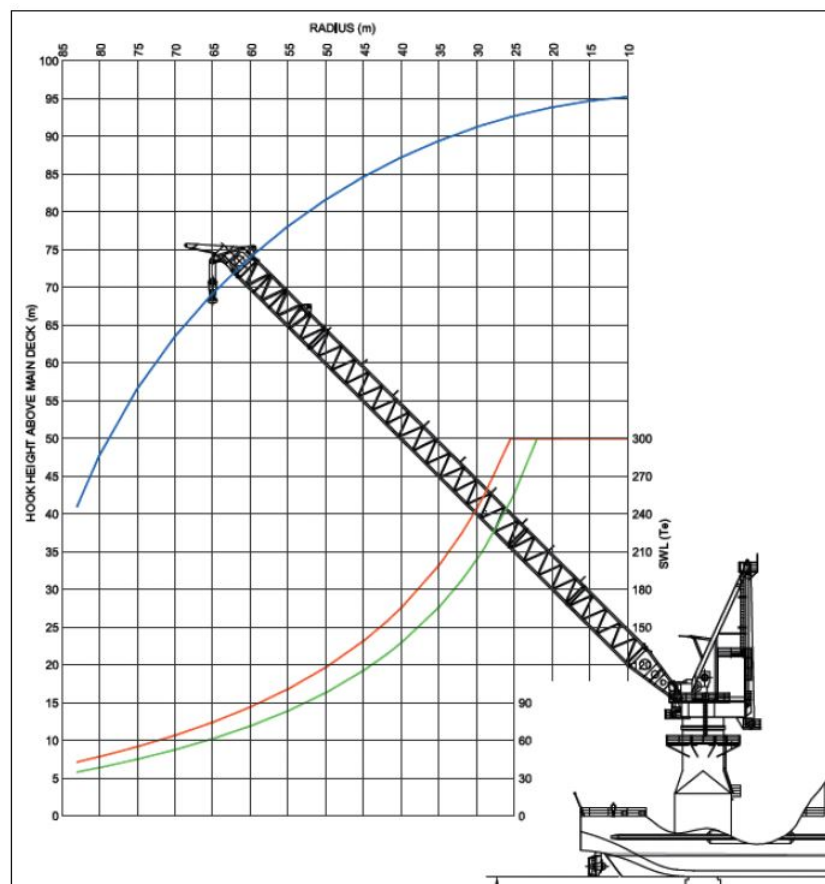


Figure 2.2: SWL vs. Radius, and Hook Height vs. Radius



# Chapter 3

## Analytical Result

Basic theoretical analysis on 'monopile upending', 'ship motion', 'coupling motion' and their effects would be shown in this chapter. Derivation of most equations using in this research would be shown at the same time. The whole process would be considered as many separate cases.

Following figure3.1 shows the upending process in practical. In order to clear the process, a simplified model was induced as figure3.2 shown. Monopile was lifted from horizontal position and a hinge connection between crane vessel and monopile used in this process. In this simplified model, dimension of monopile was neglected because it was very small compared with dimension of crane vessel.

### 3.1 Upending on Fixed Crane Vessel

In order to clear upending process, fixed crane vessel assumption was introduced. Working condition of such lifting process was similar as onshore in this case. In other words, onshore upending process would be analyzed in the following.

#### 3.1.1 Description of Monopile Upending

Monopile working as the foundation of offshore wind turbine, could be transported to the wind farm through two different scenarios. One is the monopile staying on the crane vessel during whole transportation, the other will use an extra barge to hold monopile. The former method



Figure 3.1: Upending Process in Practical

would be discussed in this part. Monopile could be arranged along the breadth of vessel. When it to be upending, about one fifth of monopile would be outside of the crane vessel and a kind of hinge used to connect the vessel and monopile just as figure 3.2 shown. From 2D concept, hinge connection limited the horizontal and vertical motion just allowing rotation as freedom. Upending was a monopile rotation process until it standing vertically. In this process crane and support point(hinge connection) would provide forces to maintain the rotation motion. In practical, there was a plate kind structure at the end of monopile to prevent it sliding into water. In the whole process, crane lifting limitation, yield stress of plate kind structure and strength of support point would challenge the upending motion. For this reason, motion and mechanism analysis should be carefully done. In this analysis, monopile could be seen as mass point at the centre of gravity or the mass of it could be seen uniformly distributed along the length. In the following, these two assumptions would be discussed separately.

### 3.1.2 Concentrated Mass Assumption of Monopile

When the mass concentrated to the center of gravity, angular acceleration would not provide inertia moment to the monopile. Such inertia moment would be discussed in the next section. Before dynamic analysis, the static analysis of monopile in random angle of  $\theta$  would be done.

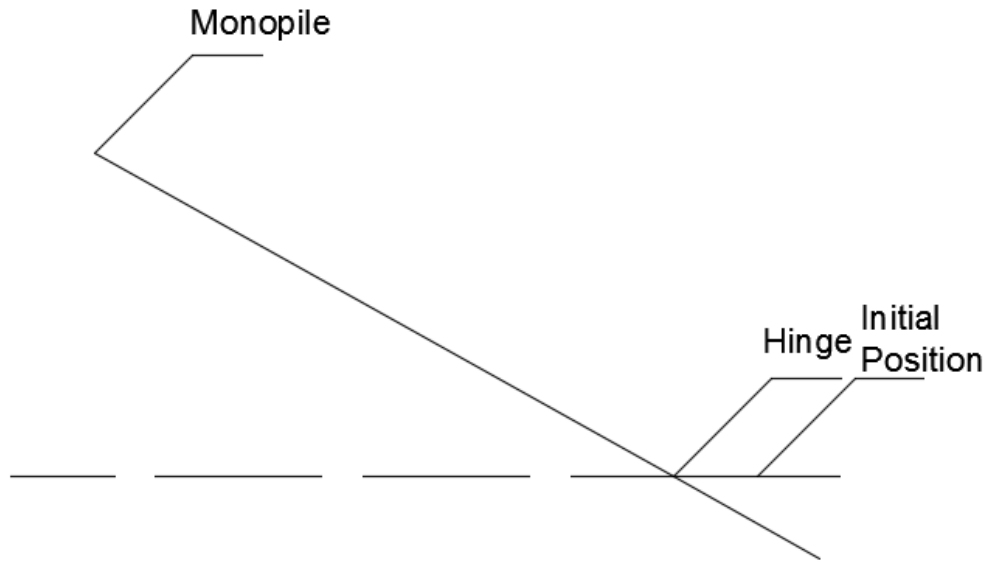


Figure 3.2: description of upending process

### Static Analysis

In static analysis, there was no acceleration and velocity of monopile, the forces on monopile were shown as figure 3.3. Force in the lift wire and support point will balance the gravity. Equation 3.1 and 3.2 shows the result of this condition.

In vertical direction

$$F_{line} + F_{supporty} = G \quad (3.1)$$

where,

- $F_{supporty}, F_y^S$  means vertical support force of hinge connection
- $F_{line}, F_l$  means lift wire force
- $G$  means gravity of monopile

Sum of moment at center of gravity

$$\begin{aligned} F_{line} * x1 &= F_{supporty} * x2 \\ x1 &= l/2 \cos(\theta), x2 = l_3 \cos(\theta) \end{aligned} \quad (3.2)$$

where,

- $\theta$  means inclination angle of monopile

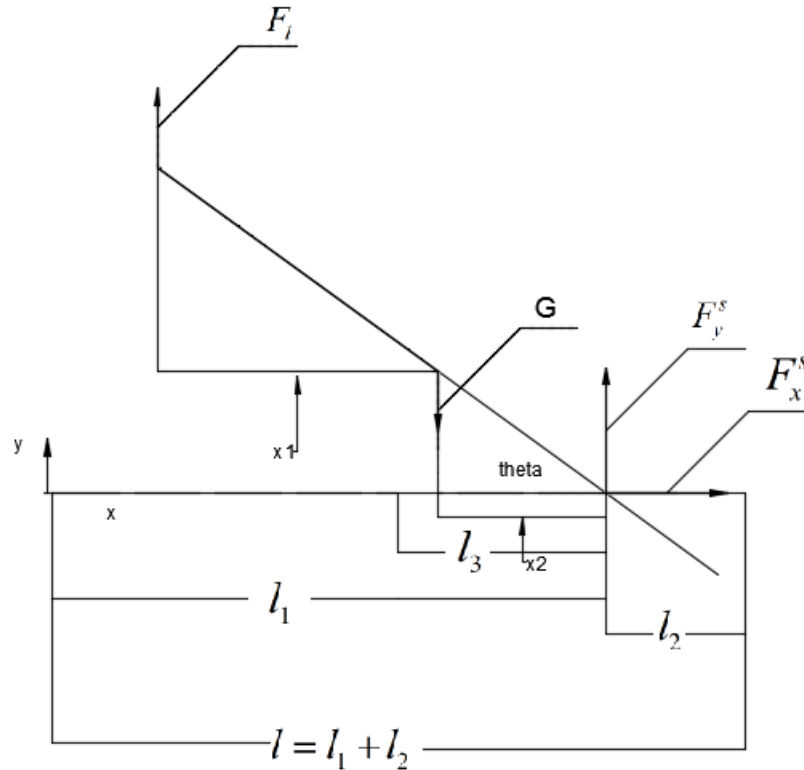


Figure 3.3: Forces on Monopile in Static Condition

In this process, length of monopile was 60 meters and the total mass of it was 500,000kg. Based on above equations, values of lift wire force( $F_{line}$ ) and vertical support force( $F_{supporty}$ ) would keep constant while the value of 'theta' changing in the process. In other words, the support point only provided vertical force. Monopile could keep any position even if it stood on a mirror without friction when neglect rotation acceleration and velocity. Figure3.4 shows the result of forces with the changing of theta.

However, rotational acceleration and velocity due to upending process would be taken into account in dynamic analysis. In order to describe clearly, three kinds of lifting process would be shown. Firstly, constant angular velocity, then constant vertical lifting velocity and last one fixed location of crane tip. Mechanism analysis including all kinds of forces on monopile in dynamic condition was shown in figure3.5.

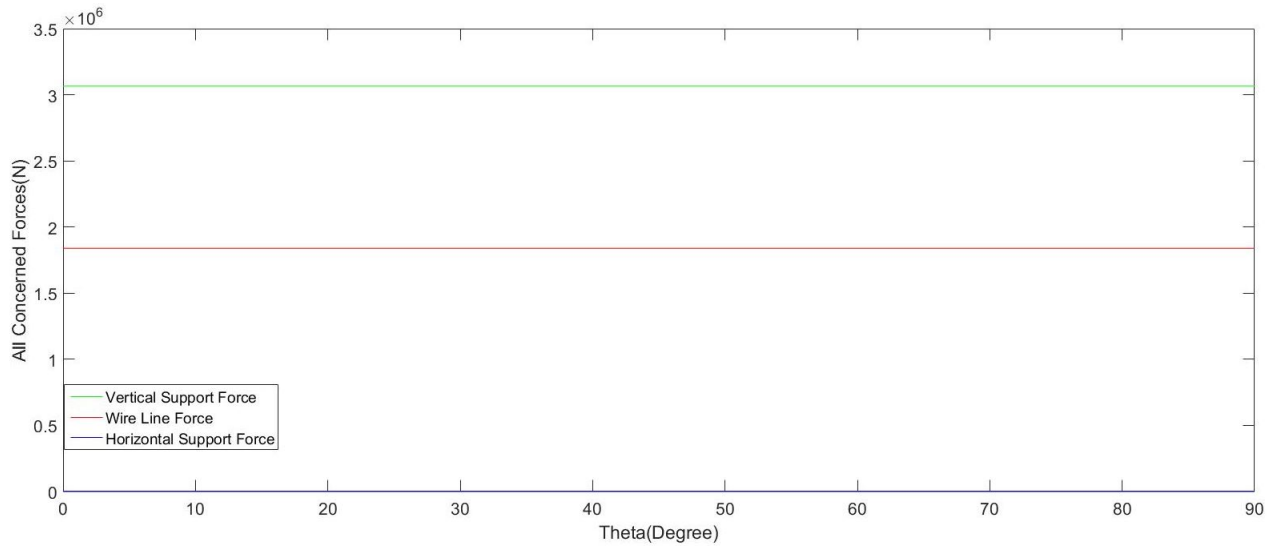


Figure 3.4: Static Result of All Concerned Forces

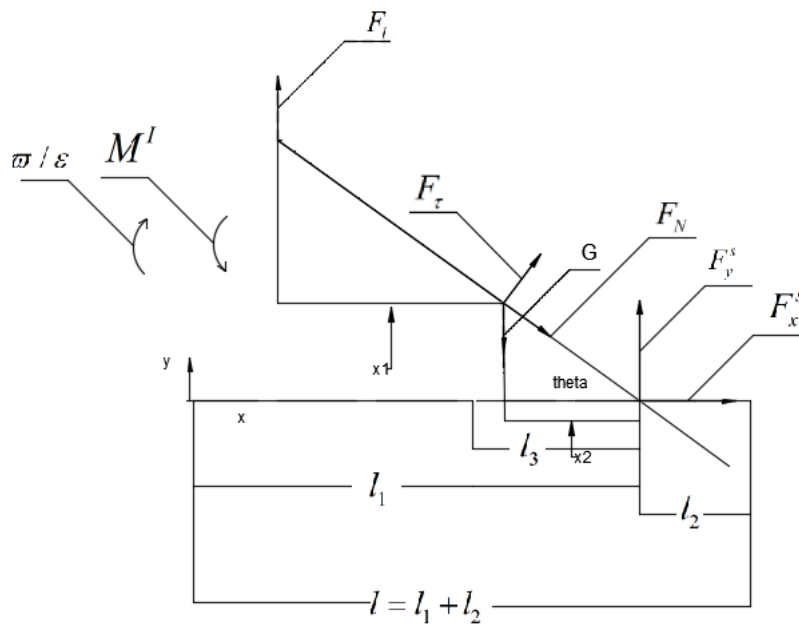


Figure 3.5: Forces on Monopile in Dynamic Condition

### Constant Angular Velocity

When the angular velocity of upending process assumed constant, there was no angular acceleration ( $\epsilon'$  in figure 3.6). All forces are shown in figure 3.6. Furthermore, ' $F_\tau$ ' which relied on angular acceleration in talked condition was also zero. When the constant angular velocity ( $\omega$ ) assumed, the following equations 3.3 would be got. Based on such equations, the result of concerned forces in the lift wire and support point were got as function 3.4 shown.

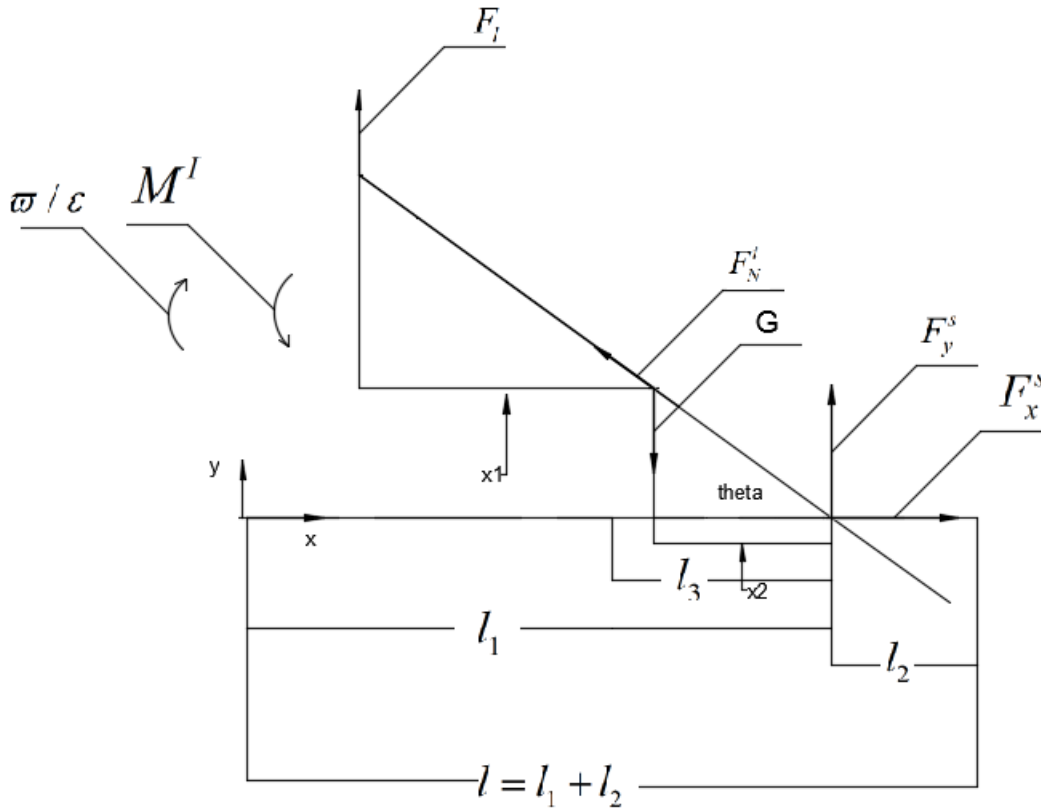


Figure 3.6: Forces in Constant Angular Velocity Condition

$$\begin{aligned}
 a^n &= \omega^2 * l_3 \\
 F^n &= a^n * m \\
 \left\{ \begin{aligned}
 F_{line} + F_{supporty} - m * g &= F^n \\
 F_{supportx} &= F^n \cos(\theta) \\
 F_{line} * l/2 * \cos(\theta) &= F_{supporty} * l_3 * \cos(\theta) + F_{supportx} * \sin(\theta)
 \end{aligned} \right. \quad (3.3)
 \end{aligned}$$

where,



- $\omega$  means angular velocity of monopile rotation

$$\left\{ \begin{array}{l} F_{line} = 3/8 * m * g \\ F_{supportx} = F^n \cos(\theta) \\ F_{supporty} = 5/8 * m * g - F^n \sin(\theta) \end{array} \right. \quad (3.4)$$

Following figure3.7 shows the changing of forces in lift wire and support point with different 'θ'. From this figure, changing of horizontal support force was obviously. Lift wire and vertical support forces could be seen as constant. However, figure3.8 shows the vertical support force keep changing with different 'θ'. The changing of it was very small because the main part of vertical support force coming from constant term which was 5/8 of gravity. Based on such discussion, lift wire force and vertical support force could be seen as constant with different 'θ' and the values of them were much larger than horizontal support force.

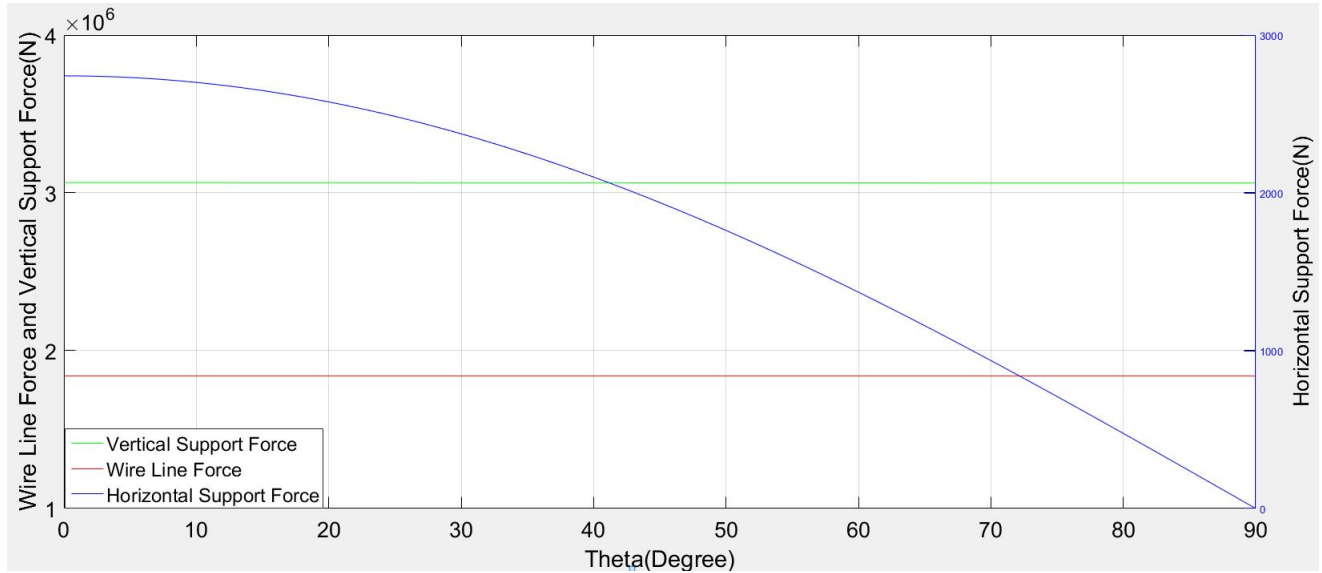


Figure 3.7: Force versus Theta in Constant Angular Velocity Condition

### Constant Vertical Lifting Velocity

In this part, the vertical lifting velocity of lift wire was assumed as constant, which means the angular acceleration ('ε' in figure3.9) was not zero. All forces in the system under such condition were shown in figure3.9. Moreover,  $F_t$  which relied on angular acceleration in this condition

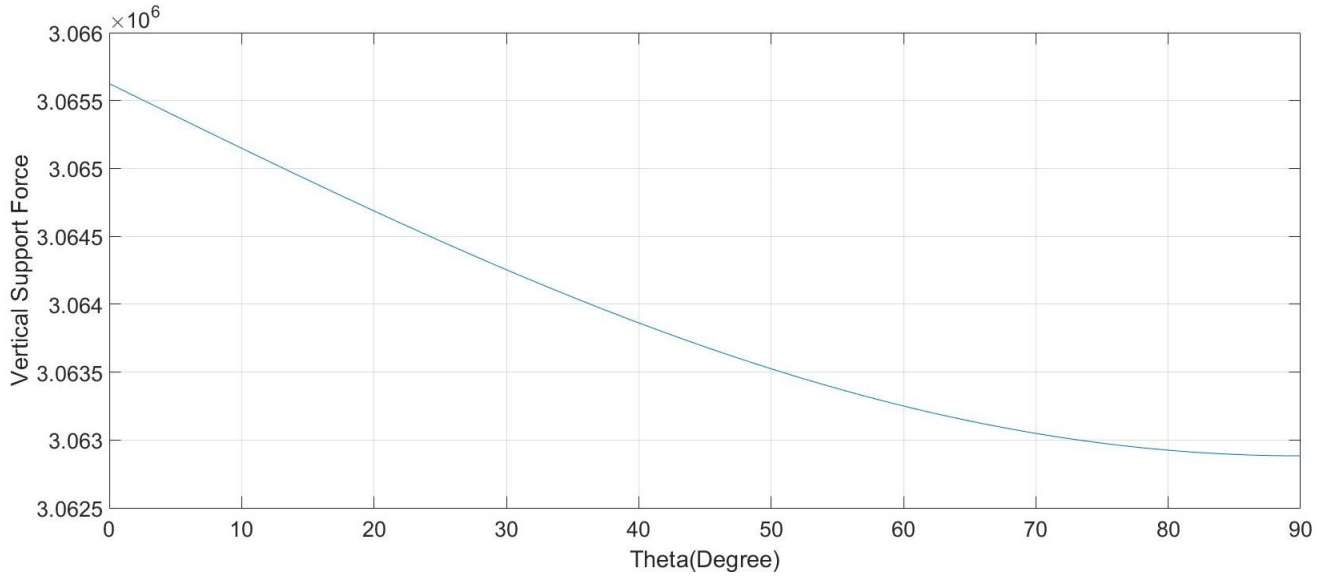


Figure 3.8: Vertical Support Force Versus Theta in Constant Angular Velocity Vondition

was no longer zero. When the constant velocity was assumed as 'v', the following equations 3.5, which based on the sum force in x and y directions were zero and bending moment on support point was also zero, show the mechanism. From such equations, the results of forces in lift wire and support point were got shown in equations 3.6.

$$\begin{aligned}
 \omega &= \frac{v}{\cos(\theta) * l_1} \\
 \cos(\theta) &= \frac{\sqrt{l_1^2 - (vt)^2}}{l_1} \\
 \varepsilon &= \frac{d\omega}{dt} = \frac{v^2 t}{(l_1^2 - t^2)^{1.5}} \\
 a^T &= \varepsilon * l_3 \\
 a^n &= \omega^2 * l_3
 \end{aligned} \tag{3.5}$$

$$\left\{ \begin{aligned}
 F_{supportx} &= (a^n * \cos(\theta) + a^T * \sin(\theta)) * m \\
 F_{line} + F_{supporty} &= (a^T * \cos(\theta) - a^n * \sin(\theta)) * m + m * g \\
 F_{line} * l_1 * \cos(\theta) &= a^T * m * l_3 + m * g * l_3 * \cos(\theta)
 \end{aligned} \right.$$

$$\left\{ \begin{aligned}
 F_{supportx} &= (a^n * \cos(\theta) + a^T * \sin(\theta)) * m \\
 F_{line} &= \frac{3 * m * (g * \cos(\theta) + a^T)}{8 * \cos(\theta)} \\
 F_{supporty} &= (a^T * \cos(\theta) - a^n * \sin(\theta)) * m + m * g - F_{line}
 \end{aligned} \right. \tag{3.6}$$

where,

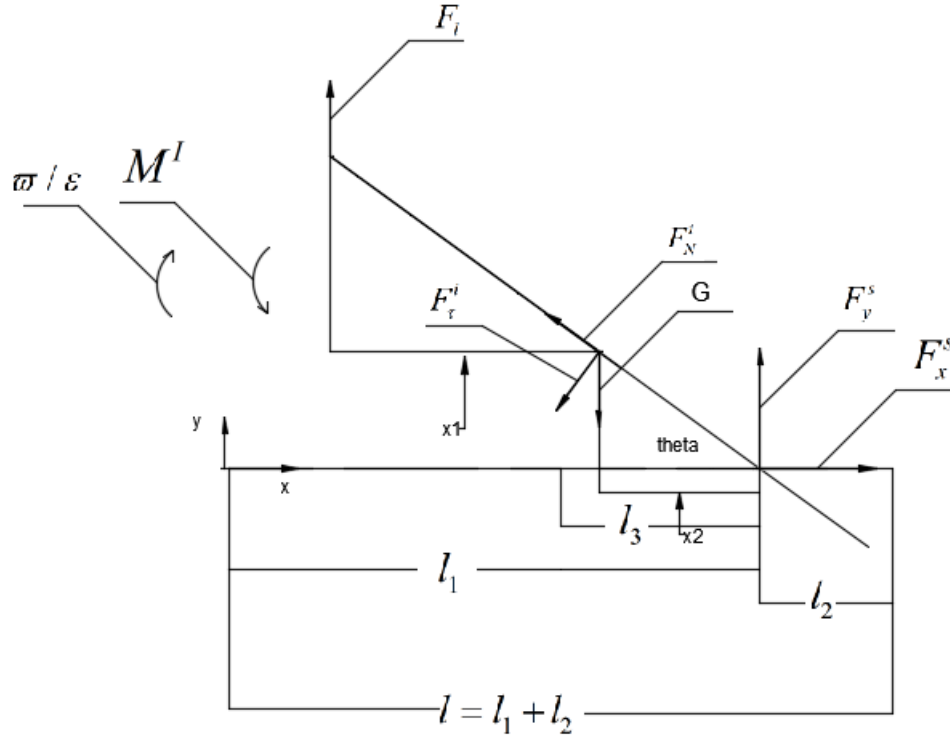


Figure 3.9: Mechanism Analysis Based on Constant Vertical Lifting Velocity Condition

- $F_x^S, F_{Supportx}$  means horizontal support force
- $\epsilon$  means angular acceleration of monopile rotation

The following three figures show the result of forces with the changing of 'time' and ' $\theta$ '. From figure3.10 and figure3.11, it was easily seen that the force in lift wire almost keep constant during whole process except for the period of last seconds or final angles. The reason was that the velocity of lifted point equaled to

$$\frac{v}{\cos(\theta)}$$

, which means that with the ' $\theta$ ' approaching to 90 degree, the rotational velocity could be infinite. In other words, the angular acceleration would also be very large. From the equation3.6, force in lift wire relate to angular acceleration. Such reason also led similar trend of horizontal and vertical support force of hinge connection. Figure3.12 shows the changing of forces in last tow degrees of ' $\theta$ ' (from 88 to 90). It was obviously seen that the changing in final angles was more obvious and the changing rate increased very fast at the end of process. Even in such an idealistic model, lifting velocity should be reduced at end of process to limit maximum value of

lift wire and support force.

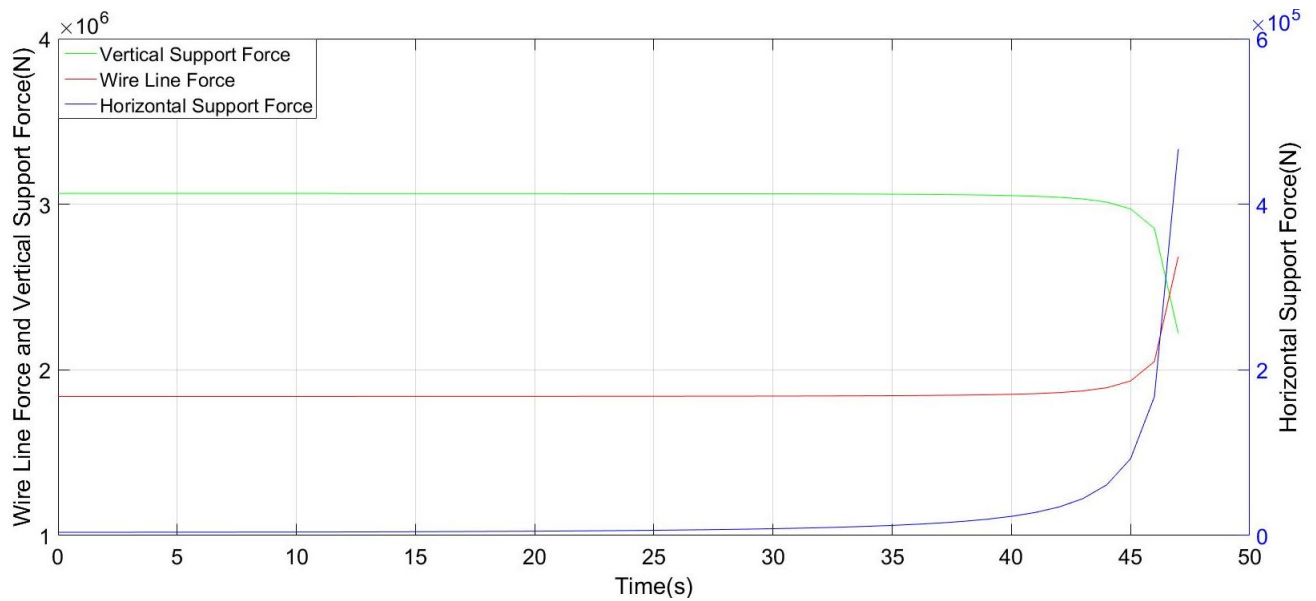


Figure 3.10: Time Series of Concerned Forces

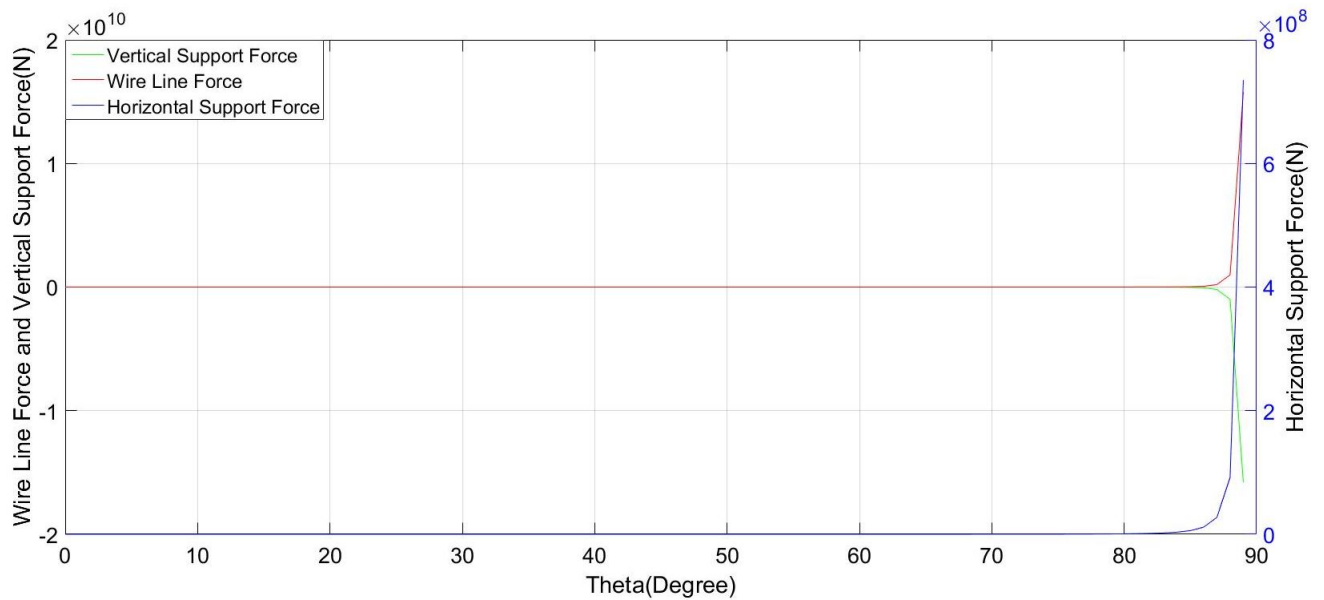


Figure 3.11: Concerned Forces Versus Theta

### Fixed Crane Tip

Another condition would be discussed here, which was the crane tip has no horizontal motion. But the velocity of lift wire was also constant. Figure 3.13 shows the geometrical relation between

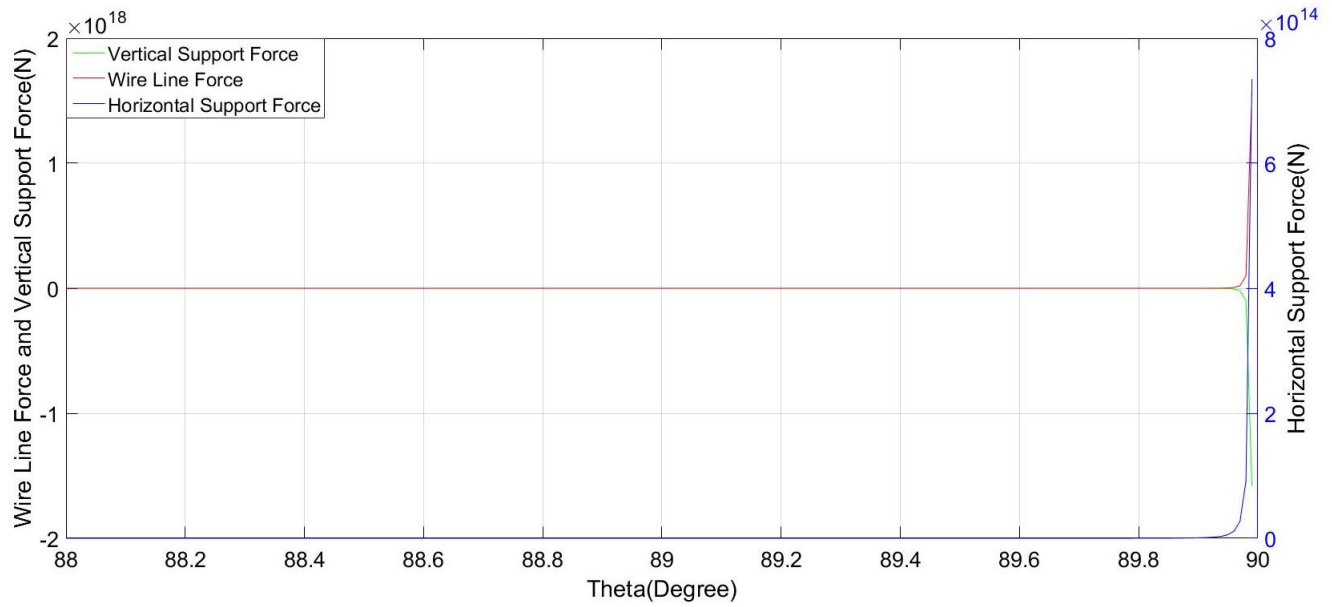


Figure 3.12: Concerned Forces Versus Theta(88-90)

crane tip and monopile. This method was not a reasonable choice due to the final position of monopile appeared when the monopile and lift wire consist a straight line. There were two circles in the figure3.13, hinge point acted as a center of one circle with the length of monopile acting as radius. The other has the center of crane tip, and the length of lift wire acted as radius in this circle. At each time step the length of lift wire could be exactly calculated. The connection point between these two circles would be seen as the connection point between monopile and lift wire. From coordinate of the connection point, angle ' $\alpha$ ' and ' $\theta$ ' would be sure. Then the following equations3.9 would be got to find forces of lift wire and support point. In order to simplify analysis process, force in support point was divided into tangential direction ( $f_{support\tau}$ ) and radial direction ( $f_{supportn}$ ) the same as force in lift wire as the figure3.14 shown. Even though, this was not a reasonable method, time series of concerned forces were also shown in figure3.15. From this figure, it was easily seen that the changing trend of all three forces were similar as the constant vertical lifting velocity condition. In other words, the value of angle ' $\alpha$ ' was very small in the whole process with little effect to the result.

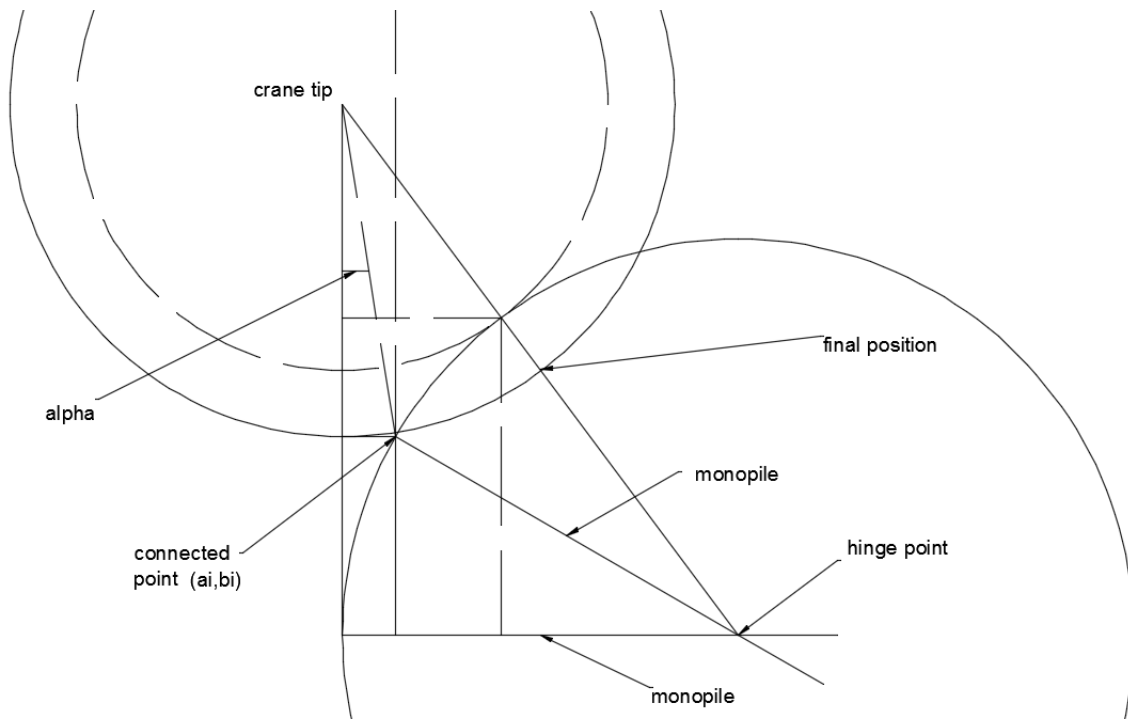


Figure 3.13: Fixed Crane Tip Position

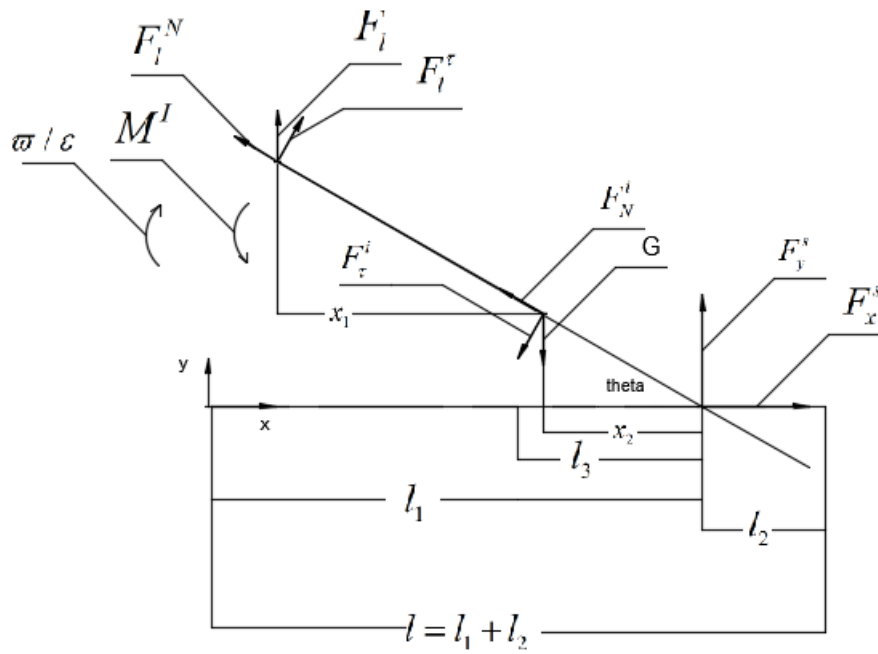


Figure 3.14: Mechanism Analysis for Fixed Crane Tip Condition

$$\begin{aligned}
 a^t &= \varepsilon * l_3 \\
 a^n &= \omega^2 * l_3 \\
 F_I^t &= -ma^t \\
 F_I^n &= -ma^n
 \end{aligned}
 \tag{3.7}$$

$$\begin{cases}
 F_{linetau} + F_{supporttau} = F_I^t + mg \cos(\theta) \\
 F_{line} = F_{linetau} / \cos(\theta + \alpha) \\
 F_{linetau} * (l_1 - l_2) = F_{supporttau} * l_3
 \end{cases}
 \tag{3.8}$$

$$\begin{cases}
 F_{linetau} * l_1 = m * g * l_3 * \cos(\theta) + F_I^t * l_3 \\
 F_{line} = F_{linetau} / \cos(\theta + \alpha) \\
 F_{supporttau} * l_1 = m * g * (l_1 - l_2) * \cos(\theta) + F_I^t * (l_1 - l_2) \\
 F_{supportn} = F_{line} * \sin(\theta + \alpha) + F_I^n - m * g * \sin(\theta)
 \end{cases}
 \tag{3.9}$$

where,

- $F_{linetau}, F_I^t$  means lift wire force in tangential direction
- $F_{linen}, F_I^n$  means lift wire force in radial direction

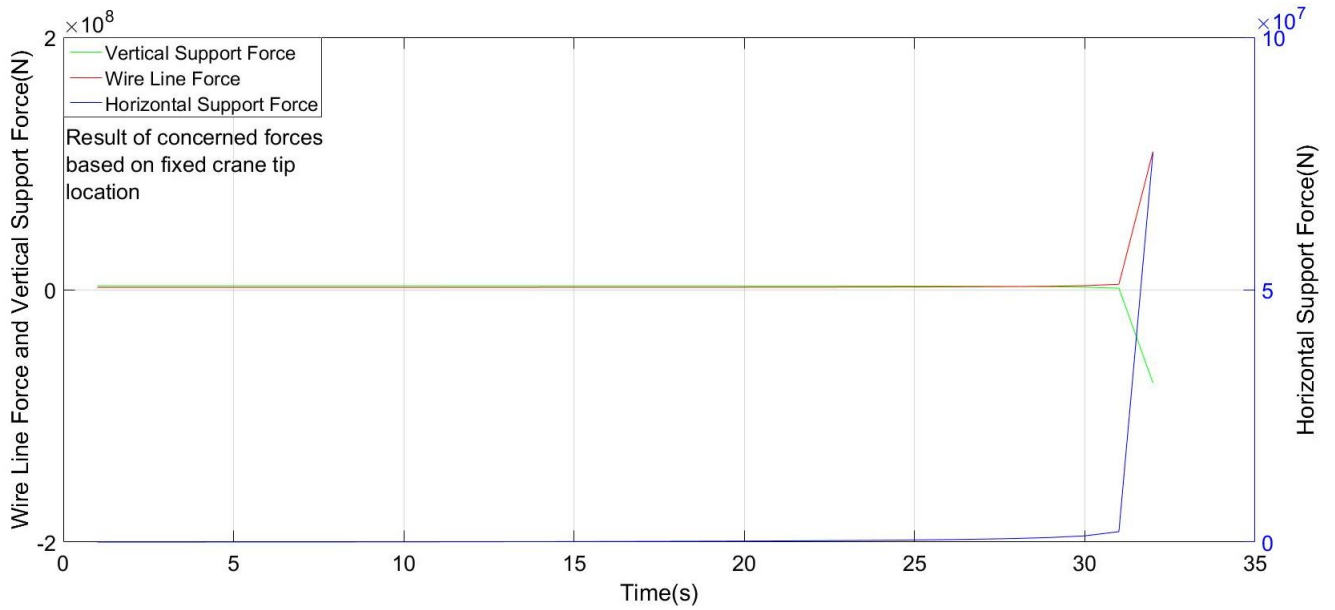


Figure 3.15: Time Series of Concerned Forces in Fixed Crane Tip Condition

### 3.1.3 Distributed Mass Assumption of Monopile

In practical, mass of monopile cannot be concentrated at one fixed point. Distributed mass would affect the inertia moment ' $M^I$ ' in figure 3.14. If assumed the whole monopile consist of finite number of mass element, the ' $M^I$ ' could be got from equation 3.10, where 'r' was the distance from each element to center of Gravity(COG). This moment was the key difference between concentrated and distributed mass assumptions in this process. From equation 3.10, it was easily seen that ' $M^I$ ' relied on the angular acceleration. In other words, static and constant angular velocity conditions had no difference after correcting the distribution of mass due to no angular acceleration.

$$M_I = 2 * \int_0^{l/2} \frac{m}{l} \epsilon r^2 dr = \frac{m * l^2}{12} \epsilon \quad (3.10)$$

### Constant Vertical Velocity

Distributed mass had no effect on acceleration of monopile which relied on upending process. So in this part the angular velocity and acceleration were the same as former concentrated mass condition. The only difference was an extra inertia moment ' $M^I$ '. The following equations 3.11, show the mechanism of the whole structure. Result of all concerned forces were shown in equations 3.12. Changing of all concerned forces with upending time and angle (' $\theta$ ') were shown in the figure 3.16 and 3.17. It was easily seen that effects to all three forces due to inertia moment were very limited. From equation 3.10, value of inertia moment which depended on mass and angular acceleration was much smaller than moment due to gravity and upending process itself. However, evenly distributed mass assumption had to be used in the following simulation.

$$\left\{ \begin{array}{l} F_{supportx} = F_I^n * \cos(\theta) + F_I^t * \sin(\theta) \\ F_{line} + F_{supporty} = m * g + F_I^t * \cos(\theta) - F_I^n * \sin(\theta) \\ F_{line} (l_1 - l_3) * \cos(\theta) = \frac{m * l^2 * \epsilon}{12} + F_{supporty} * l_3 * \cos(\theta) + F_{supportx} * l_3 * \sin(\theta) \end{array} \right. \quad (3.11)$$



$$\left\{ \begin{aligned} F_{supportx} &= F_I^n * \cos(\theta) + F_I^t * \sin(\theta) \\ F_{line} &= \frac{3 * m * \cos(\theta) * (g + a^t * \cos(\theta)) + 3 * F_{supportx} * \sin(\theta)}{8 * \cos(\theta)} \\ F_{supporty} &= (a^t * \cos(\theta) - a^n * \sin(\theta)) * m + m * g - F_{line} \end{aligned} \right. \quad (3.12)$$

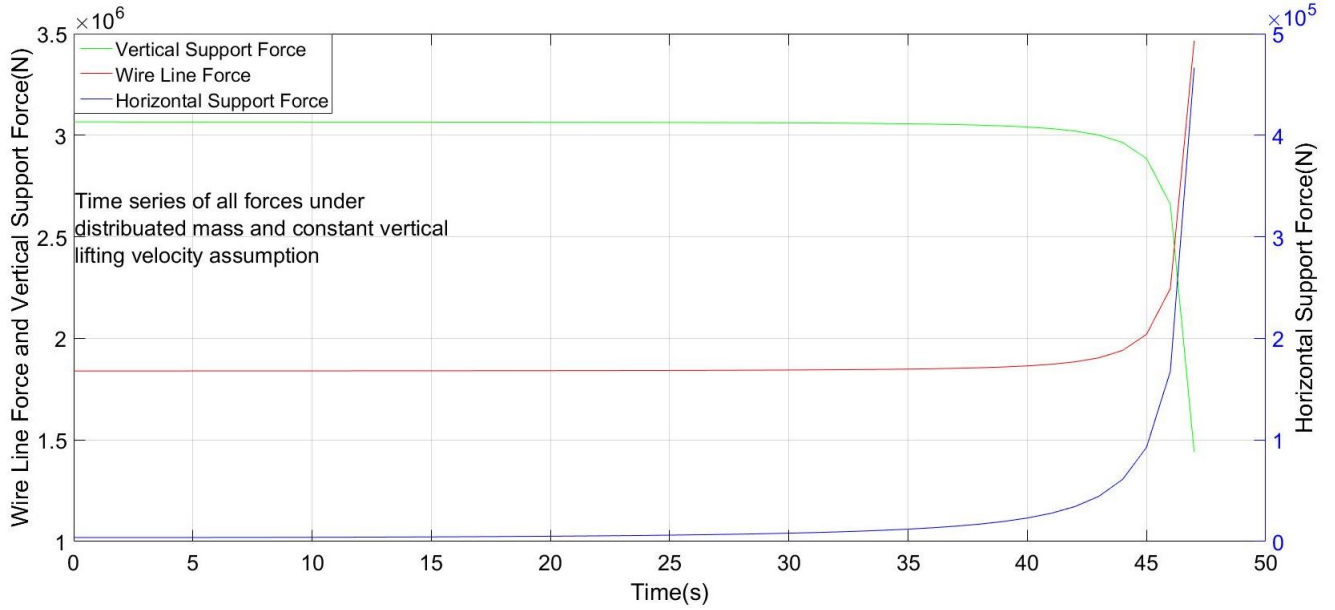


Figure 3.16: Time Series of All Forces Under Constant Vertical Lifting Velocity Assumption

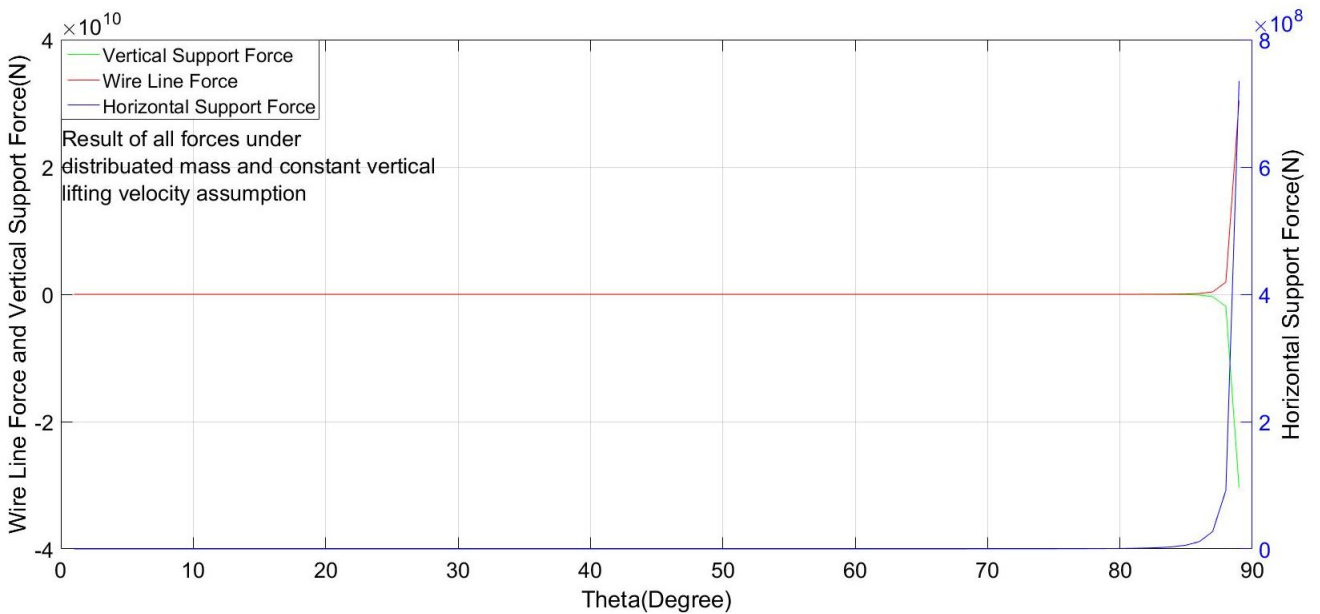


Figure 3.17: Theta Series of All Forces Under Constant Vertical Lifting Velocity Assumption

## Linear Moving Crane Tip Condition

As discussed in part 3.1.2, fixed crane tip was not a reasonable choice due to final position of monopile in upending process. In order to correct this case, horizontal velocity of crane tip was taken into account, which means the crane tip in figure 3.13 could move to right during upending process to get reasonable final position of monopile. Horizontal velocity of crane tip was concerned by moving position of circle with crane tip as center. Analysis of this condition was similar as 'Fixed Crane Tip' condition except the talked moving circle. Result of this case was shown in figure 3.18 when assumed horizontal velocity of crane tip as 1m/s same as lifting velocity. This result was similar as 'Constant Vertical Velocity' condition. Because the upending time equaled to crane tip moving time. When the horizontal velocity changed to 0.5m/s. Time series of concerned forces shown in figure 3.19, it could be seen as an unidealized case but more practical. All three forces got maximum value around 43s, which means monopile and wire line consisted a straight line. Compared with former result, horizontal support force had negative value for most part of the process rather than keep zero. Velocity of crane tip made this result. This condition could be more similar with numerical one in following chapter than any other theoretical case. Detail comparison would be shown in next chapter.

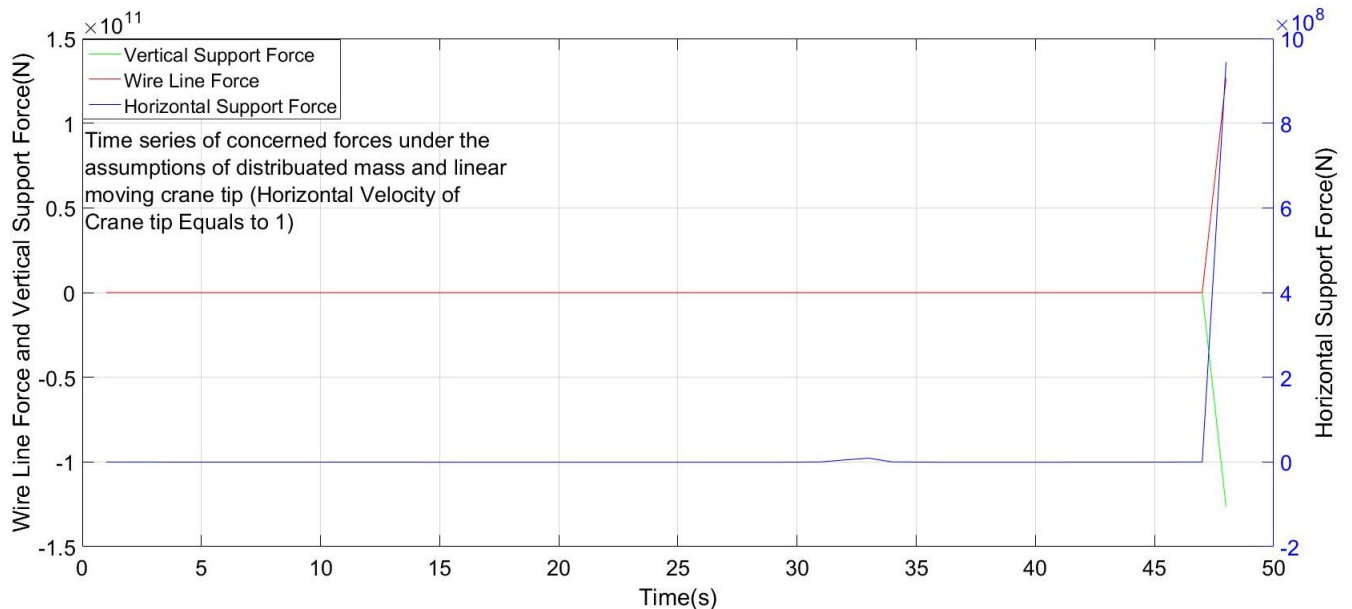


Figure 3.18: Time Series of All Forces under Linear Moving Crane Tip Assumption(1m/s)

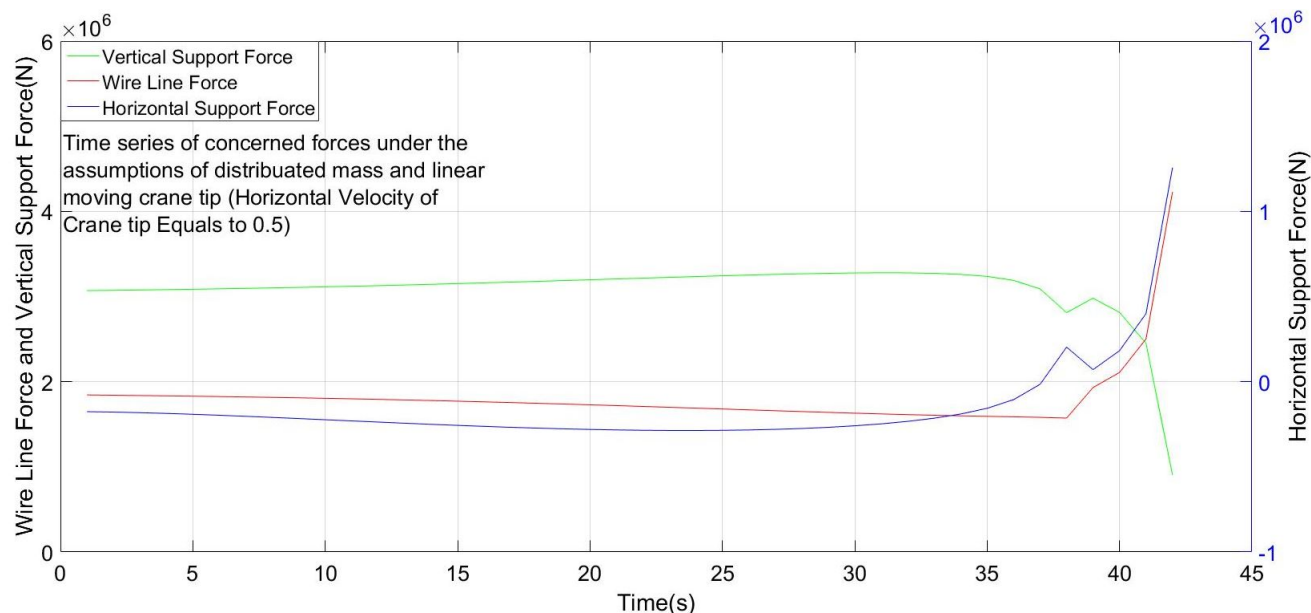


Figure 3.19: Time Series of All Forces under Linear Moving Crane Tip Assumption(0.5m/s)

## 3.2 Results Based on Constant Lifting Velocity and Lift Wire Force

From former discussion, the case of 'Fixed Crane Tip' led to 'un-totally' upending process, which means monopile could not be upended any more when the monopile and lift wire connect crane tip and support point straightly. Even though, moving crane tip to keep wire line vertically was an ideal case, that was the best choice in upending process. Following numerical and theoretical analysis could base on such assumption. Lifting force and velocity of crane lift wire had upper limit which corresponding to the largest power of crane. In this part, different values of lifting force and velocity would be discussed in detail.

### 3.2.1 Results Based on Constant Lifting Velocity

Constant lifting velocity was assumed as 1m/s in former discussion. In order to clear effects on concerned forces due to such lifting velocity, series simulations were done based on different lifting velocities. Vertical support force took as an example as figure 3.20 and 3.21 shown. These two figures show vertical support force versus ' $\theta$ ' within range of 0-90 and 0-60 respectively. It was clearly from figure 3.20, ' $\theta$ ' series of vertical support force were little affected by different lifting velocities. This means that amplification of vertical support force due to large value of lifting

velocity was very small compared with upending process. From figure 3.21, force increased with the increasing of lifting velocity but the increasing level was limited. This phenomenon could also be seen from equations 3.5 and 3.6. Terms in lift wire and vertical support forces which based on lifting velocity was very small compared with term due to gravity. 'θ' series of lift wire and horizontal support forces with different lifting velocities would be shown in appendix.

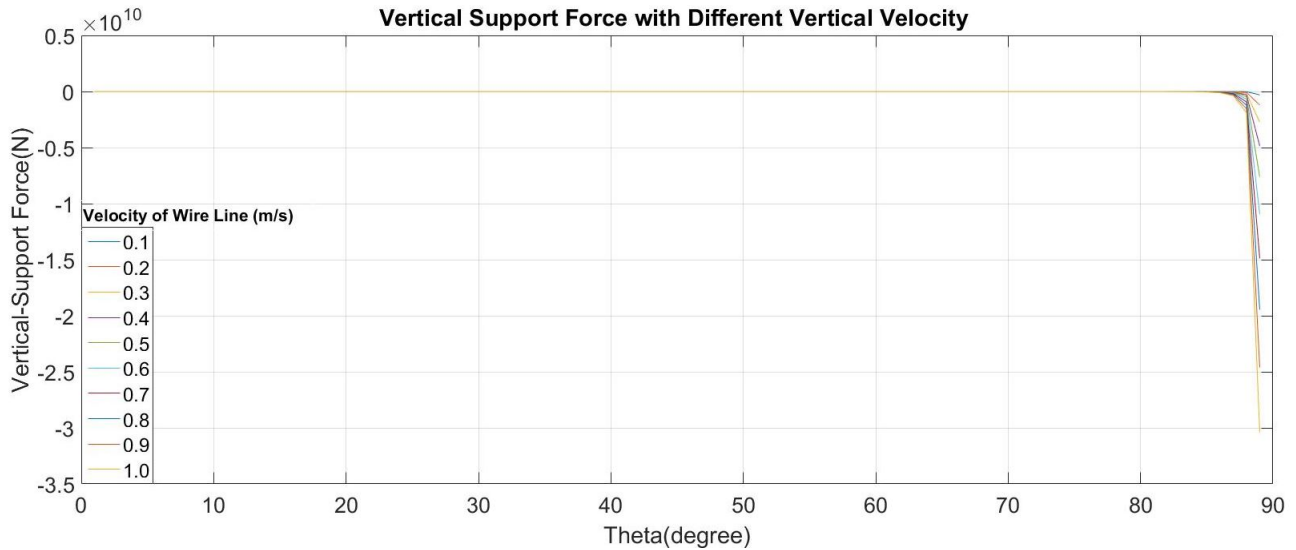


Figure 3.20: Theta Series of Vertical Support Force for Different Lifting Velocity

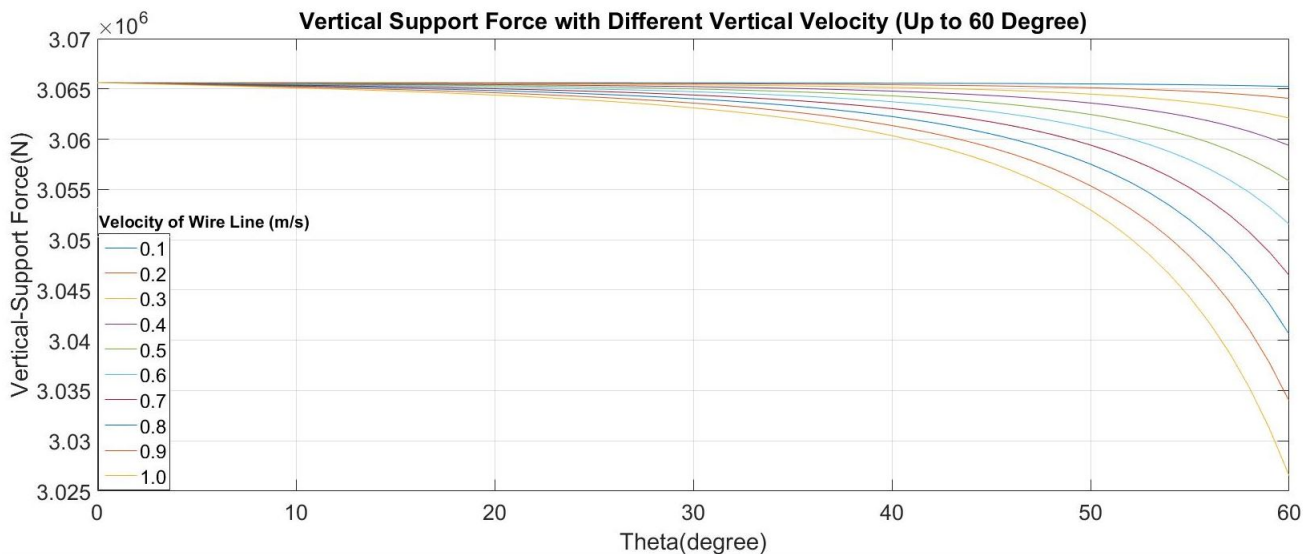


Figure 3.21: Theta Series(0-60) of Vertical Support Force for Different Lifting Velocity

### 3.2.2 Results Based on Constant Lifting Force

Effects to support force and lifting velocity due to different lift wire forces would be show in this part. Based on energy conservation law of rotation, the following equations 3.13 show the relation between angular velocity and acceleration when the theta( $\theta$ ) using as a given value. Then a weight value 'a' was assumed in a range from 0.4 to 0.85 to define constant value of lift wire force in each circle. Figure 3.23 shows 'θ' series of lifting velocity. In these cases, lift wire was assumed vertical during whole process. From talked series, average and peak values of lifting velocity increased with larger lift wire force. Peak values of all series show too large lifting velocity of on-board crane. Minimum peak value appeared when constant lifting force assumed as 0.4G, which was around 6m/s. From survey of on-board crane, such velocity had exceeded upper limit. From this discussion, constant lift wire force condition was not a reasonable choice for upending process.

Following lift wire velocity, concerned forces would be discussed. Vertical support force was taken as an example. From 'θ' series of vertical support force shown as figure 3.22, shape of such series was very different from former one. Constant value of lift wire force made lifting velocity changing with theta( $\theta$ ). From equations 3.5, angular velocity and acceleration would also changing with lifting velocity. Moreover, maximum value of vertical and horizontal (shown in appendix) support force was a reasonable value rather than infinite in other conditions. Constant lift wire force was not a suitable choice to upend monopile in practical, but it provided exact relation between concerned forces and lifting velocity. This relation could be used to limit maximum value of all three forces in numerical simulation by decreasing lifting velocity at the end of process.

$$\begin{aligned} \frac{1}{2} I_z \omega^2 &= M * \theta = I_z \int_0^{\theta} \varepsilon * d\theta \\ \omega^2 &= 2 * \int_0^{\theta} \varepsilon * d\theta \end{aligned} \quad (3.13)$$

$$a * G * l_1 * \cos(\theta) = G * l_3 * \cos(\theta) + \left( \frac{ml^2}{12} + m * l_3^2 \right) * \varepsilon \quad (3.14)$$

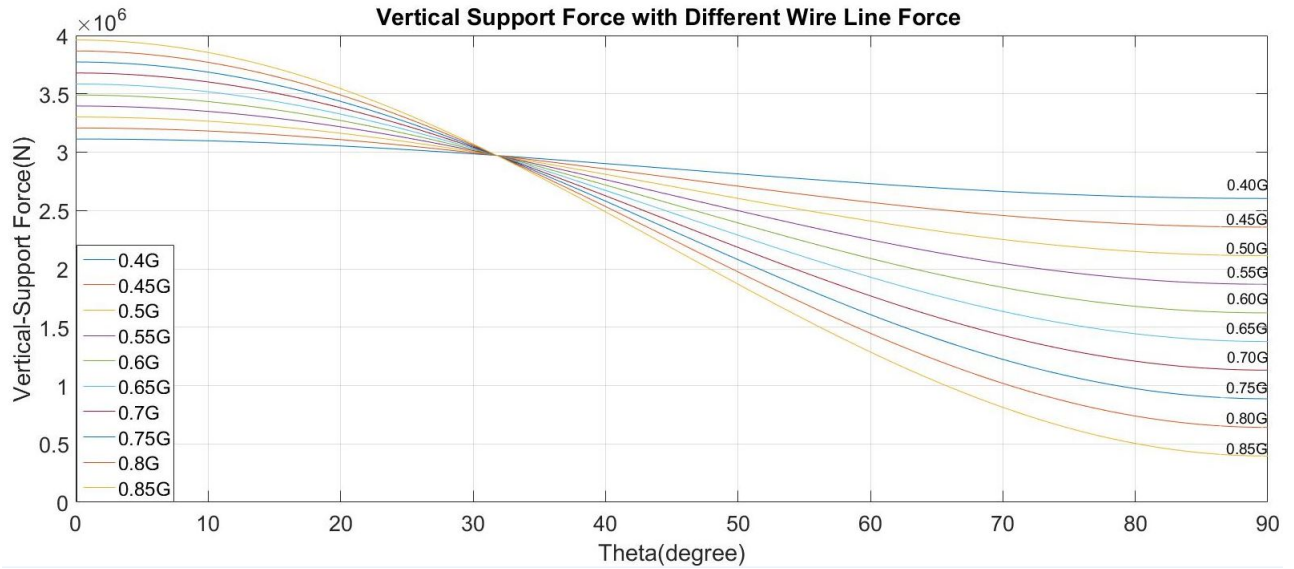


Figure 3.22: Theta Series of Vertical Support Force for Different Lifting Forces

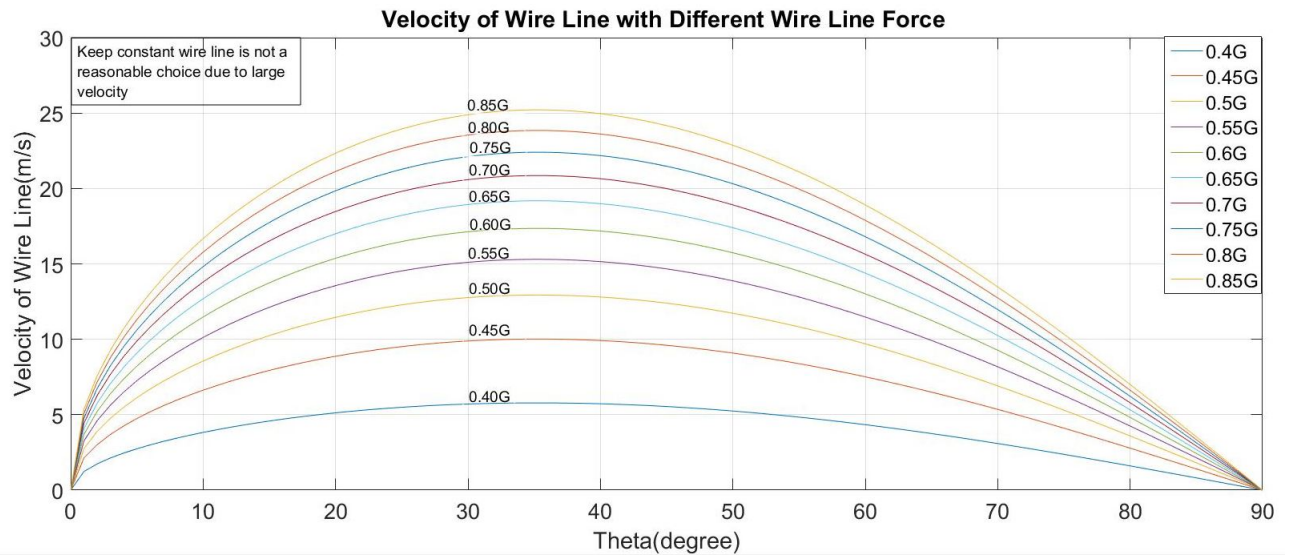


Figure 3.23: Theta Series of Lifting Velocity for Different Lifting Forces

### 3.3 Regular Heave Motion of Crane Vessel

All of former discussions were based on jack-up vessel assumption. From this part, motion of crane vessel would be taken into account. All six possible motions of crane vessel including surge, sway, heave, roll, pitch and yaw were divided into two kinds. One was translation the other rotation. The former kind just provided extra accelerations to the system, which means only relative and convected motion would be considered to couple upending and vessel vessel motions. Latter kind was a little complicated, which brought one more second order acceleration(Coriolis Acceleration) to the system than vessel translation condition. Details of such two kinds would be shown by some examples. Heave and roll motions were chosen as examples to show effects from these two kinds of motions. Firstly, heave motion of vessel would be discussed in theory analysis then frequency and amplitude of such motion would be verified to show their effects to concerned three forces.

#### 3.3.1 Theory Analysis of Coupled Motion

Different from jack-up vessel condition, an extra force( $F_I^H$ ) which means inertia force due to vessel heave motion was taken into account. This force could be seen as finite force elements evenly averaged along length of monopile. For the reason of same direction of every force element. This distributed force could be seen as a concentrated force on the COG of monopile without extra inertia moment. The only difference between jack-up vessel and floating vessel condition was the extra vertical force in equilibrium equation of y-direction.

In the analysis of heave motion condition, motion of vessel could be assumed regularly as equation 3.15 shown. Then the velocity and acceleration of such motion would also be got. From this result inertia vertical force on monopile could get by the acceleration times mass. Similar as former fixed vessel condition, lift wire velocity assumed constant as 'v'. Following this, upending angular velocity and acceleration would be got as equation 3.16 shown. Moreover, vertical force equilibrium equation and sum moments for support point were got as equations 3.17 to calculate concerned forces. Vessel heave motion had effects in horizontal force. So the horizontal support force had no difference between jack-up vessel and floating vessel condition.



$$\begin{aligned}
y &= A \sin(\omega_0 t) \\
v_H &= \omega_0 A \sin(\omega_0 t) \\
a_H &= -\omega_0^2 A \sin(\omega_0 t)
\end{aligned} \tag{3.15}$$

$$\begin{aligned}
a_N &= \omega^2 l_3 \\
a_\tau &= \varepsilon l_3 \\
v_{line} &= v \\
v_{Rotation} &= \frac{v}{\cos \theta} = \frac{l_1 v}{\sqrt{l_1^2 - (vt)^2}} \\
\cos \theta &= \frac{\sqrt{l_1^2 - (vt)^2}}{l_1} \\
\omega &= \frac{v}{R} = \frac{v}{\sqrt{l_1^2 - (vt)^2}} \\
a_N &= \frac{v^2}{l_1^2 - (vt)^2} l_3 \\
a_\tau &= \frac{tv^3}{[l_1^2 - (vt)^2]^{1.5}}
\end{aligned} \tag{3.16}$$

$$\begin{cases} F_{line} l_1 \cos(\theta) + F_I^H l_3 \cos(\theta) = mg l_3 + \left( \frac{ml^2}{12} + l_3^2 m \right) \varepsilon \\ F_I^N \sin(\theta) + F_{line} + F_S^y + F_I^H = mg + F_I^\tau \cos(\theta) \end{cases} \tag{3.17}$$

### 3.3.2 Effects Based on Heave Amplitude

Heave motion of the crane vessel would be different in varied sea states. From given heave RAO for beam sea, amplitude of it could be varied from 0m to 1m. Based on equations 3.16 and 3.17, larger amplitude of heave motion would increase peak value of lift wire and vertical support force time series. Lift wire force was chosen as an example to show such phenomenon as figure 3.24. It was easily seen, that peak value of lift wire force increased a little with larger heave amplitude but the percent of increment was very limited compared with value without heave motion. Shape of all time series were similar as jack-up vessel condition. Because the terms in lift wire force which depended on vessel heave motion were much smaller than terms due to gravity. Values of lift wire force would be very large even be infinite at end of upending process. Such result based on upending process with no relation to vessel motion. Almost same result for vertical support force which would be shown in appendix. Similar as discussed before, vessel heave motion had no effects to horizontal support force as figure 3.25 shown. Result of



horizontal support force was same with jack-up vessel condition.

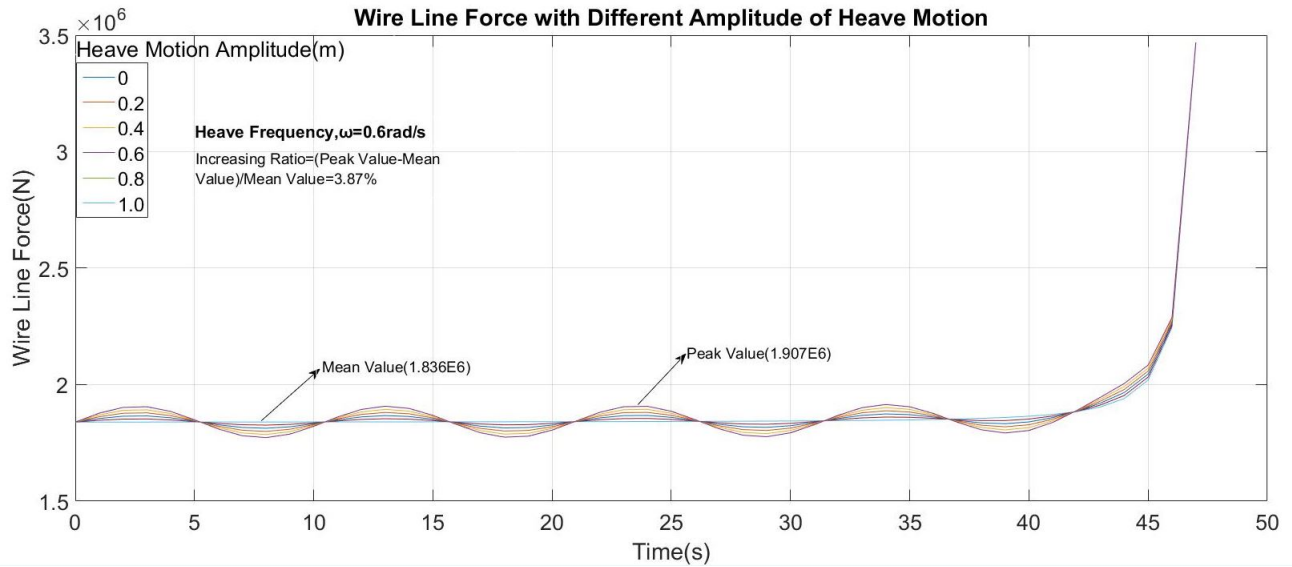


Figure 3.24: Time Series of Wire Line Force with Different Heave Amplitude

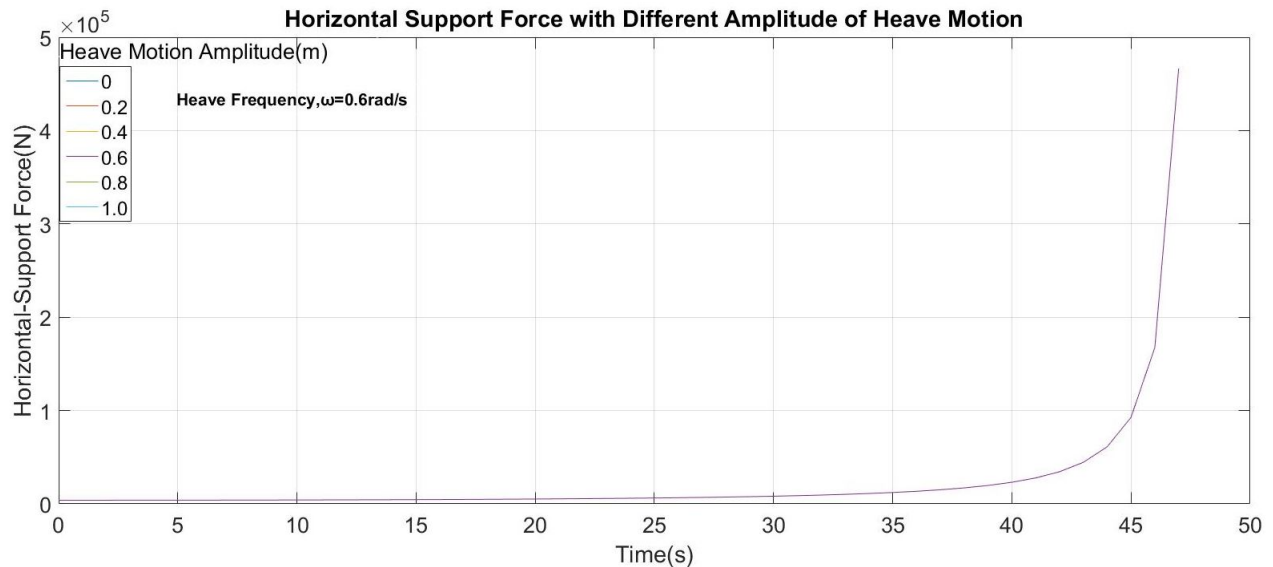


Figure 3.25: Time Series of Horizontal Support Force with Different Heave Amplitude

### 3.3.3 Effects Based on Heave Frequency

Effects to concerned forces due to different heave frequencies would be discussed in this part. Similar as heave amplitude effects. Frequency of heave motion had no relation to horizontal

support force which would be shown in appendix. Both lift wire and vertical support forces were a little affected by different frequencies. Heave amplitude in this condition was constantly assumed as 1m. Figure 3.26 shows result of time series of lift wire force as an example of concerned forces. It was easily seen, that the peak value had little difference with the mean value which based on no heave motion condition. Ratio between (peak value-mean value)/(mean value) was shown on the figure as 4.32 percent. Compared with the effects due to different heave amplitude, frequency provided much larger effects. Period of each time series was different due to heave frequencies. Similar as former discussed, maximum value of lift wire force had almost no relation with heave frequency. Only upending process lead appearance of maximum.

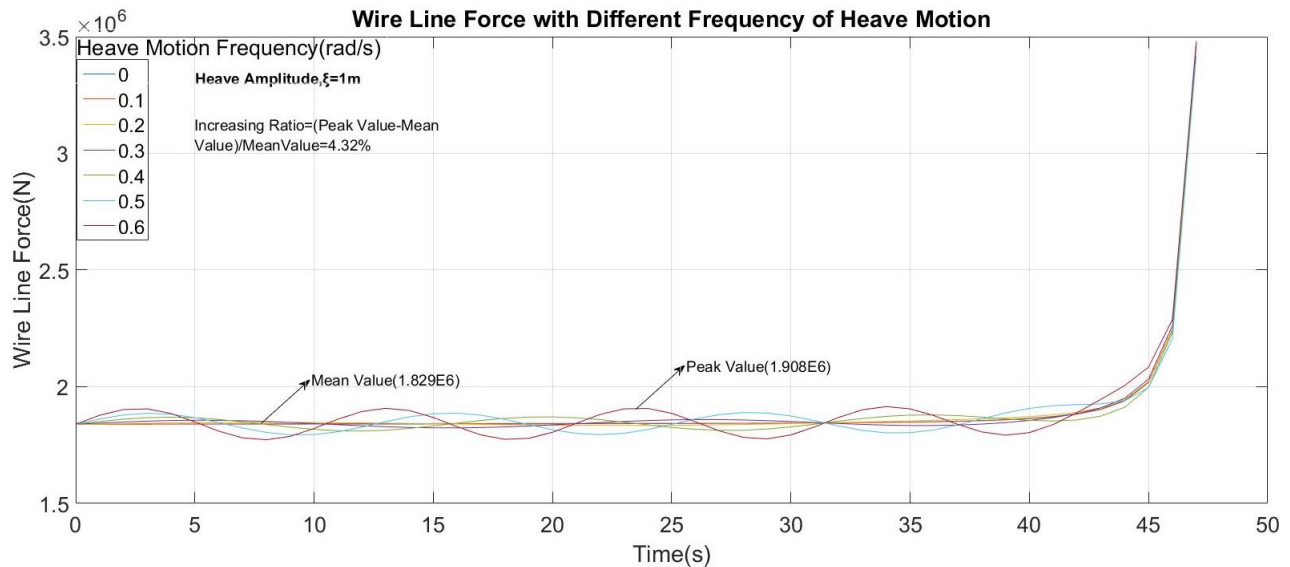


Figure 3.26: Time Series of Wire Line Force with Different Heave Frequency

### 3.4 Regular Roll Motion of Crane Vessel

Roll motion of crane vessel would be discussed in this part as an example of rotation. Different from heave motion discussed above, roll motion provide extra second order acceleration. Directions of convected and second order accelerations due to roll motion kept changing in whole process, which leaded horizontal force in support point. In other words, much larger effects to concerned forces due to roll motion than heave. In the following part, mechanism analysis of roll motion would be given. Weight of each term in concerned forces due to different kinds of

accelerations would also be shown. Effects from different amplitudes and frequencies of vessel roll motion would be discussed at the end of this part.

### 3.4.1 Mechanism Analysis of Coupled Motion

In this part, regular roll assumption was used to simulate vessel motion. Then angular velocity and acceleration could be got from differentiation of motion. Just as equations 3.18 shown. Figure 3.27 shows the relation between vessel roll motion and upending process. 'r' in such figure shows the distance between any point on monopile to COG of vessel, which could be got from equation 3.19, 'x' and 'y' in such equation means coordinate of any point in monopile. When roll motion of crane vessel was considered, convected system could be seen as a rotation one. Moreover, absolute acceleration would be got from three different parts shown as equation 3.20. First two terms show convected acceleration. Third term shows the relative one and last term shows the second order one. It was easily seen discussed three accelerations leaded extra forces in horizontal and vertical directions compared with jack-up vessel assumption. Equations 3.21 shown result of convected acceleration. Extra forces on monopile during whole process could be assumed as figure 3.28 shown.

$$\begin{aligned} y &= \xi \sin(\omega_0 t) \\ \omega_1 &= \omega_0 \dot{\xi} \cos(\omega_0 t) \\ \varepsilon_1 &= -\omega_0^2 \xi \sin(\omega_0 t) \end{aligned} \quad (3.18)$$

$$r = \sqrt{\left(x - \frac{B}{2}\right)^2 + (y + 1)^2} \quad (3.19)$$

$$a_a = \varepsilon_1 \times r + \omega_1 \times (\omega_1 \times r) + a_r + 2\omega_1 \times v_r \quad (3.20)$$

$$\begin{aligned} a_e^{T_0} &= \varepsilon_1 r \\ a_e^{n_0} &= \omega_1^2 r \\ \begin{cases} a_e^T = a_e^{T_0} \cos(\beta) - a_e^{n_0} \sin(\beta) \\ a_e^n = a_e^{T_0} \sin(\beta) + a_e^{n_0} \cos(\beta) \end{cases} \end{aligned} \quad (3.21)$$

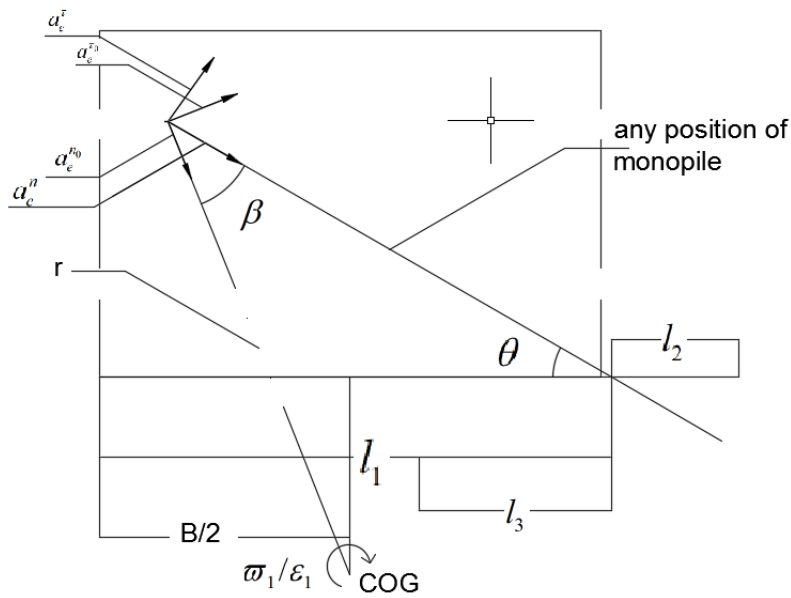


Figure 3.27: Mechanism Analysis of Relation Between Roll and Upending Process

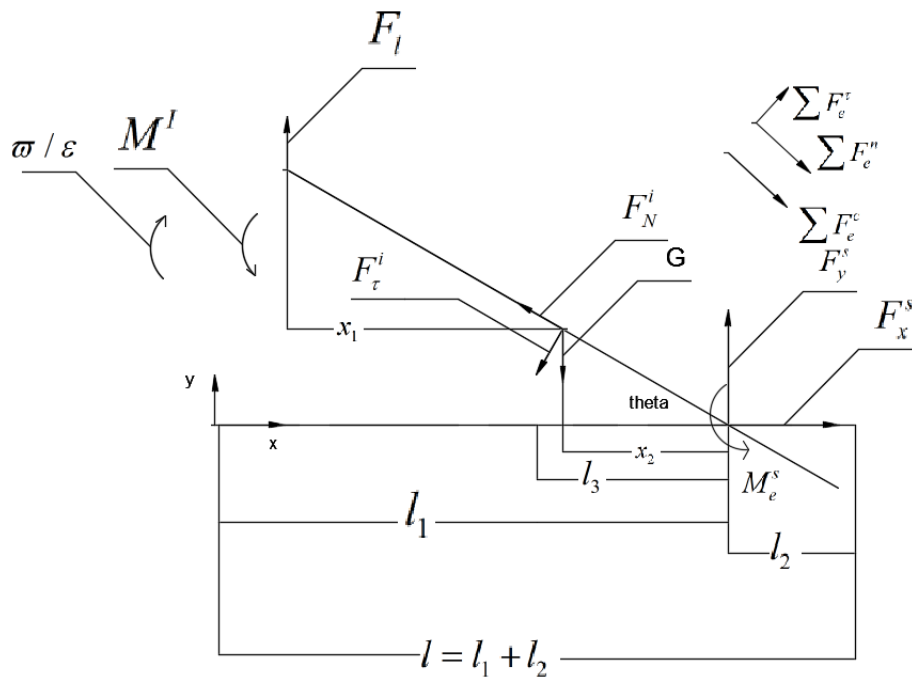


Figure 3.28: Extra Forces under Regular Roll Assumption

Distribution mass assumption was used in this part, which means the inertia forces due to roll motion were different in each position of monopile. From this discussion, convected and second order forces could be got from integration along length of monopile just as equations 3.22 and 3.23 shown. Forces due to relative motion was the same as jack-up vessel assumption as discussed former. Then equilibrium equations of sum forces in 'x', 'y' directions and sum of moments of support point were used to calculate time series of lift wire, horizontal and vertical support forces. Equations 3.24 show the talked equilibrium.

$$\begin{aligned}
 F_e^r &= \int_l a_e^r \frac{m}{l} dl = \int_{l_1 - l_1 \tan(\theta)}^{l_1 + l_3 \tan(\theta)} a_e^r \frac{m}{l \cos(\theta)} dx \\
 F_e^n &= \int_l a_e^n \frac{m}{l} dl = \int_{l_1 - l_1 \tan(\theta)}^{l_1 + l_3 \tan(\theta)} a_e^n \frac{m}{l \cos(\theta)} dx \\
 M_e^{\text{sup}} &= \int_{l_1 - l_1 \tan(\theta)}^{l_1 + l_3 \tan(\theta)} a_e^r \frac{m}{l \cos(\theta)} \frac{48-x}{\cos(\theta)} dx
 \end{aligned} \tag{3.22}$$

$$\begin{aligned}
 a_c &= 2\omega v_r \\
 F_c &= \int_{l_1 - l_1 \tan(\theta)}^{l_1 + l_3 \tan(\theta)} a_c \frac{m}{l \cos(\theta)} dx
 \end{aligned} \tag{3.23}$$

$$\left\{ \begin{array}{l}
 \sum M_{\text{sup}} = 0 \rightarrow F_{\text{line}} l \cos(\theta) + M_e^s = M_I + mgl_3 \cos(\theta) + F_I^r l_3 \\
 \sum F_y = 0 \rightarrow F_{\text{line}} + F_s^y + F_e^r \cos(\theta) + F_I^n \sin(\theta) = F_e^n \sin(\theta) + mg + F_I^r \cos(\theta) + F_c \sin(\theta) \\
 \sum F_x = 0 \rightarrow F_s^x = F_I^n \cos(\theta) + F_I^r \sin(\theta) - F_e^r \sin(\theta) - F_e^n \cos(\theta) - F_c \cos(\theta)
 \end{array} \right. \tag{3.24}$$

### 3.4.2 Weight of Different Part

From above discussion, each forces consisted of three parts. Weight of each part would be discussed in the following. Figure 3.29 shows the weight of each part in horizontal support force. It was easily seen that convected term take the main part, which means crane vessel roll motion was the source of horizontal force. This phenomenon could also be shown in equations 3.24. Different from horizontal support force, weight of different parts in vertical support force were shown in figure 3.30. It was easily seen, that relative term was the most important part in vertical support force, which means that accelerations due to vessel roll motion was small compared

with gravity and the ones due to upending process. Lift wire force was also mainly affected by relative term, which would be shown in appendix.

Based on above discussion, all three concerned forces were affected by vessel roll motion in different level. From such phenomenon control maximum value of each forces should base on different methods. For example, maximum value of lift wire force was decided by upending process but horizontal support force relied on rotation motion of crane vessel and upending process. When different parts of system considered as critical, various control system would be introduced.

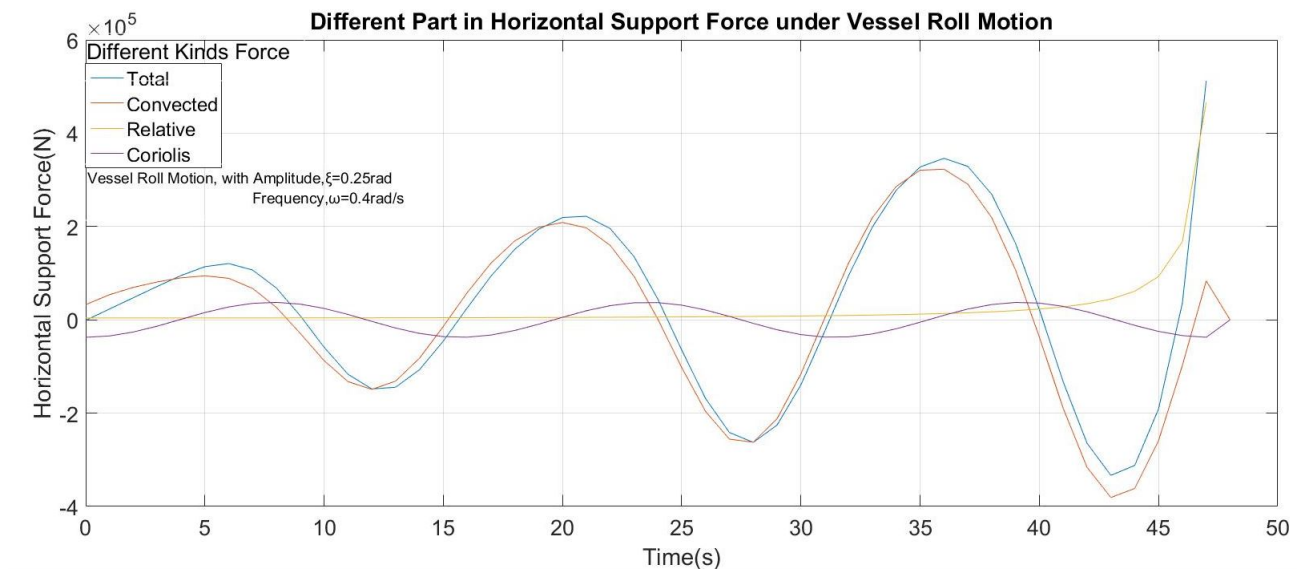


Figure 3.29: Different Parts in Horizontal Support Force due to Roll Motion

### 3.4.3 Effects Based on Roll Frequency

As discussed above, roll motion of crane vessel affected three concerned forces in different levels. Regular roll motion was assumed as  $(y = \xi \sin(\omega_0 t))$ , frequency ( $\omega_0$ ) and amplitude ( $\xi$ ) could decide the such roll motion. In order to clear effects due to roll motion, different frequencies would be discussed firstly.

As shown before, horizontal support force was seriously affected by convected motion. But lift wire and vertical support forces mainly depend on upending process. In this part, horizontal support and lift wire forces were taken as examples. Figure 3.31 shows time series of horizontal support force with different roll frequencies. It was clearly seen, that large value of frequency

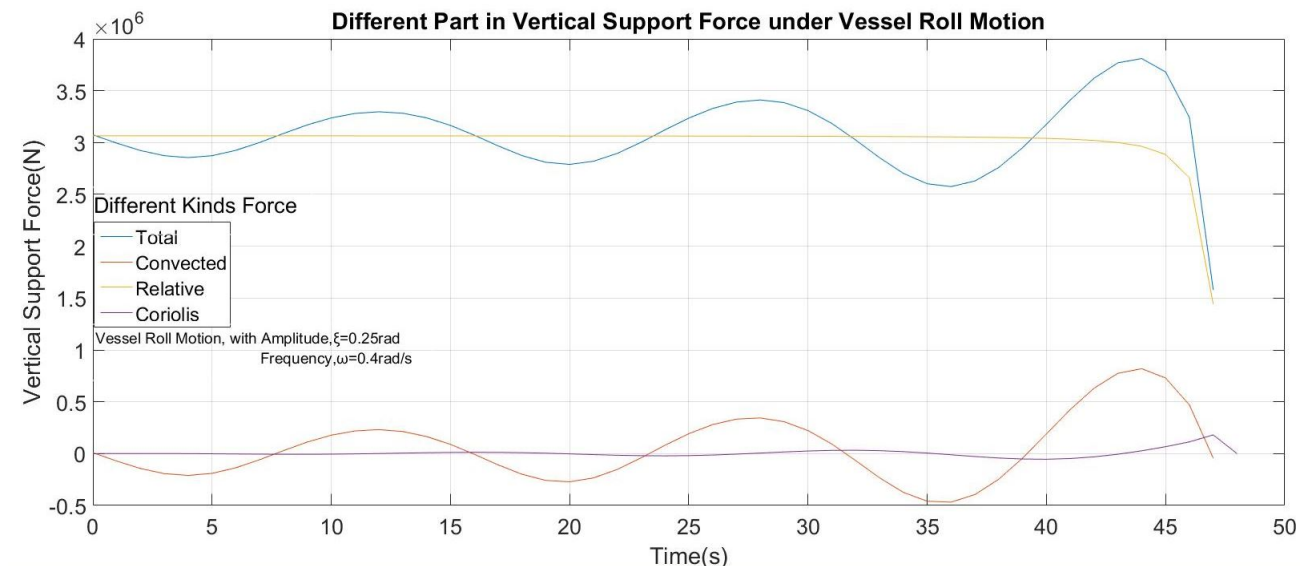


Figure 3.30: Different Parts in Vertical Support Force due to Roll Motion

lead larger maximum value and short period. And the effect due to roll motion was amplified as progressing of upending process. In other words, peak value in time the series became larger and larger. However, different phenomena could be got for lift wire force. Figure 3.32 shows time series of lift wire force with different roll frequencies. Similar as horizontal support force, peak value of each series increasing a little with large frequency. And period decreased a lot for large frequency. But the maximum value of each series would appear at the end of upending process and were almost no affected by different roll frequencies. Reason of that was the main part of lift wire force coming from relative motion rather than vessel motion. Rule of vertical support force was almost same as lift wire one. Result figure would be shown in appendix.

### 3.4.4 Effects Based on Roll Amplitude

As discussed in former section, frequency and amplitude decided regular roll motion of crane vessel. Effects due to roll motion amplitude would be discussed in this part. Similar as former discussion, horizontal and lift wire forces were taken as examples.

Figure 3.33 shows the result of time series of horizontal support force with different roll amplitudes. Each peak value was much larger than the value based on jack-up vessel assumption. Larger value of roll amplitude leded larger value of horizontal support force. Due to constant roll frequency used in this part, periods of every series were the same. And value of such force

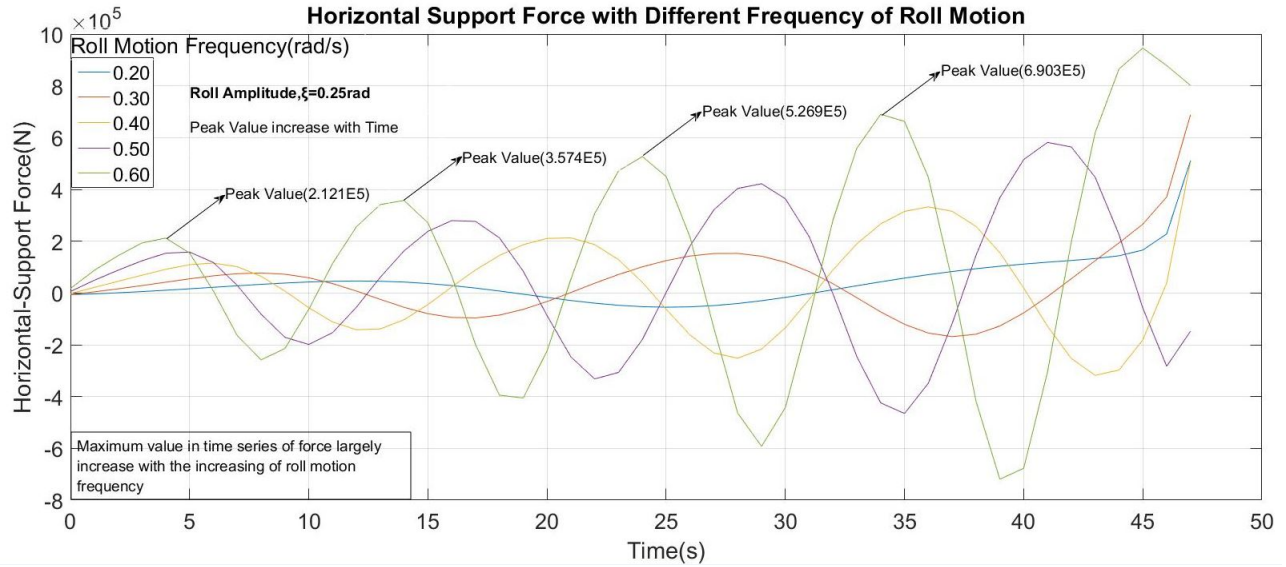


Figure 3.31: Time Series of Horizontal Support Force With Different Roll Frequency

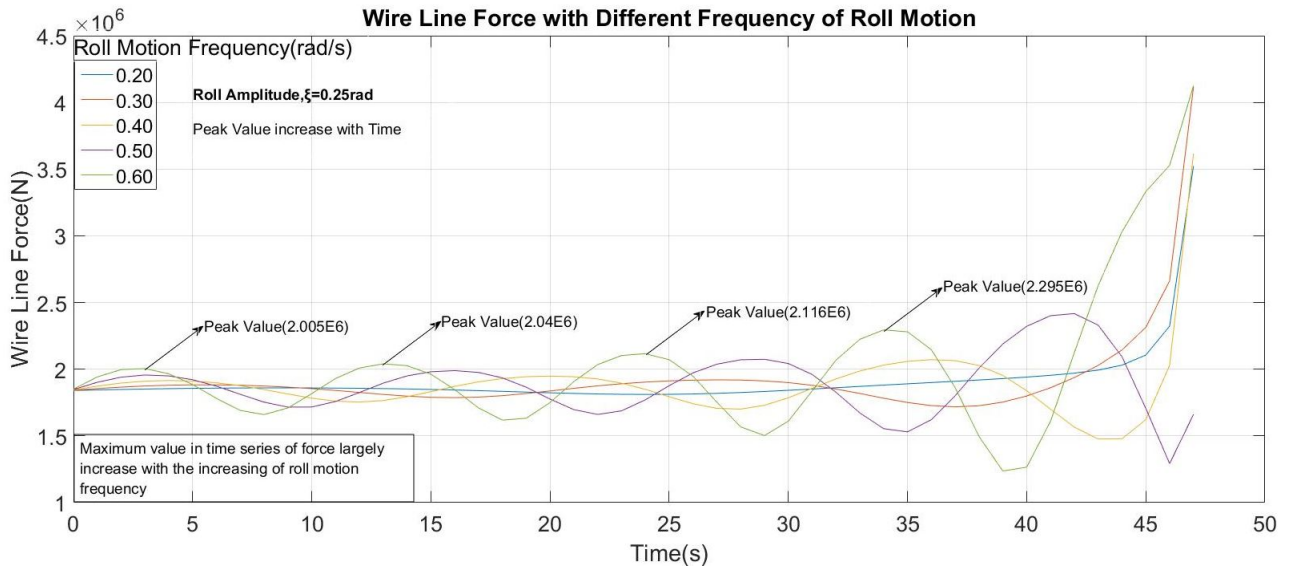


Figure 3.32: Time Series of Wire Line Force With Different Roll Frequency



went to very large at end of upending process. Increment due to roll motion was obvious from the figure. On the contrary, lift wire force had different rule. Figure 3.34 shows time series of lift wire forces with different roll amplitudes. There was an increment due to roll motion and the level of it was more obvious with larger roll amplitude. The increment rate was considerable small compared with horizontal support force. Maximum value of lift wire force appeared at the end of process which means effects due to roll amplitude was not as serious as upending itself.

Based on above discussion, roll motion control could limit maximum value of horizontal support force. But when the lift wire or vertical support forces became the critical part. Roll motion control cannot be seen as useful. Even if roll motion had little effects to lift wire and vertical support forces, anti-roll equipment should be used on the crane vessel. Because horizontal support force mainly relied on friction between monopile and support shelf on crane vessel. With progressing of upending process, pressure between monopile and support shelf would be decreased sharply. For this reason, limited value of horizontal support force would be provided and anti-roll equipment should be used.

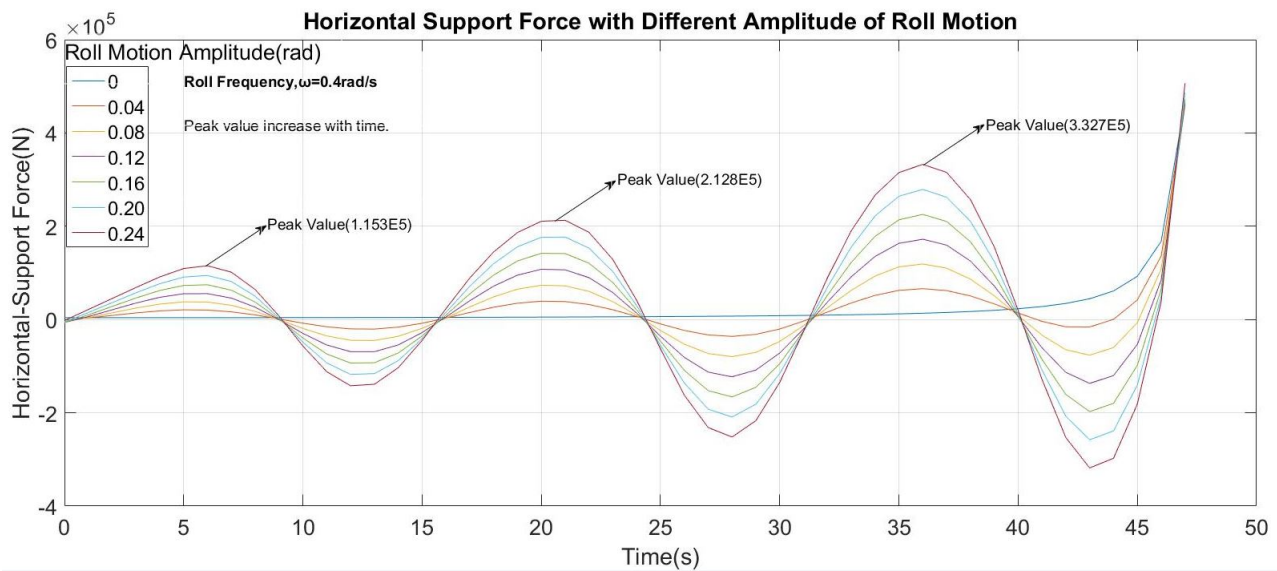


Figure 3.33: Time Series of Horizontal Support Force With Different Roll Amplitude

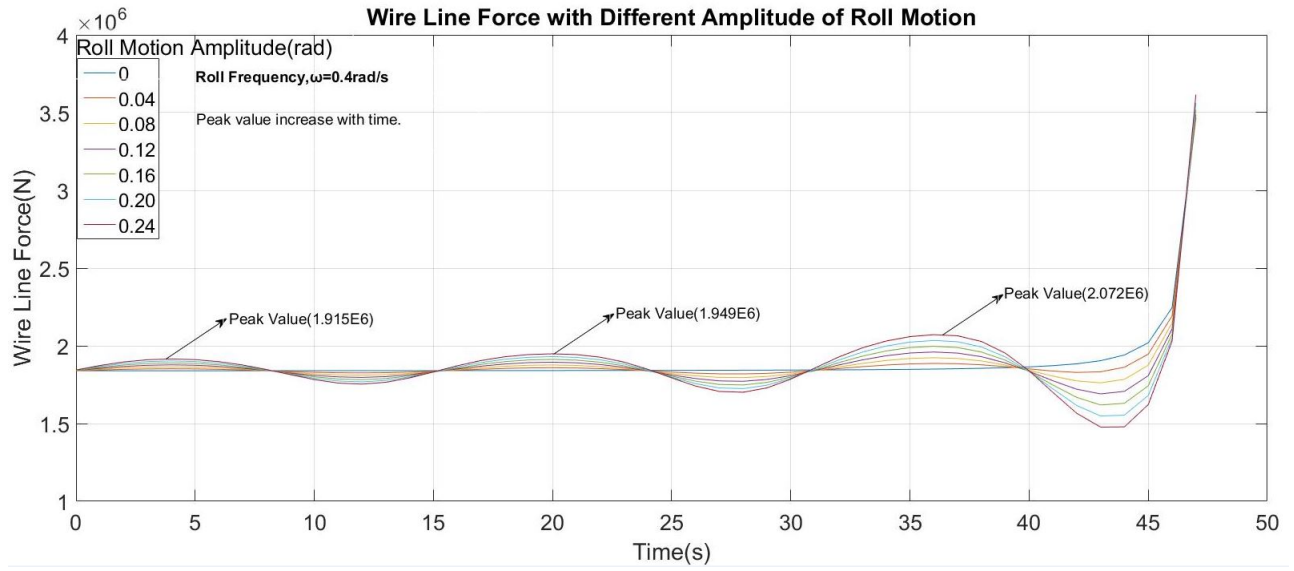


Figure 3.34: Time Series of Wire Line Force With Different Roll Amplitude

# Chapter 4

## Numerical Model and Analysis

After clearly theoretical analysis, numerical method was used to check the accuracy of former result and take complex environmental loads into account. In order to do time domain analysis, hydrodynamical characters of crane vessel was got from senior student as known information without checking. Such characters based on panel model analysis in HydroD, which means average draft assumption would be used in the following simulation. SIMA was chosen as numerical analysis tool in this thesis to do time domain simulation.

### 4.1 Model Discription

Whole numerical model consisted of three parts which were vessel, crane and monopile. All of them would be described in detail with advantages and disadvantages.

#### 4.1.1 Vessel

Crane vessel model used here given by senior student with all known parameters such as mass, damping and hydrostatic stiffness. Figure 4.1 shows the given information. It was clearly seen, there were eight mooring lines with the crane vessel which used to decrease the second order motion in whole process. All mass of the concerned vessel assumed at a very small box compared with geometry of it, which was the red one in figure. Detail geometry of crane vessel shown in table 4.1. The vessel was a monohull heavy lift vessel with 52,000 tons as displacement. Mooring line position system allowed the operations of the vessel in shallow water and in

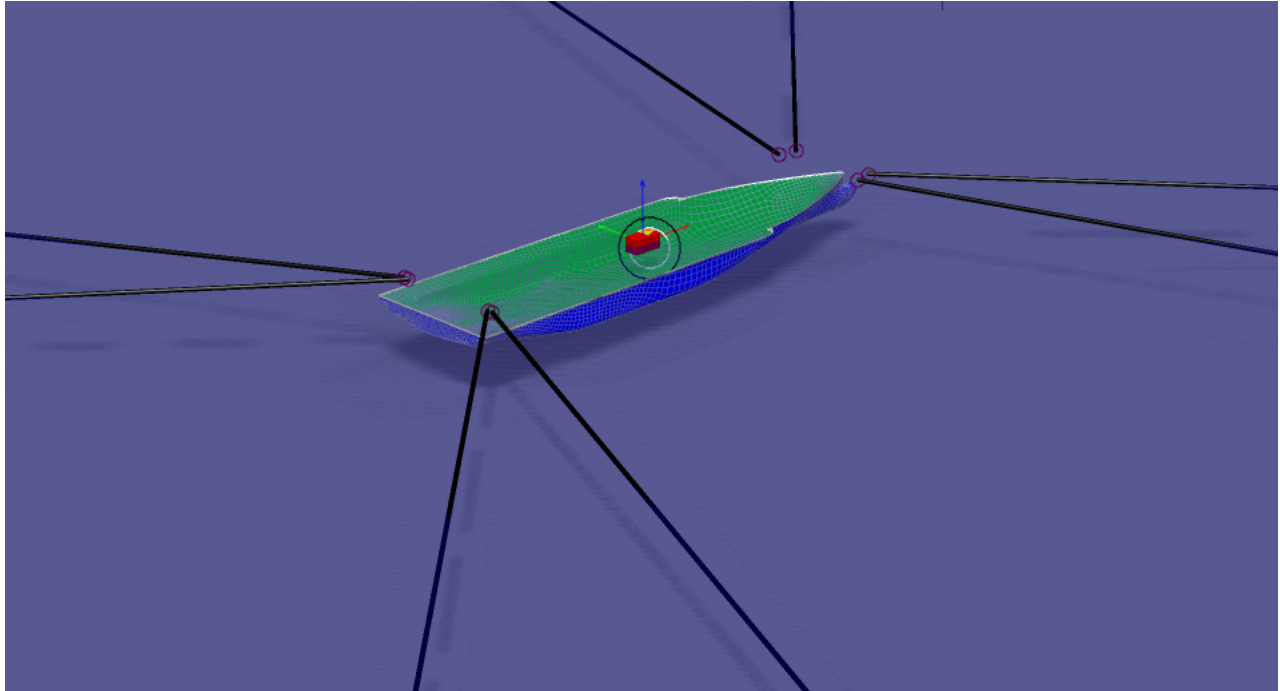


Figure 4.1: Crane Vessel Model Got From Senior Student

Table 4.1: Main parameters of the crane vessel

Vessel		
Length Overall	[m]	183
Breadth	[m]	47
Operational Draft	[m]	12
Displacement	[tons]	52000

close proximity to other structures. The water depth for the concerned operation was 25 meters. Mooring system could be considered as springs in this system to keep position of crane vessel.

### 4.1.2 Crane

In order to give a prescribed motion to the crane. 'Articulated structure' which was suitable for crane simulation was used in SIMA. Figure 4.2 shows the theory of it which consist of one master body and one rigid body. The rigid member of the structure was connected in a master-slave fashion. In the present version of SIMA a time history of prescribed motion can be specified for each member of such a mechanism. In this case, crane was considered as three rigid members which could rotate along vertical and horizontal axis. Figure 4.3 shows the outlook of whole model. Crane bottom fixed on the deck of vessel with 79.156m from origin of local coordinate

system of vessel. It could rotate along vertical axis to keep the tops of inclined column and monopile in the same plane. Vertical column had the same motion as crane bottom, which used to make the model similar as the crane in practical. Moreover, inclined column move with the vertical column in horizontal plane and rotate along y-axis in vertical plane. Both the motions of bottom and inclined column were used to keep the lift wire vertical. However, rotation velocity of such motions cannot be defined as a function of time in present version of SIMA. It means that the lift wire cannot be always vertical. This limitation introduced difference between numerical and theoretical result, which would be shown in the next chapter. Mass of crane was considered as a part of vessel which is not on the crane itself. This assumption made the crane vessel have no motion in static analysis which was the same as theoretical analysis.

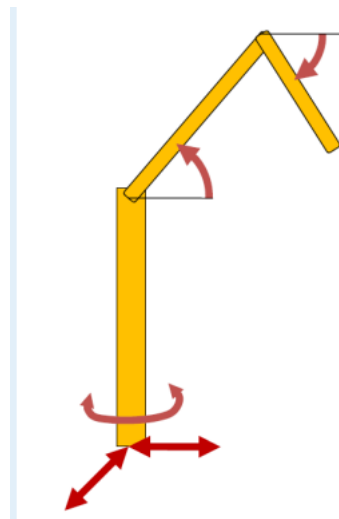


Figure 4.2: Model for Crane

### 4.1.3 Monopile

Monopile was described as a cylinder in y-axis in the SIMO model. Main parameters of it as shown in table 4.2. Mass of it was assumed evenly distributed along the length, which is similar as reality and easy to compare with theoretical result. Empty core structure of such monopile was neglected due to no water move in it during whole process.

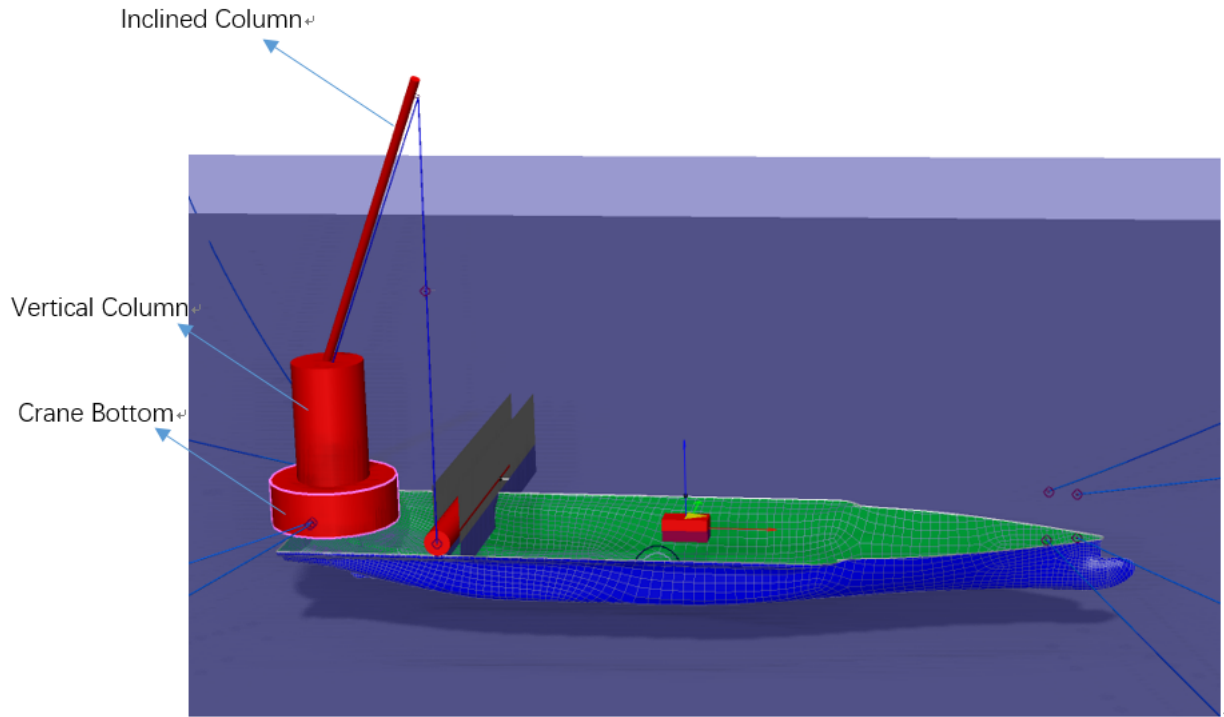


Figure 4.3: Whole Model Outlook

Table 4.2: Main Parameters of the Monopile

Monopile		
Total Mass	[tons]	500
Length	[m]	60
Outer Diameter	[m]	5.7
Thickness	[m]	0.06

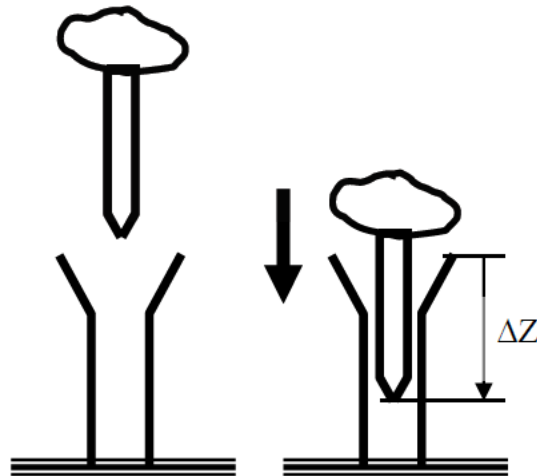


Figure 4.4: Theory of Docking Cone

#### 4.1.4 Connection between Monopile and Vessel

Connection between monopile and vessel was assumed as a hinge in this case from beginning. However, there was no such type of connection in present version of SIMA. Two docking cones and point fenders were taken to replace the hinge. Figure 4.4 shows the theoretical meaning of docking cone, which limit the motion of pin in perpendicular direction to the cone. And the motion along cone was allowed in docking cone connection. Figure 4.5 shows the theory of point fender, which provided restoring force when point and fender plane had certain distance. Two docking cones and point fenders were arranged as the figure 4.6 shown. Two docking cones limit the vertical motion of monopile. Moreover the motion along left-right direction was also limited. Two point fenders limited front-back motion of monopile. With these four connections, monopile could only rotate along horizontal axis, which is similar as hinge connection. From meaning of hinge connection, five degrees of freedom were fixed with only one left. In order to meet this requirement, stiffness of docking cone and point fender should be set as infinite. But this cannot be done in SIMA due to unacceptable acceleration. For this reason, stiffness of talked connections were set large as possible but not infinite. However, this replacement was not an ideal choice which may lead some difference between numerical and theoretical result. This would be discussed in the following chapter.

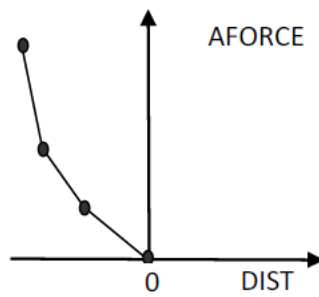
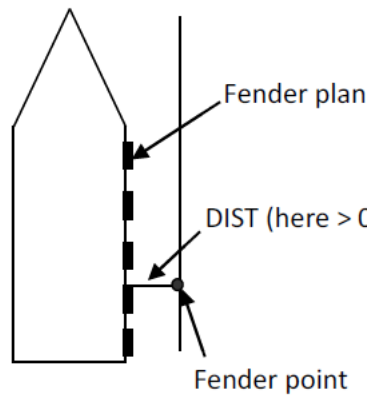


Figure 4.5: Theory of Point Fender

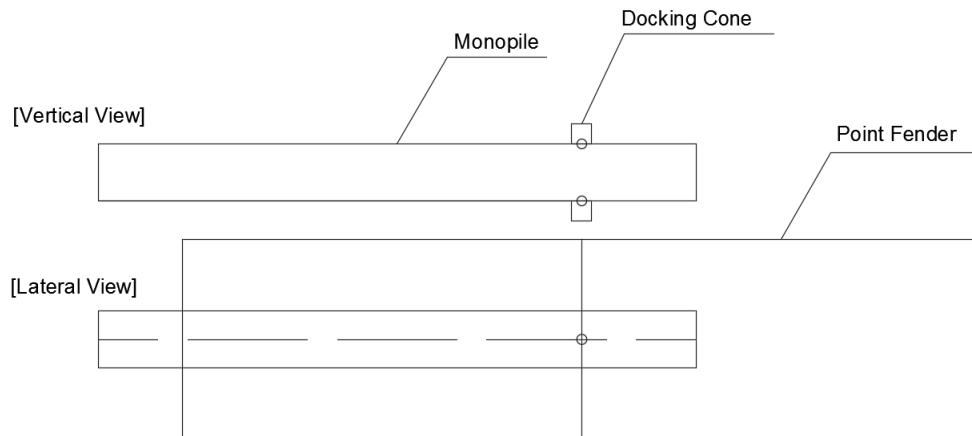


Figure 4.6: Arrangement of Docking Cone and Point Fender



## 4.2 Motion Setting of Crane Bottom and Inclination Column

Velocities of crane and winch were set with suitable values to make the lift wire keep vertical. From figure 4.3, bottom and inclined part would have different motions respectively. Constant upend velocity was assumed in this case, figure 4.7 shows the theory of it. Whole process could be divided into two parts. Firstly, inclined column at the right side of bottom and then at the left side. It was clearly seen that the right end of monopile move from zero to 42.14m in vertical direction during first part. And the whole lift distance would be 49 meters in the concerned process. By that with constant lifting speed, first part experienced much longer period than second. Equation 4.1 shows the angular velocity of crane bottom and inclined column, where  $\omega_1^f$ ,  $\omega_1^l$  and  $\omega_2$  in this equation means bottom velocity in first part, second part and angular speed of inclined column. When the lifting velocity assumed constant as 0.2 m/s during whole process, first part would be 200s while second part 34s. However, the moving angle of bottom in first part was 45 degree and 46.2 degree in second part. This means the bottom would rotate much faster in second part. As told former, velocity cannot set as a function of time in present version of SIMA, this means the velocity could only be set as constant in each time step. In the uniform time step assumption, cumulative errors in second part was more significant, which lead unreasonable result of simulation. There was a clear vibration of horizontal support force at end of upending process in numerical result shown in figure 4.8.

Based on such discussion, different time steps would be assumed in following discussion. In detail, time step in first part was 1s and 0.1s in second part. In order to keep the lift wire vertical in whole process, winch velocity would also be modified in the simulation rather than constant assumption. This would be discussed in latter part.

$$\begin{aligned}
 \omega_1^f &= \frac{1}{1+(1-\frac{\Delta x}{l_1-l_2})^2} * \frac{-1}{24} * v^2 t [l_1^2 - (vt)^2]^{-0.5} \\
 \omega_1^l &= \frac{1}{1+(1-\frac{\Delta x}{l_1-l_2})^2} * \frac{1}{24} * \left[ l_1^2 - (\sqrt{l_1^2 - l_2^2} + vt) \right]^{-0.5} * \frac{1}{2} * (2v\sqrt{l_1^2 - l_2^2} + 2v^2 t) \\
 \omega_2 &= \left[ \frac{1}{\sqrt{1-\frac{1}{8\cos^2\theta_{(1/2)}}}} * \frac{1}{2\sqrt{2}} * (\cos\theta_{(1/2)})^{-2} * \sin\theta_{(1/2)} \right] * \omega_1
 \end{aligned} \tag{4.1}$$

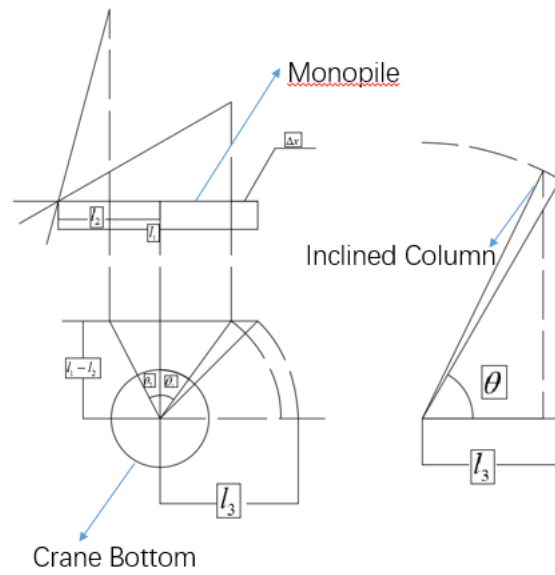


Figure 4.7: Theory of Two Part Motion

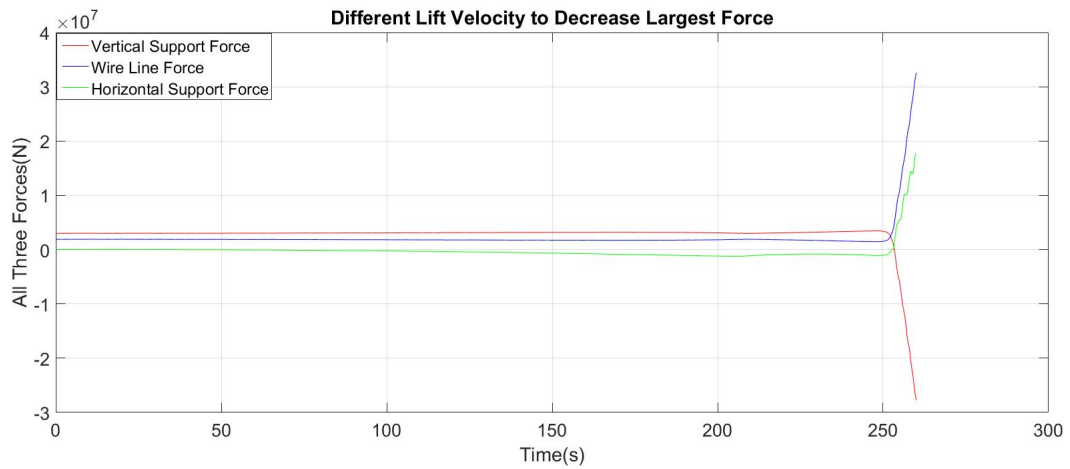


Figure 4.8: Numerical Result of Constant Lift Velocity

## 4.3 Decrease Maximum Value of Concerned Forces in Numerical Simulation

Both numerical and theoretical result in this case show similar result, all concerned forces would be infinite at the end of upend process. Attempts to decrease such maximum value would be shown in this part. Effects from environmental load factors such as 'significant wave height ( $H_s$ )' and 'peak period ( $T_p$ )' would be discussed. Moreover, factors affected the upend motion would also be talked.

### 4.3.1 Environmental Load Factor

Two parameters ( $H_s, T_p$ ) 'JONSWAP' spectrum was chosen to simulate irregular wave in this part. Such two parameters were used to describe the wave energy distribution with different wave frequencies ( $\omega$  rad/s). In this part, significant wave height would be discussed firstly. Figure 4.9 shows the result of lift wire force with different  $H_s$ . when the  $T_p$  was assumed constant as 12s. It was easily seen, that the effect from different values of  $H_s$  was very small. Increment due to  $H_s$  was not at the same level as increasing at the end of process which due to upending motion. When concerned horizontal support force just as figure 4.10 shown, irregular wave introduced significant vibration of horizontal support force during upend process. However, the effects due to  $H_s$  was also limited. Vertical support force was affected by  $H_s$  similar as lift wire force, irregular wave had almost no effect to the time series of them.

Following discussion of  $H_s$ , effects due to  $T_p$  would be concerned here. Figure 4.11 shows the result of lift wire force with different  $T_p$  when  $H_s$  assumed as constant (2.5m). Effect due to irregular wave was larger than the result of different  $H_s$ . This means  $T_p$  was more important than  $H_s$  for lift wire force. It was clearly seen that turning part of the figure was affected seriously. From discussion in 4.2, this time of series correspond to the end of first part. Before turning part, numerical simulation is similar as reality. But large difference appeared from this time. Similar as effect due to  $H_s$ ,  $T_p$  gave a little effects to lift wire force but not as important as upending motion influence. Figure 4.12 show the result of horizontal support force which was heavily influenced by irregular wave. Peak value of each time series increased with the larger  $T_p$ . But the most significant effect was also due to upend motion. Vertical support force had similar

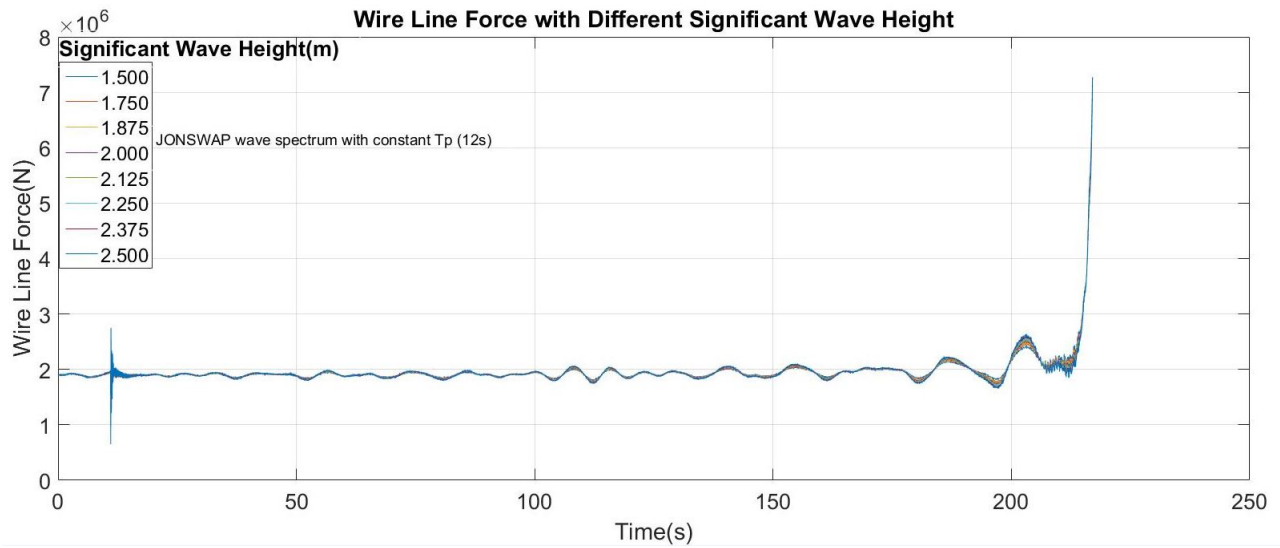


Figure 4.9: Wire Line Force with Different Hs

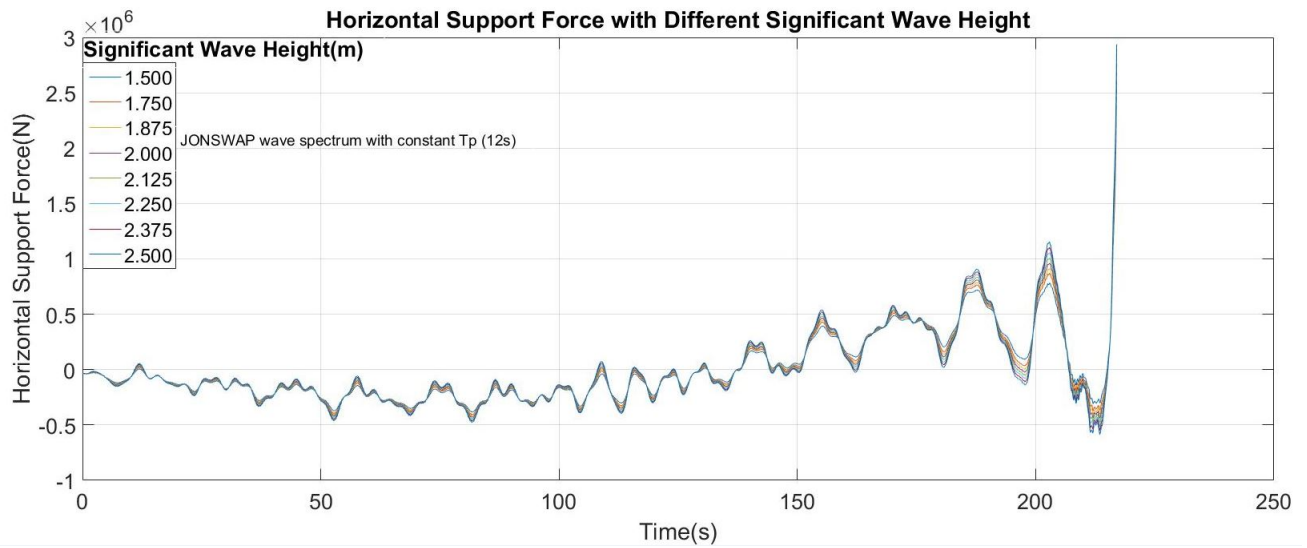


Figure 4.10: Horizontal Support Force with Different Hs

trend as lift wire force, which was not shown here.

Based on above discussion, environmental load factors only had limited effects to all three forces. In order to meet the requirement of maximum force in lift wire and support, upending motion could be modified.

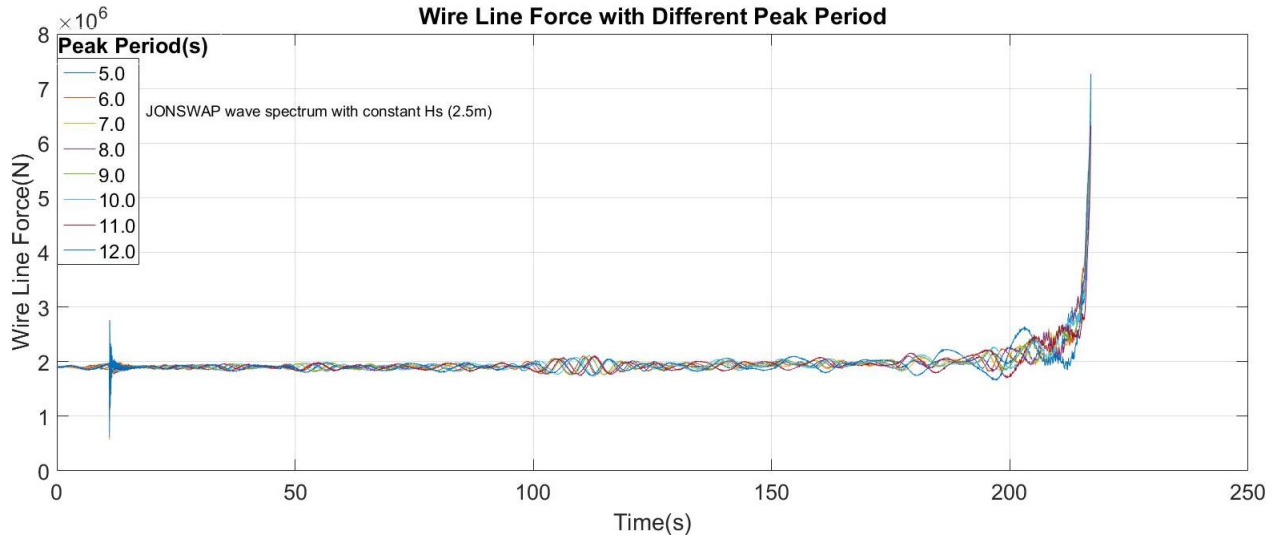


Figure 4.11: Wire Line Force with Different  $T_p$

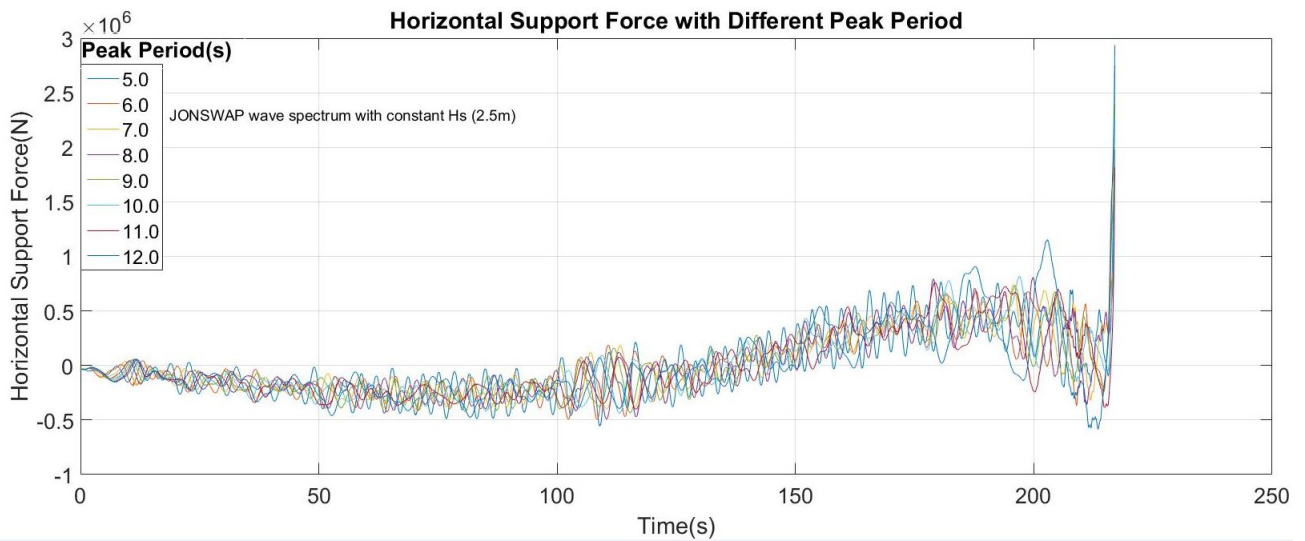


Figure 4.12: Horizontal Support Force with Different  $T_p$

### 4.3.2 Upend Motion

After analysis of environmental load factor, maximum value of wire line force and support force cannot be decreased with the changing of  $H_s$  or  $T_p$ . Above discussion show that the upend motion would decide the maximum value of result. Time step of crane bottom rotation and lift velocity would be discussed in this part.

Based on the discussion in 3.2, concerned upend process could be divided into two parts due to geometrical relation between top of inclined column and the monopile. Effects of environmental load factor was considered based on constant lifting velocity assumption. Such assumption would lead different accuracy level to result of first and second part. Lifting velocity of the second part was decreased to 0.01m/s in this part. From such changing, all maximum value of concerned three forces were in the safety range of wire line and support point(5000tons). From figure 4.13, maximum wire line force was around  $4.5E06$ . For the reason of large vessel motion, time series of concerned forces were not same as theoretical result especially in second part. Suddenly changing of lifting velocity lead a serious vibration of concerned forces at the beginning of second part. And the vessel motion due to upending process was in a considerable level. Such motion was not considered in former theoretical analysis. Accuracy of numerical and theoretical analysis would be shown in latter chapter.

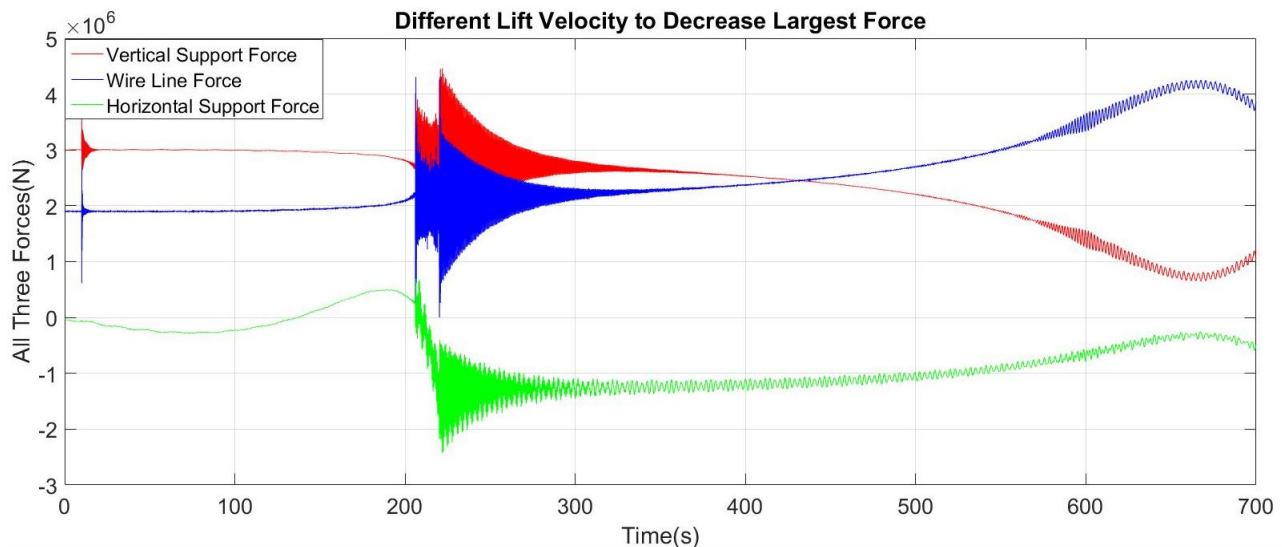


Figure 4.13: Result after Modification

## 4.4 Effects From Different State

In order to clear effects due to different load conditions, various sea states were selected in this numerical simulation. Different couples of significant wave heights( $H_s$ ) and peak periods( $T_p$ ) were chosen to represent various load conditions based on stochastic theory. Because limitation of computer disk space and allowable CPU time, 64 couples of  $H_s$  and  $T_p$  with 20 realizations of each were used in this simulation.

### 4.4.1 Location of Selected Sea and Its Representative Value

Concerned wind turbine planned to build in Norwegian North Sea shown as area 15 in figure 4.14. Based on JONSWAP Spectrum which suitable for Norwegian North Sea,  $H_s$  and  $T_p$  were seen as only parameters to describe different sea states. From calculations give by Li et al. (2015), typical values of  $H_s$  and  $T_p$  were corresponding to 8.66m and 6.93s. So concerned ranges of  $H_s$  and  $T_p$  were set as (1-5.5m) and (1-12s). 20 random values within range of (0,360) were used as phase angles in each realization. 8\*8\*20 simulations were done in this part. In this lift-off operation, all three concerned forces keep changing due to progressing. And maximum values of them mainly depended on process. For this reason, mean values and stand deviations of concerned forces time series were chosen as representative. However, these mean values and stand deviations should correspond to the time period before obvious changing due to upend process. In this case, part one which defined in section 4.2 was chosen as concerned period.

### 4.4.2 Result of Different Sea States Effect

Statistic result of vertical support and lift wire forces were shown in following figures. Mean values of vertical support force corresponding to each sea state were shown in figure 4.15. It was easily seen that the maximum mean values appeared at up-right position which means large  $H_s$  and  $T_p$  condition. Equation 4.15 which based on 'Dissipation Equation', shows the relation between particle velocity and wave period. So large period induced large velocity and then large wave force. This might be the reason of 'red area' appeared in up-right zone of figure 4.15. From color-bar on right margin of the figure, difference of mean values was very limited. This phenomenon also shows environmental load has slightly effect to the process same as theoretical





Figure 4.14: Location of 18 Potential European Offshore Sites

result in chapter3.

Following figures 4.16 and 4.17 show the result of stand deviation in the same weather conditions as former one. But results of them were different from former. Figure 4.16 shows the stand deviation of vertical support force. Though there was obvious 'red area' in the up-right position, down-right part also showed a little higher result. This phenomenon was similar in figure 4.17, which showed stand deviation of lift wire force. Based on linear wave assumption, wave length could also be got from equation 4.2. However, breaking limit of ratio between wave height and wave length is 10 percent which was smaller than 0.2 of this condition. So most wave have already broken in this condition. For this reason, linear wave theory could not be available in this part and unreliable result was introduced. Main trend shown in these two figures that stand deviation increased from down-left to up-right part was almost correct.

Different sea states led some difference in concerned forces which mainly depended on rotation motion of vessel. Similar as theoretical result, environmental loads did not lead obvious changing. But high level of sea state provided serious vibration in concerned forces which also challenge safety of lift-off operation.



$$v = \frac{\lambda}{T} = \frac{gT}{2\pi^2} \quad (4.2)$$

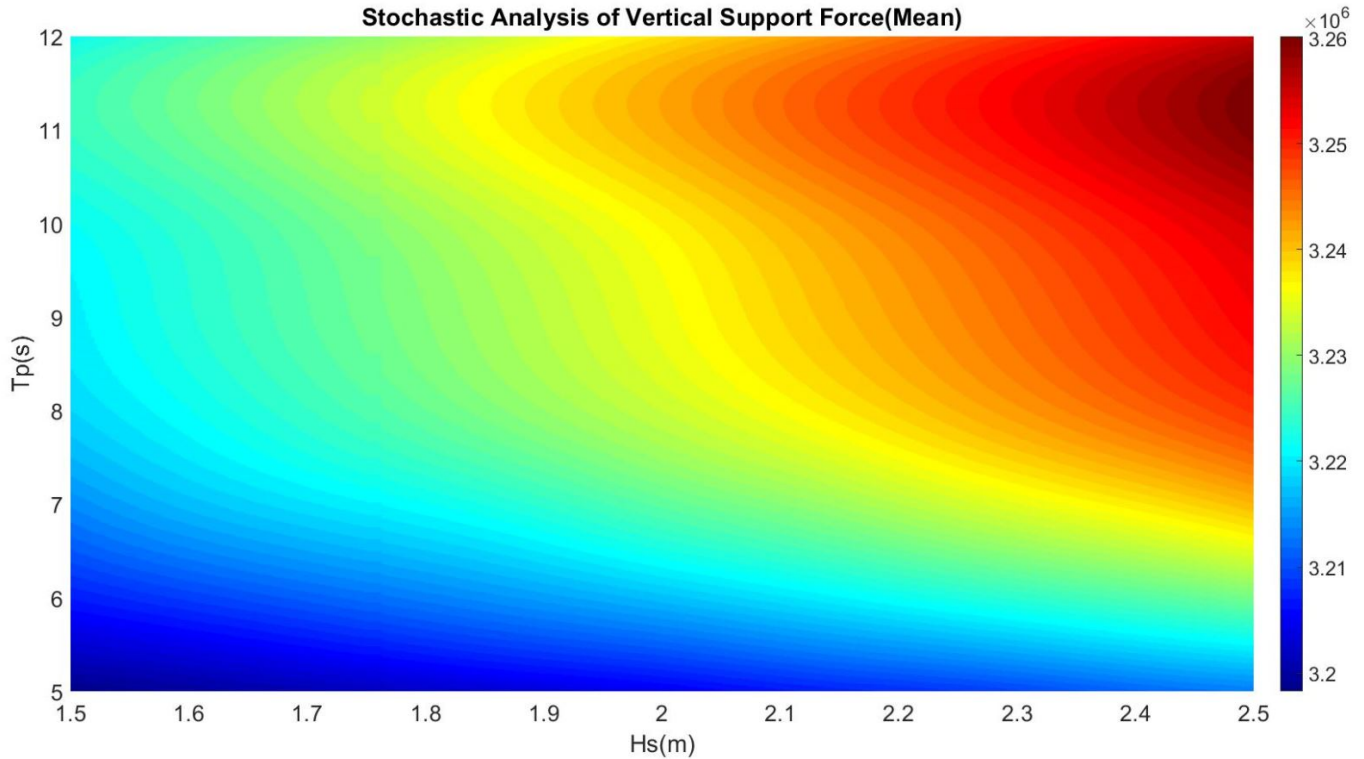


Figure 4.15: Result of Mean Vertical Support Force in Different Sea States

## 4.5 Two Vessels Scenario

In order to consider the scenario with one crane vessel and one transport barge, new panel model was built in HydroD. Hydrodynamic effects due to different distances between barge and crane vessel would be considered in this part. Therefore barge model cannot build directly in SIMA for the reason of interaction between crane vessel and barge.

### 4.5.1 Panel Model in HydroD

A FEM model was firstly built in GeniE with 91.44m long, 27.432m wide. And the displacement was assumed as 9011 tons. Then it was transported into HydroD and multi-body model was chosen to consider interaction. Panel model in HydroD was shown in figure 4.18. Panel model

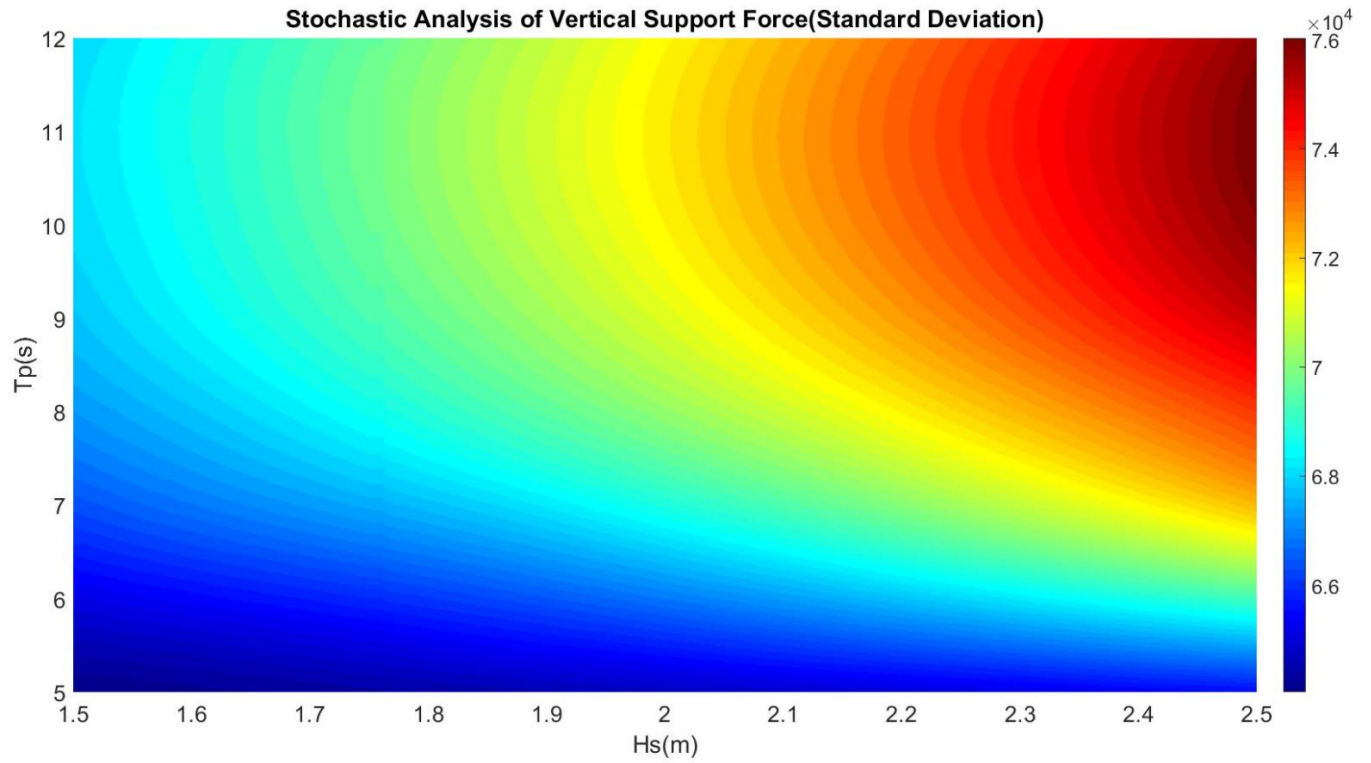


Figure 4.16: Result of Vertical Support Force Standard Deviation in Different Sea States

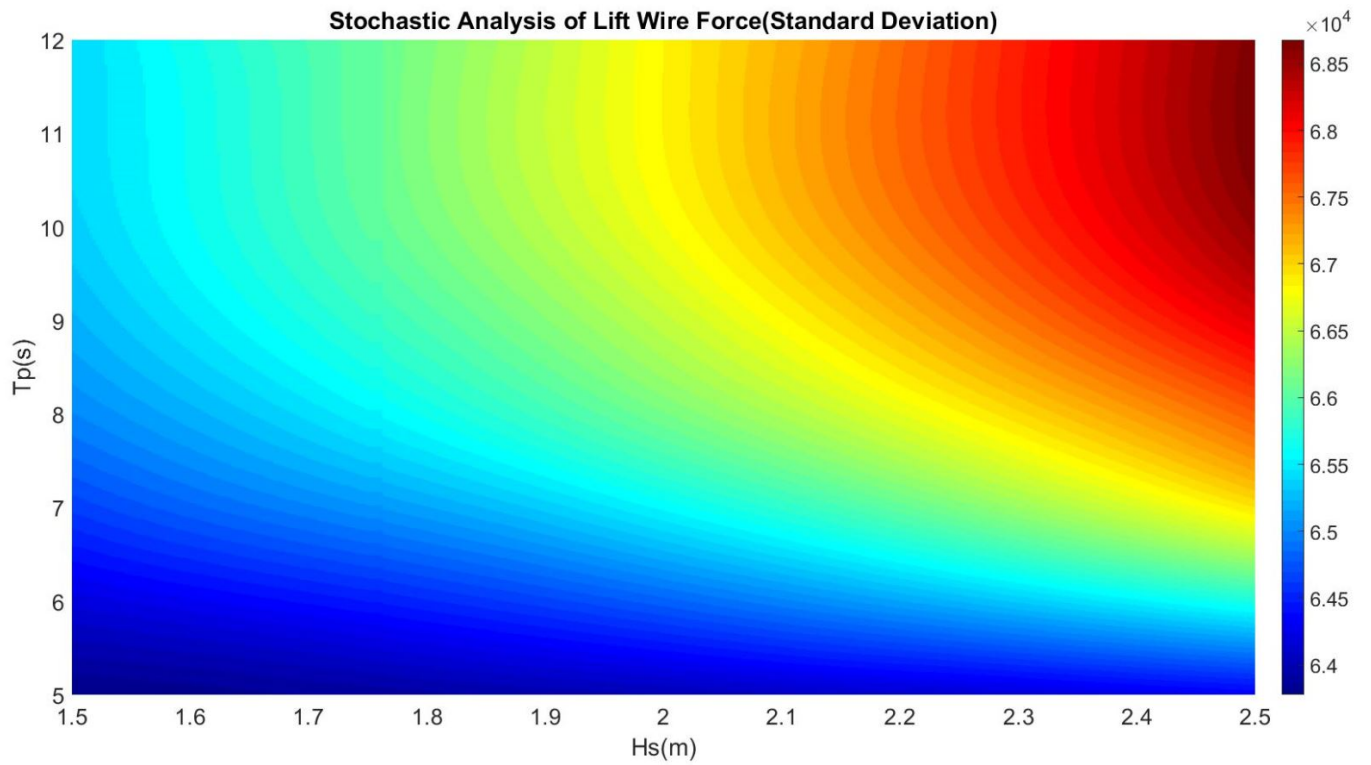


Figure 4.17: Result of Lift Wire Force Standard Deviation in Different Sea States

could provide reasonable result when draught of vessel kept almost constant. However, water surface in the gap between crane vessel and barge was heavily affected by the value of gap. In order to find reasonable result, several HydroD model were built with different gaps.

Sea condition was same as former scenario, which including water depth, wave incident direction and sea state characters. Based on HydroD analysis, a 'WAMIT' result file was got with suitable hydrodynamic factors. Then it would input into SIMA to do time domain analysis.

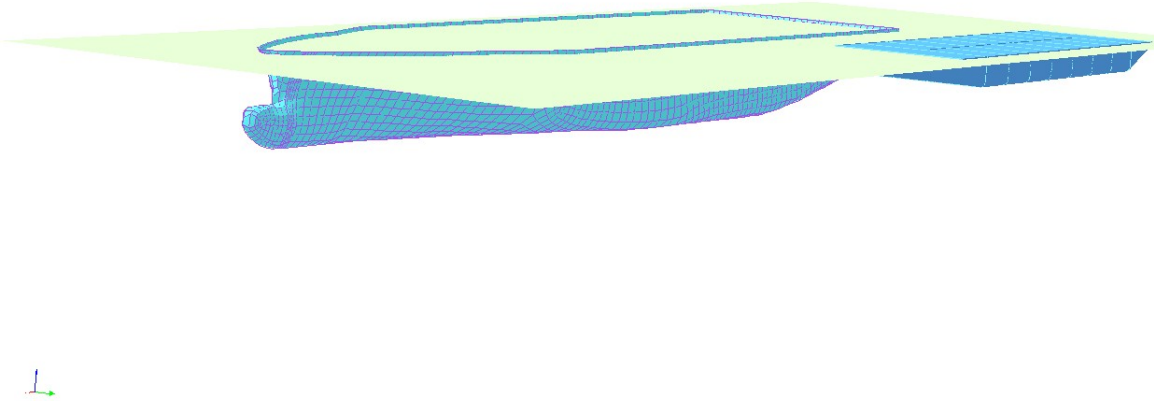


Figure 4.18: Panel Model of Two Vessels

#### 4.5.2 Model in SIMA

Same mooring system of vessel, on-board crane and monopile were used in this case, just as figure 4.19 shown. Relative motion between crane vessel and barge may lead overloading or slack of lift wire. For this reason, lift wire force would be calculated when monopile on the barge. When monopile lifted from barge, lift wire force had almost no relation with barge. For this reason, two cases corresponding to monopile on barge and lift-off process were considered respectively. In order to clear effect due to gap length, short period time duration was concerned as 3 hours. Following that, lift-off part which mainly rely on crane vessel would be discussed.

Based on former discussion in theory part, small distance between barge and crane vessel might lead large force in horizontal direction. Strong dynamic position system would be used on barge. Maximum force and minimum changing time from maximum to minimum thrust would be changed for different gap values. And mooring system was also enforced due to similar reason. Figures 4.20 show steps of two vessels lift-off scenario.

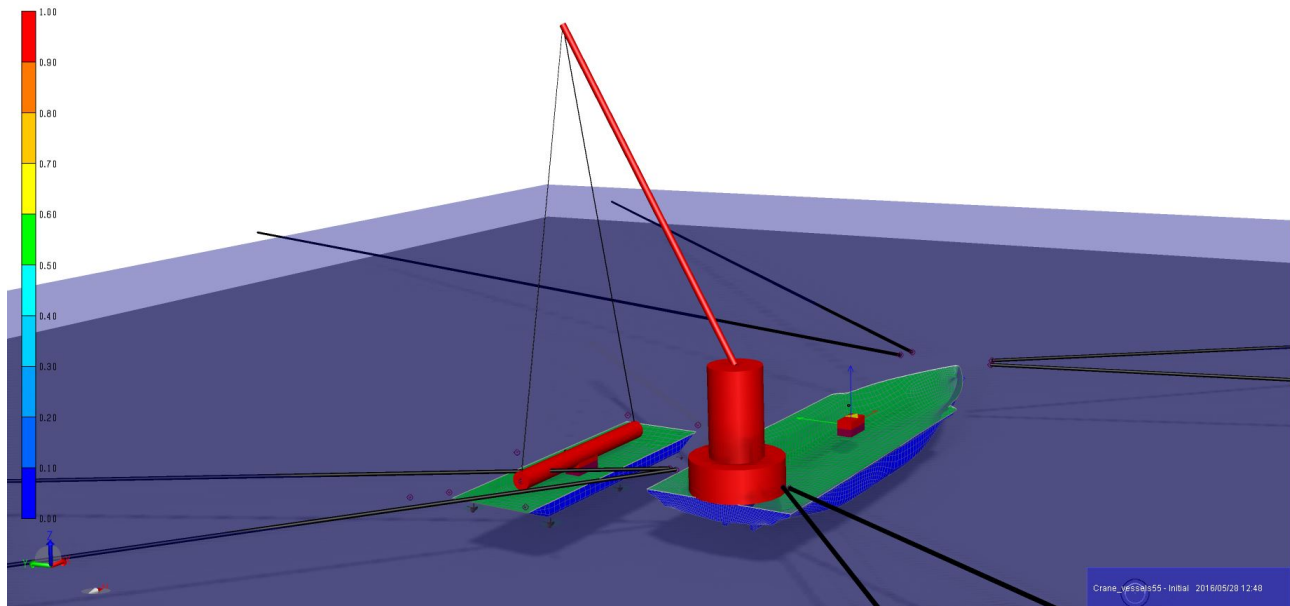


Figure 4.19: Two Vessels Model in SIMA

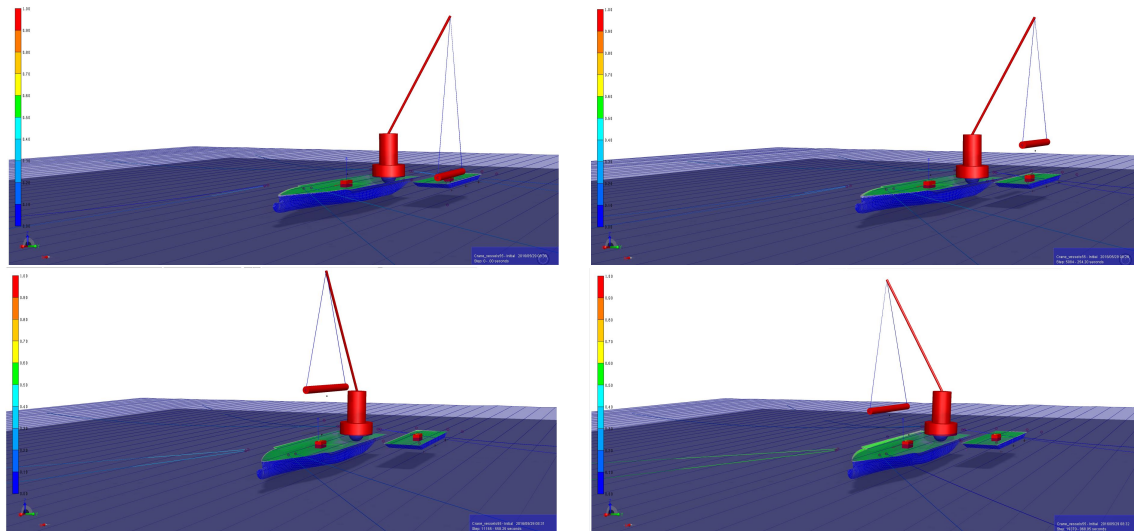


Figure 4.20: (a) Step 1 in Two Vessels Scenario. (b) Step 2 in Two Vessels Scenario. (c) Step 3 in Two Vessels Scenario. (d) Step 4 in Two Vessels Scenario.

### 4.5.3 Numerical Result of Two Vessels Scenario

Table 4.3 shows the results of lift wire force, crane vessel heave and roll motion. Environmental load in this part was assumed as only wave load. For the reason of beam sea was most critical, wave load was assumed in beam direction. JONSWAP spectrum was used to make the simulation more reliable in Norwegian North Sea with  $H_s=1.5\text{m}$  and  $T_p=12\text{s}$ . It was easily seen that all of these concerned results increased with the decreasing of gap value. When the gap value decreasing from the wide of crane vessel (47m), hydrodynamic effect became obvious. And the effects due to resonance of water in the gap area were decreased by increasing damping of the motions to minimize errors leaded by numerical method. Moreover, thruster was also increased a lot when the gap decreased. When the gap value increased to minimize its effect, large horizontal scale of crane column was needed. Based on discussion in chapter 2, lift capacity of crane vessel was limited with the increasing of horizontal range. Moreover, ballast water needed to balance the extra moment due to hanged monopile was increased a lot when large gap value concerned shown in table 4.4. In this case, under water shape of crane vessel was assumed as constant to fit calculated hydrodynamic factors. For this reason, extra roll damping (from bilge keel) of crane vessel was hardly to get. In order to balance talked moment, extra point mass was used as ballast water at the position of crane bottom. This extra mass cannot be very large because it would affect displacement and initial pitch angle of crane vessel. In this case added point mass used to balance the moment from monopile was too large when the gap equaled to 53meters, which condition was given up.

Table 4.3: Result of Two Vessels Scenario with Different Gap Values

Gap (m)	Lift Wire Force-90 (N)	Crane Vessel Heave-90 (m)	Crane Vessel Roll-90 (degree)
48	3.97E+07	8.74E-01	1.27E-02
38	4.08E+07	9.55E-01	8.35E-02
28	4.87E+07	2.24E+00	9.62E-02
18	4.96E+07	4.18E+00	1.71E-01
13	4.99E+07	4.52E+00	1.81E-01
8	5.30E+07	5.54E+00	2.29E-01

whole lift-off process would be considered in the following. Just as shown in figures 4.20, monopile would be lifted from barge then move to other side of crane vessel and finally lift

Table 4.4: Ballast Water for Different Gaps

Gap (m)	Ballast Water (ton)
48	1808.51
38	1595.74
28	1382.98
18	1170.21
13	1063
8	650

down to sea. Time series of lift wire force was shown in figure 4.21. It was easily seen, that the lift wire force was almost same in the whole process and a little larger in step 3 when it moving to other side of crane vessel. Rotation motion would lead second order force on monopile which increased lift wire force. Moreover, there were four extreme large values of concerned force. Each of them appeared at the beginning of each step. This was a mistake leading by numerical theory. Velocity of lift wire could decrease zero at end of second step. And rotation motion of crane bottom was also decreased to zero at end of step three. These talked velocities changing happened in a very short period, which means large acceleration on the monopile. For this reason, lift wire force increased a lot at that time. And went back to mean value quickly.

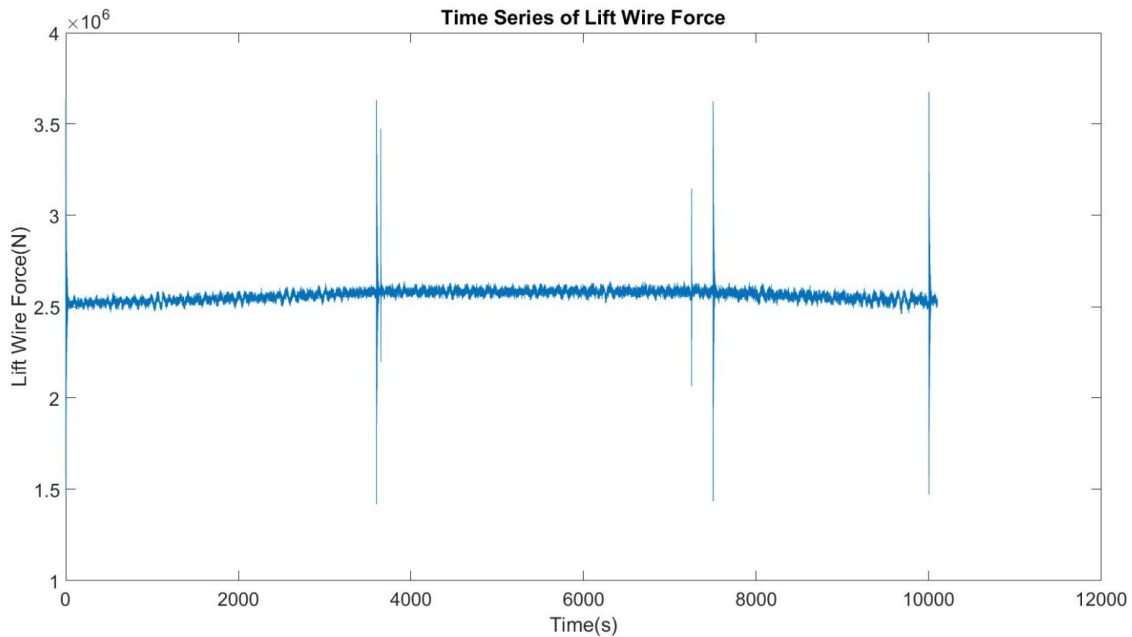


Figure 4.21: Time Series of Lift Wire Force



Generally speaking, lift wire force was almost same as gravity of monopile which was  $5E6N$ . Two lift wires shared this gravity so the mean value in figure 4.21 was around  $2.5E6N$ . When the horizontal motions of barge and crane vessel were limited by thruster and mooring system, gravity was the main part in lift wire force. Distance between barge and crane vessel challenge this scenario mostly.





# Chapter 5

## Comparative Study

Accuracy of numerical simulation would be checked by comparison between its result and theoretical one. Firstly, basic assumptions of numerical simulation would be shown. Then the comparison between theoretical result and numerical one would be listed based on given motion of crane vessel. In the last part of this chapter, result of concerned forces under irregular wave assumption would be shown to clear effects from vessel motion.

### 5.1 Basic Assumption of Numerical Simulation

Mass, geometry, motion, damping, pretension and external forces could be seen as key parameters for dynamic problem. All of them would be discussed in detail, including effects due to talked assumption and difference between hypothesis of theoretical simulation and numerical one.

#### 5.1.1 Mass Distribution

Mass of monopile assumed as concentrated point mass at the center of gravity(COG). Moments of inertia in different directions were considered individually. This setting could be seen similar as evenly mass distribution along length. A solid cylinder replaced an empty-core pipe structure in this case. However, the concerned inertial moment of monopile was a little affected by discussed difference as equation 5.1 shown, where 'l' means length of monopile,  $r_2$ ,  $r_1$  means outer

and inner diameter respectively. Moment inertia used in numerical simulation based on equation 5.2, which was a little larger than the reality value. Based on such assumption, numerical result could be seen as conservative one due to the prescribed motion. Equation 5.3 was used in theoretical analysis which made the theoretical result a little smaller than numerical one due to smaller inertia moment. Difference of inertial moment led to dichotomy between numerical, theoretical and reality.

$$I = \frac{\pi \rho l}{12} (3(r_2^4 - r_1^4) + h^2(r_2^2 - r_1^2)) \quad (5.1)$$

$$I = \frac{1}{12} m (3r_2^2 + l^2) \quad (5.2)$$

$$I = \frac{1}{12} ml^2 \quad (5.3)$$

### 5.1.2 Geometrical Relation

Geometrical relation difference between theoretical and numerical model would also lead some deviations. Hinge connection between crane vessel and monopile was assumed at 48m from lift point of monopile in theoretical analysis while 49m in numerical. Reason for that was unideal outlook of crane vessel. This difference made the bending moment at support point a little larger in numerical result but the amplitude should be very small due to total length of monopile was much larger than this difference. Moreover, the hinge connection was assumed at the edge of monopile in theoretical analysis while at mid-point in numerical simulation. This difference based on dichotomy between thin line and cylinder assumption for monopile. This difference led to some deviations. Lift wire stiffness in theoretical analysis was assumed as infinite. By this reason, elongation of lift wire did not take into account. So time series of numerical result could be a little longer than theoretical ones based on different position of hinge connection and elongation due to a finite stiffness.

### 5.1.3 Motion of Crane

Time series of motion in theoretical analysis was smooth because velocity assumed as a function of time in theory simulation. However, this cannot be used in present version of SIMA. In the first part of process (defined in Chapter 4), this difference did not make obvious error for long period. But deviation in second part was obvious due to short period.

### 5.1.4 Motion of Crane Vessel

Vessel was assumed as jack-up or floating structure in theoretical analysis. Same situation was set in numerical tool SIMA to check the accuracy. Result of such comparison would be shown in the follow. And damping of vessel motion was neglected in theoretical analysis which just affected natural frequency of ship motion. This effect was not serious in upending process. The condition of no motion limitation of vessel did not concern in theoretical analysis due to large time consuming. Comparison between theoretical result and numerical result would be shown in the following.

## 5.2 Result Comparison

Results based on numerical and theoretical analysis would be discussed here in three different groups. These groups divided by different kinds of crane vessel motions which including jack-up vessel, regular heave and regular roll assumptions. Reasons of difference would also be highlight here.

### 5.2.1 Jack-up Vessel Assumption

Crane vessel was fixed in global coordinate without any motion. Figure5.1 shows the comparison between theoretical and numerical result. It was clearly seen, that the whole trend of all three concerned forces were almost same. In order to get stable motion for dynamic simulation. Upending process would start from 10 seconds after beginning of simulation. So the time series of numerical result shifted 10 seconds to right. There was a obvious difference for horizontal support force (green one) at the end of first part(defined in 4.2). Abrupt increasing of crane

bottom velocity led large value of acceleration. There was no such sudden changing in theoretical analysis of which result looks more smooth than numerical one. Obvious vibration of lift wire and vertical support forces shown in figure 5.1 due to start of upending process.

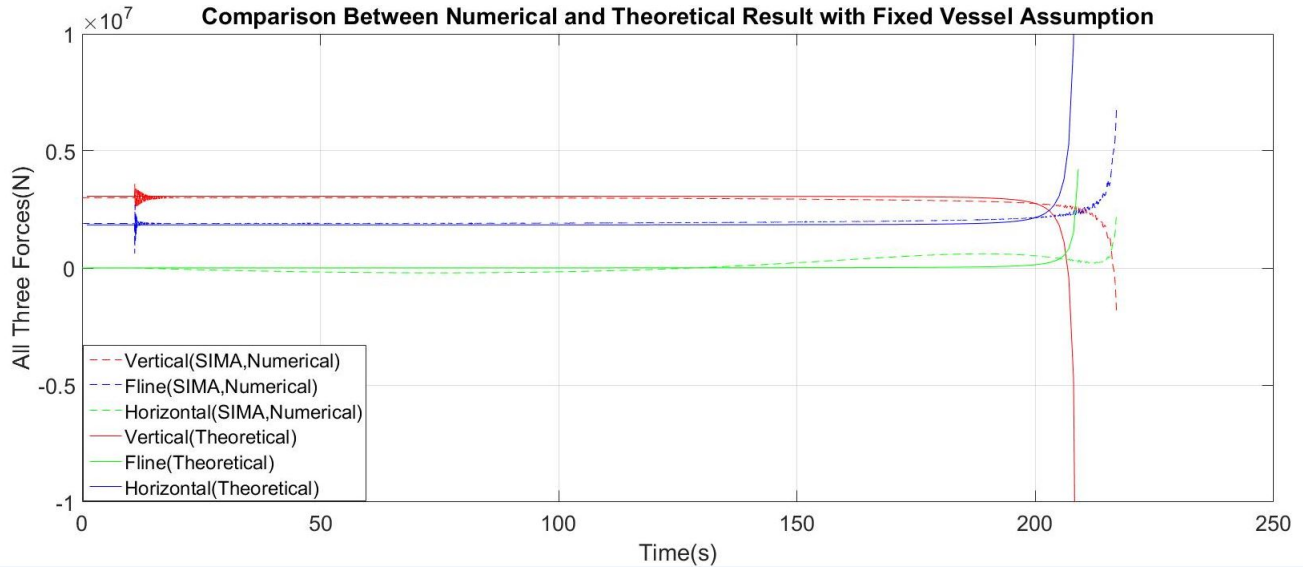


Figure 5.1: Comparison Between SIMA and Theoretical Result with Fixed Vessel

### 5.2.2 Regular Heave Motion

Vessel motion was assumed as regular heave in this part. Equation 5.4 shows regular heave motion which concerned in theoretical analysis. Other five freedoms of crane vessel were fixed in numerical analysis. Based on beam sea heave motion RAO figure, regular heave motion could be got when assumed regular incident wave with given amplitude and frequency. Figure 5.2 shows the comparison between numerical and theoretical result. It was clearly seen that the two methods had almost same result except a phase angle. Reason for clear shake at 10 second was similar as jack-up vessel assumption.

$$\xi_{heave} = \zeta_a \sin(\omega t) \quad (5.4)$$

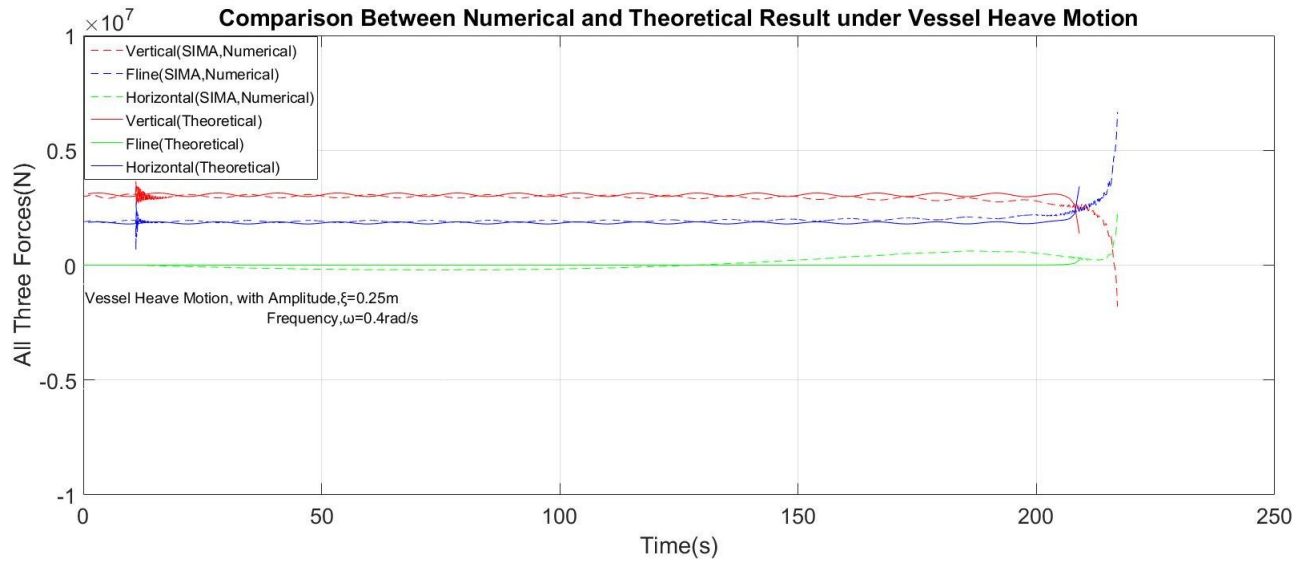


Figure 5.2: Comparison Between SIMA and Theoretical Result with Regular Heave Motion

### 5.2.3 Regular Roll Motion

Regular roll motion of crane vessel was assumed here. Similar as heave motion assumption, regular roll motion was set in theoretical and numerical analysis. Figure 5.3 shows the comparison. It was clearly seen, that the lift wire and vertical support forces were almost same for two methods. Reasons for horizontal shift of numerical result and vibration at 10 second were similar as jack-up vessel case. There was a large vibration in horizontal support force of numerical result shown in figure 5.4. Upending motion affected roll motion of crane vessel because changing position of COG of monopile. This phenomenon, which neglected in theoretical analysis led to larger horizontal support force in numerical result.

## 5.3 Comparison Between Different Freedom Setting of Vessel

Effects due to unique freedom of crane vessel in roll and heave in irregular wave condition would be considered here. Figure 5.5, 5.6 and 5.7 show time series of all concerned forces when irregular heave, roll and total motion assumed. Compared figure 5.5 and 5.6, irregular roll motion had more significant effect than heave motion, especially on horizontal support force. Main trend of each time series was almost same under these two assumptions. There was serious vibration of horizontal support force in figure 5.7. This phenomenon proved that horizontal support force

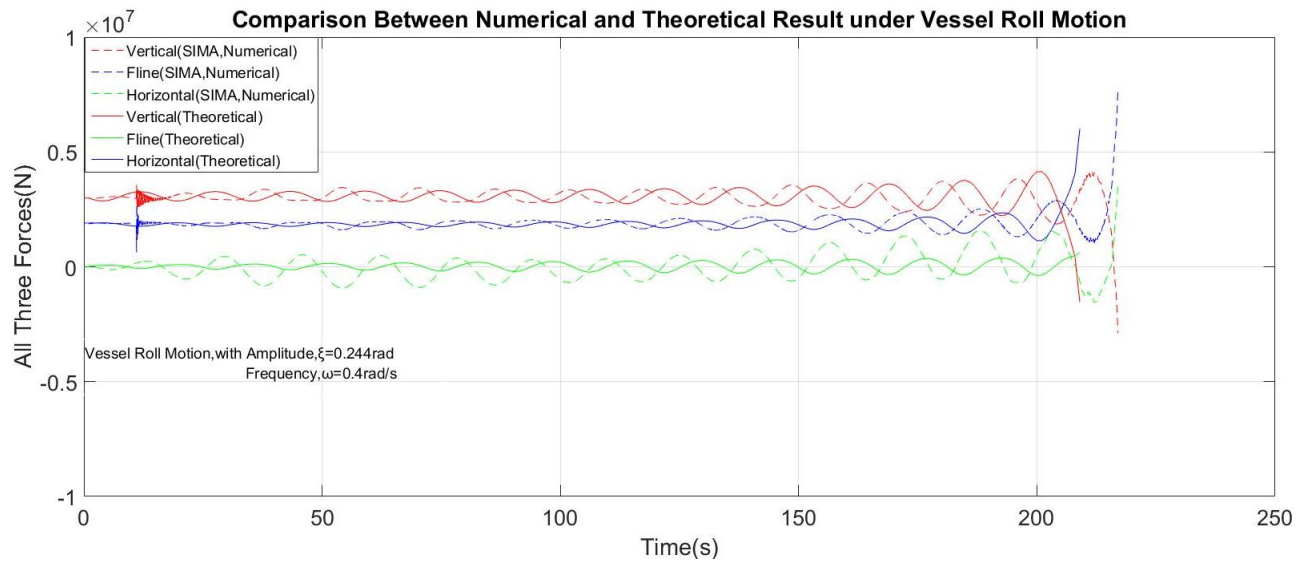


Figure 5.3: Comparison Between SIMA and Theoretical Result with Regular Roll Motion

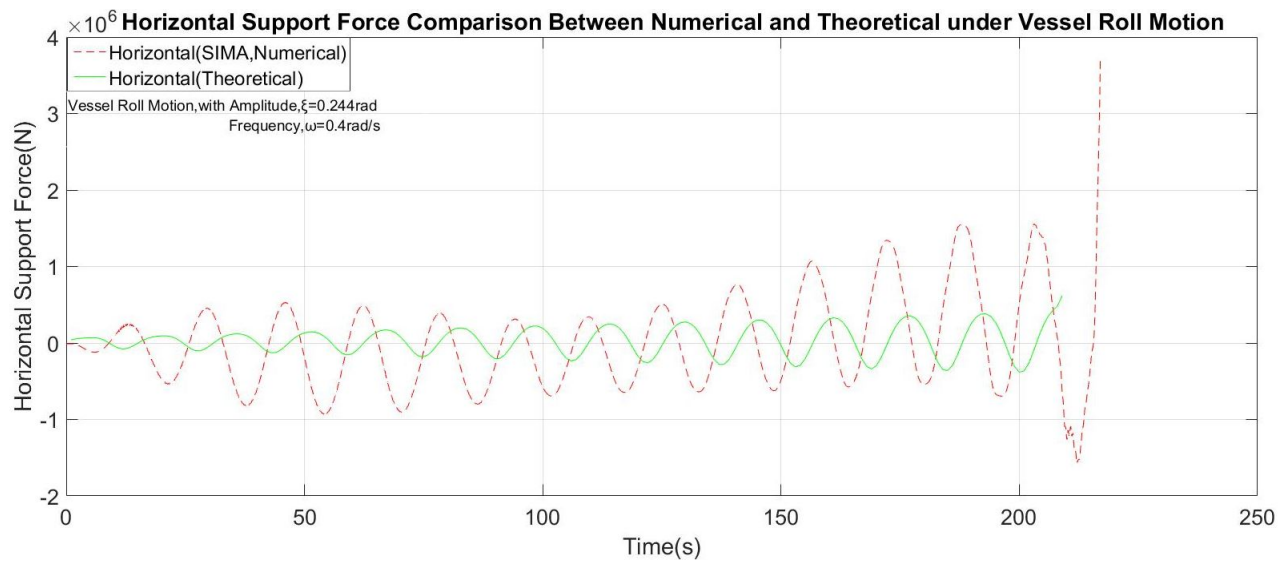


Figure 5.4: Comparison Between SIMA and Theoretical Result of Horizontal Support Force

was more sensitive to vessel motion than other two forces. And vertical support force was not affected by vessel motion. These figures also show that irregular vessel motion had nearly no effect to concerned forces. The only way to decrease maximum value of all three forces was the changing of upending process. In other word, weather condition is not very important for upending process. Choice of reasonable process is the key part to complete the upend mission.

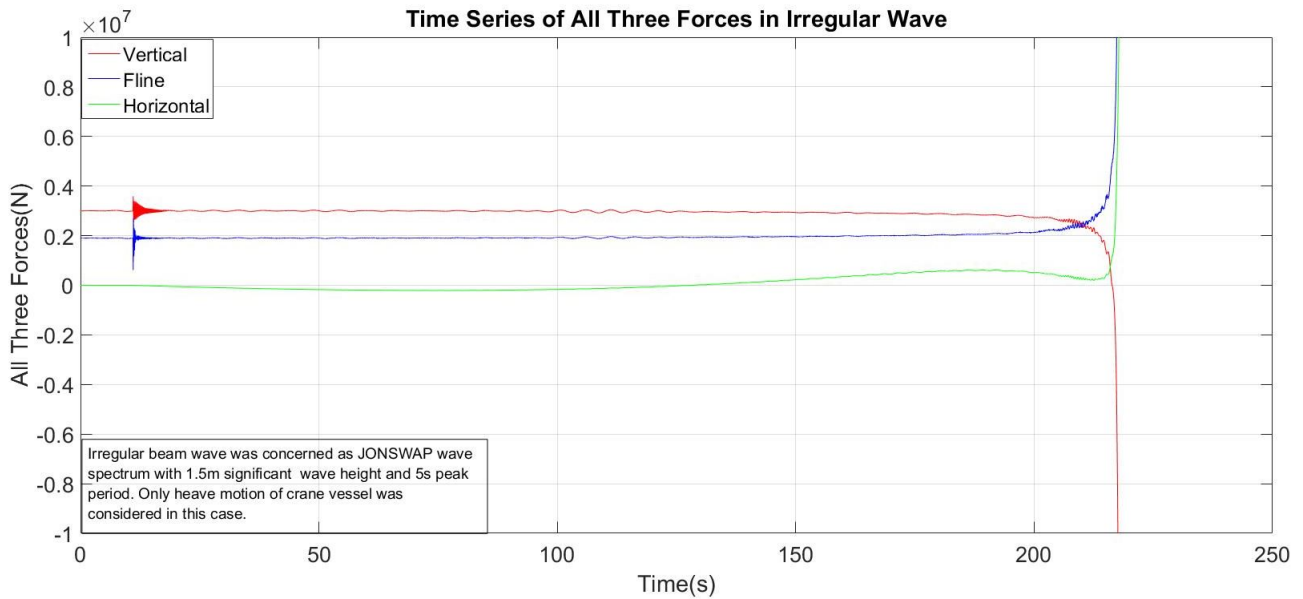


Figure 5.5: Time Series of Concerned Forces with Irregular Heave Motion

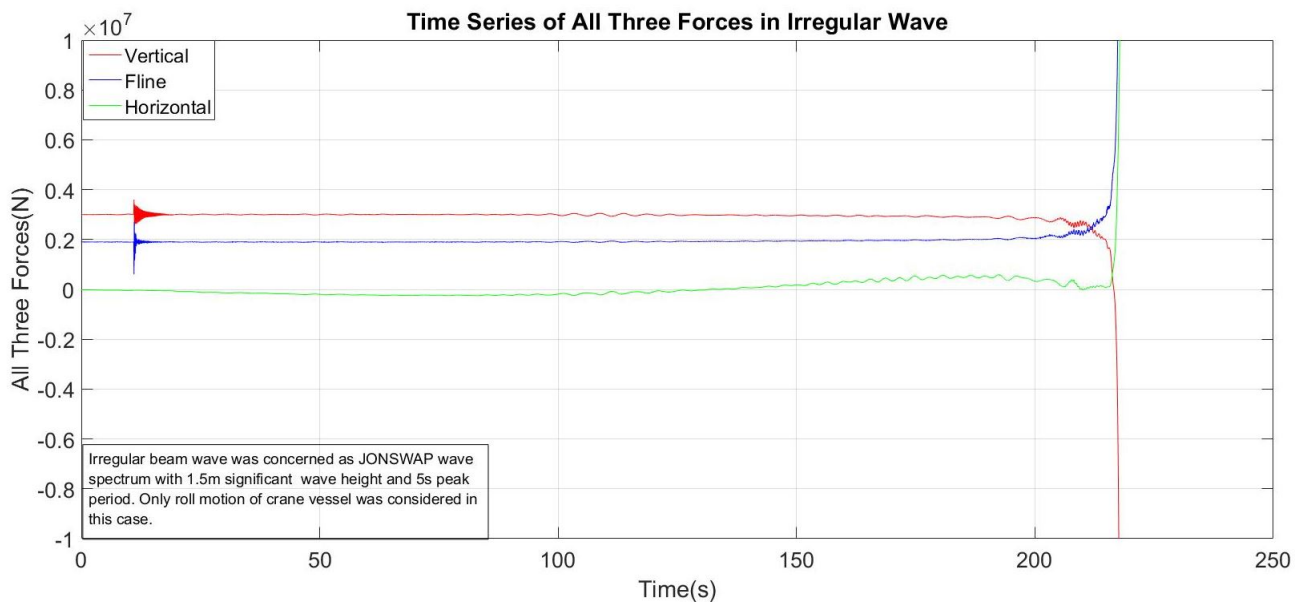


Figure 5.6: Time Series of Concerned Forces with Irregular Roll Motion

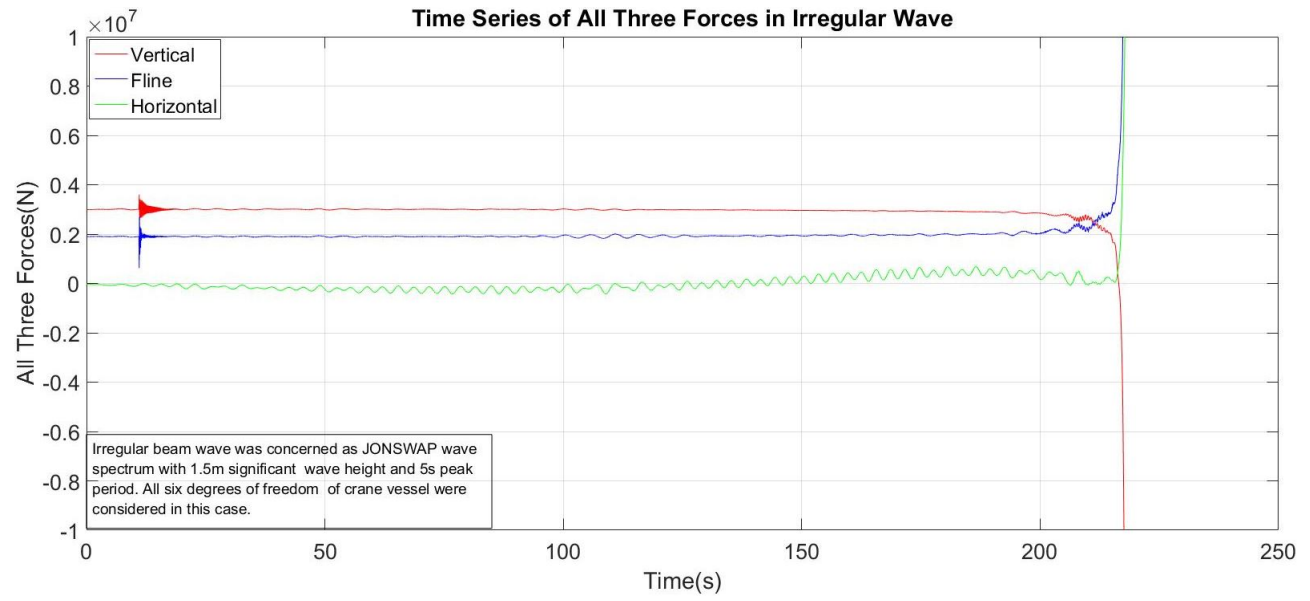


Figure 5.7: Time Series of Concerned Forces with Irregular Total Motion



# Chapter 6

## Summary and Recommendations for Future Work

In this part, conclusion of all done analysis would be drawn and some recommendations of lift-off process would also be given at the same time. At last, some further work which cannot finish for limited time would be shown.

### 6.1 Summary and Conclusions

Based on theoretical and numerical analysis of single vessel scenario, all three concerned forces lift wire, vertical support and horizontal support forces mainly depended on upending process. Lifting velocity and lift wire force were the key factors. Lift velocity had to be decreased to a very small value at the second part, which defined former to make the operation safety. From discussion of different upending process, keep lift wire vertical should be the best choice for easy control.

When the vessel motion divided into translation and rotation types, rotation ones could induce larger forces, especially roll motion. However, translation of crane vessel just had little effect on three concerned forces. From this result, some devices which used to reduce roll amplitude should be built on crane vessel such as bilge keel.

Crane vessel motion due to wave load did not seriously affect mean and maximum value of concerned forces. However, irregular wave with large  $H_s$  and  $T_p$  might lead large variance

of every force. This might lead slack or overloading of lift wire and hinge connection. So a considerable low sea state should be chosen for upending process.

When another barge was used to transport monopile from onshore to working station, distance between barge and crane vessel should be considered carefully. It should keep the distance larger than width of crane vessel. And more ballast water should flow into crane vessel to balance extra motion due to large distance and weight of monopile. Strong DP system should install on transport barge to prevent collision between barge and crane vessel in high sea state.

## 6.2 Discussion

Hydrodynamic factors used in numerical simulation were got from panel model result in SESAM. This means the changing of draft during upending process was neglected. This limit accuracy of simulation. Rotation velocity of crane bottom could not be set as a function of time made it rotate step by step, which was not similar as practical. Monopile might touch water surface at the end of upending process was also neglected in this study. Above limitations may lead some errors in whole analysis.

## 6.3 Recommendations for Further Work

For limitation of time and computer capacity, some important calculation cannot finish. Firstly, only 8 Hs and 8 Tp were considered in irregular wave condition. This was not a sufficient number of sea state to shown the final result. Though figures in chapter 4 showed larger standard deviation and mean value of concerned forces in high sea state. That figures did not represent natural period effect when changing Tp. So more sea states needed to consider to correct the result.

Changing of draft in whole process, especially for large ballast water condition, should be considered in panel model to correct hydrodynamic factors.

There were also some limitations in two vessels scenario. Only horizontal distance between barge and crane vessel was considered. Longitudinal distance and relative yaw angle were not taken into account. These two factors should be carefully concerned to keep safety of operation.

# Bibliography

Aarset, K., Sarkar, A., Karunakaran, D. N., et al. (2011). Lessons learnt from lifting operations and towing of heavy structures in north sea. In *Offshore Technology Conference*. Offshore Technology Conference.

Crol, J. (2015). *Upending of a Monopile for an Offshore Wind Turbine Foundation*. PhD thesis, TU Delft, Delft University of Technology.

Faltinsen, O. (1993). *Sea loads on ships and offshore structures*, volume 1. Cambridge university press.

Gao, Z. and Moan, T. (2009). Accuracy of the narrow-band approximation of stationary wide-band gaussian processes for extreme value and fatigue analysis. In *Proceedings of the 10th International Conference on Structural Safety and Reliability (ICOSSAR)*, pages 997–1004.

Gordon, R. B., Grytøyr, G., and Dhaigude, M. (2013). Modeling suction pile lowering through the splash zone. In *ASME 2013 32nd International Conference on Ocean, Offshore and Arctic Engineering*, pages V001T01A010–V001T01A010. American Society of Mechanical Engineers.

Graczyk, M. and Sandvik, P. C. (2012). Study of landing and lift-off operation for wind turbine components on a ship deck. In *ASME 2012 31st International Conference on Ocean, Offshore and Arctic Engineering*, pages 677–686. American Society of Mechanical Engineers.

Li, L., Gao, Z., and Moan, T. (2013). Numerical simulations for installation of offshore wind turbine monopiles using floating vessels. In *ASME 2013 32nd International Conference on Ocean, Offshore and Arctic Engineering*, pages V008T09A076–V008T09A076. American Society of Mechanical Engineers.

- Li, L., Gao, Z., and Moan, T. (2015). Joint distribution of environmental condition at five european offshore sites for design of combined wind and wave energy devices. *Journal of Offshore Mechanics and Arctic Engineering*, 137(3):031901.
- Li, L., Gao, Z., Moan, T., and Ormberg, H. (2014). Analysis of lifting operation of a monopile for an offshore wind turbine considering vessel shielding effects. *Marine Structures*, 39:287–314.
- Moller, A. (2005). Efficient offshore wind turbine foundations. *Wind Engineering*, 29(5):463–469.
- Perry, M., Sandvik, P., et al. (2005). Identification of hydrodynamic coefficients for foundation piles. In *The Fifteenth International Offshore and Polar Engineering Conference*. International Society of Offshore and Polar Engineers.
- Pre'Consuitants, B. (1997). Sima pro user manual. *The Netherlands*.
- Thomsen, K. (2014). *Offshore wind: a comprehensive guide to successful offshore wind farm installation*. Academic Press.
- Uraz, E. (2011). Offshore wind turbine transportation & installation analyses" planning optimal marine operations for offshore wind projects. *Gotland University*.
- Van der Wal, R., Cozijn, H., and Dunlop, C. (2008). Model tests and computer simulations for njord fpv gas module installation. In *Proceedings of the Marine Operations Speciality Symposium (MOSS)*.
- Zhang, Y., Yu, D., Fu, S., Guo, F., and Wei, W. (2014). Wave drift forces and resonance analysis on two ships arranged side by side. In *ASME 2014 33rd International Conference on Ocean, Offshore and Arctic Engineering*, pages V08BT06A048–V08BT06A048. American Society of Mechanical Engineers.

# Appendix A

## ROA of Crane Vessel Motion

ROA of heave and roll of crane vessel under beam sea would be shown here.

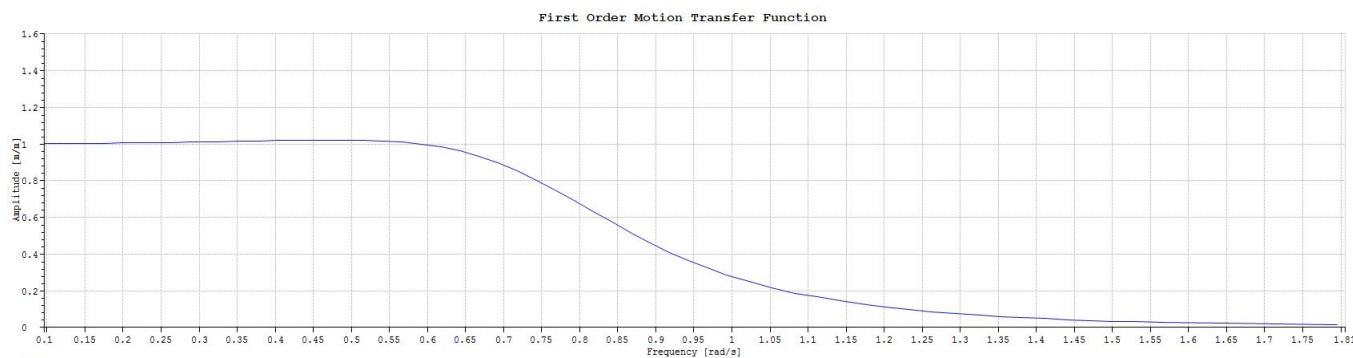


Figure A.1: ROA of Heave Motion

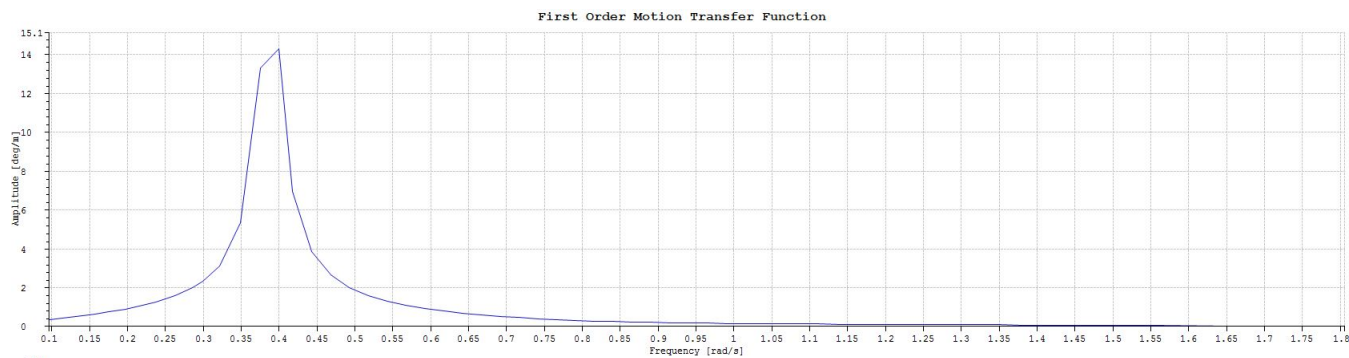


Figure A.2: ROA of Roll Motion

# Appendix B

## Result of Concerned Forces in Different Case

Some results of concerned forces did not show in the main part of thesis due to limited pages would be shown here.

### B.1 Result in Different Lifting Velocities

Figures B.1, B.2, B.3 and B.4

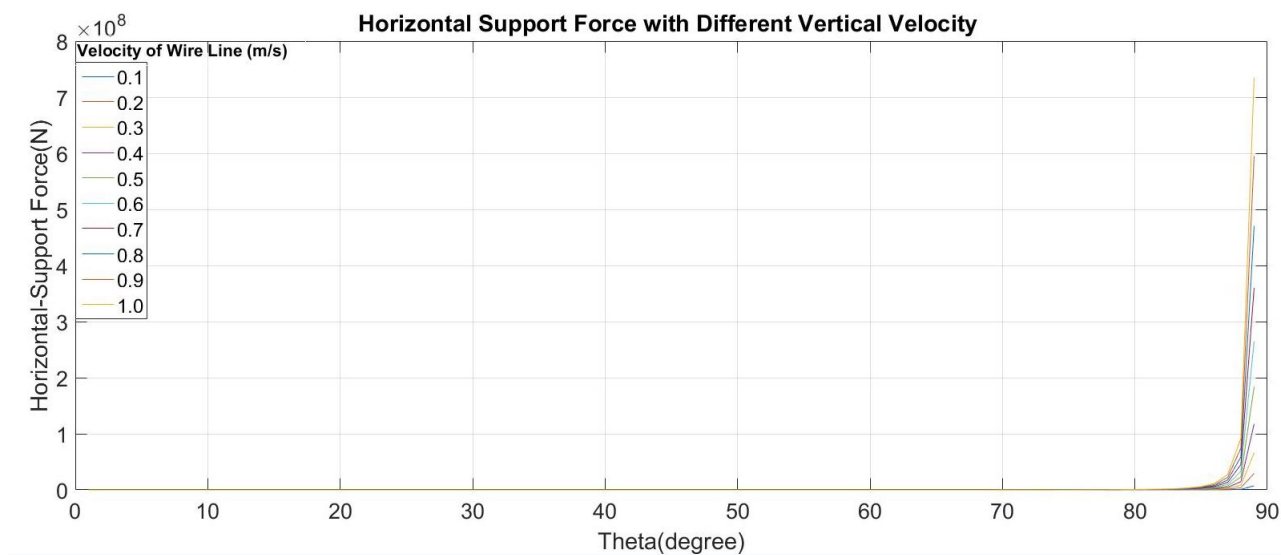


Figure B.1: Theta Series of Horizontal Support Force for Different Lifting Velocity

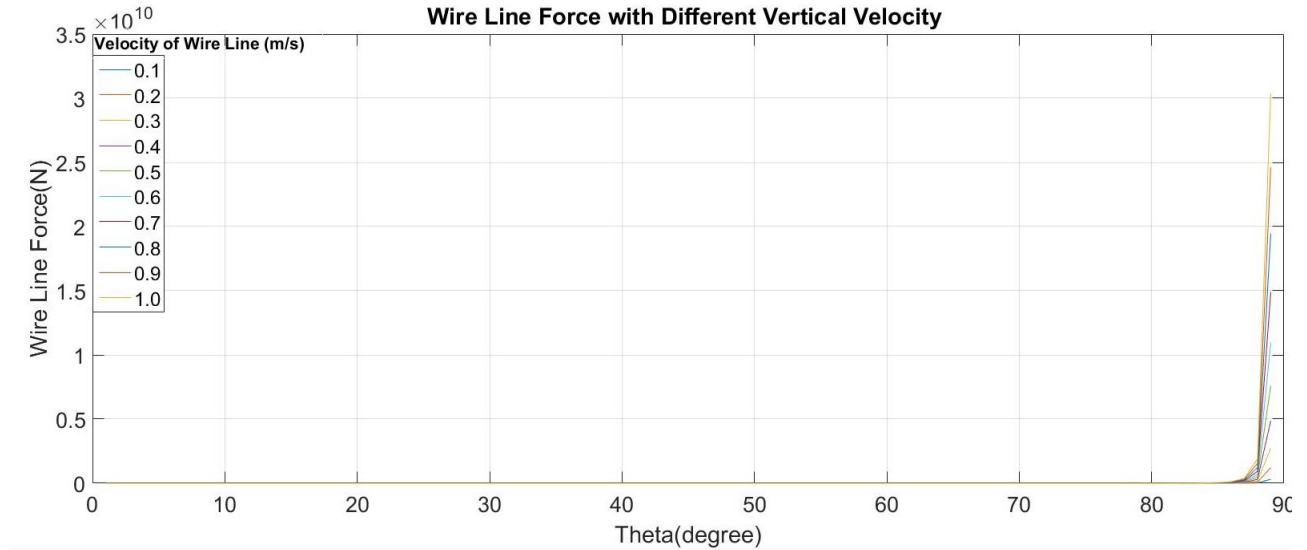


Figure B.2: Theta Series of Lift Wire Force for Different Lifting Velocity

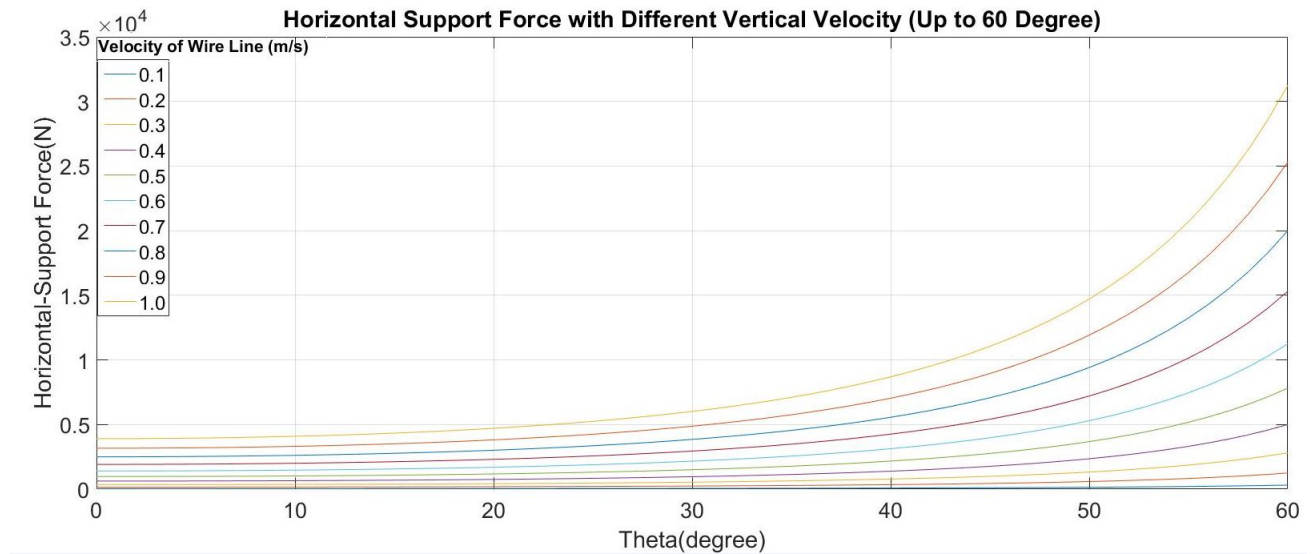


Figure B.3: Theta Series of Horizontal Support Force for Different Lifting Velocity(60)

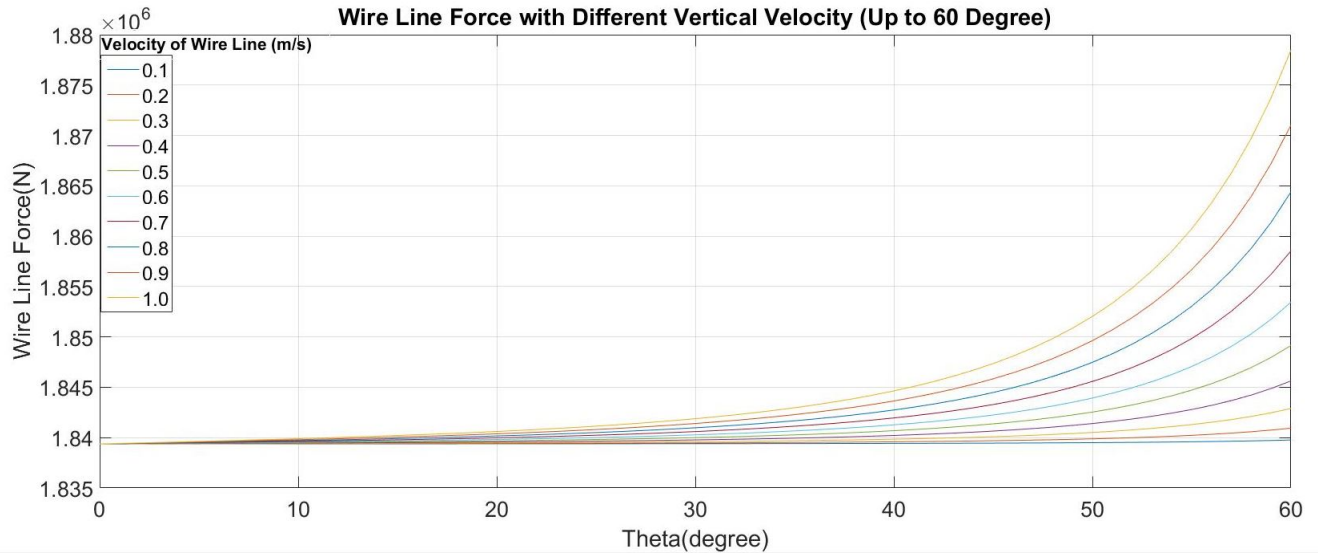


Figure B.4: Theta Series of Lift Wire Force for Different Lifting Velocity(60)

## B.2 Result in Different Lifting Forces

Figure B.5

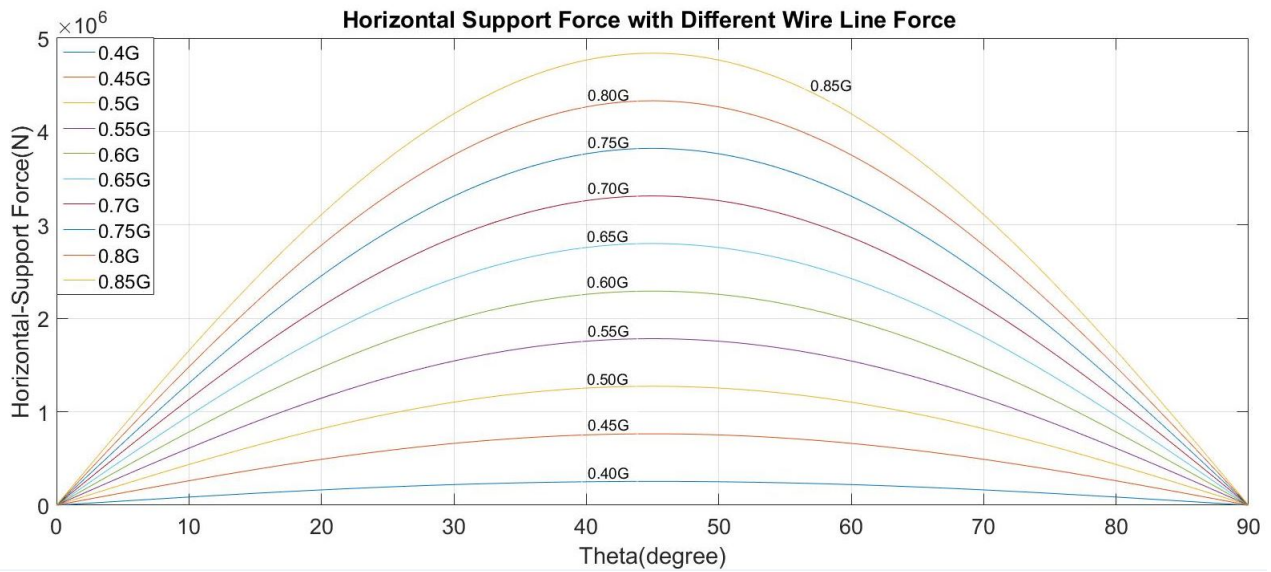


Figure B.5: Theta Series of Horizontal Support Force for Different Lift Force

## B.3 Result under Different Heave Amplitude

Figure B.6



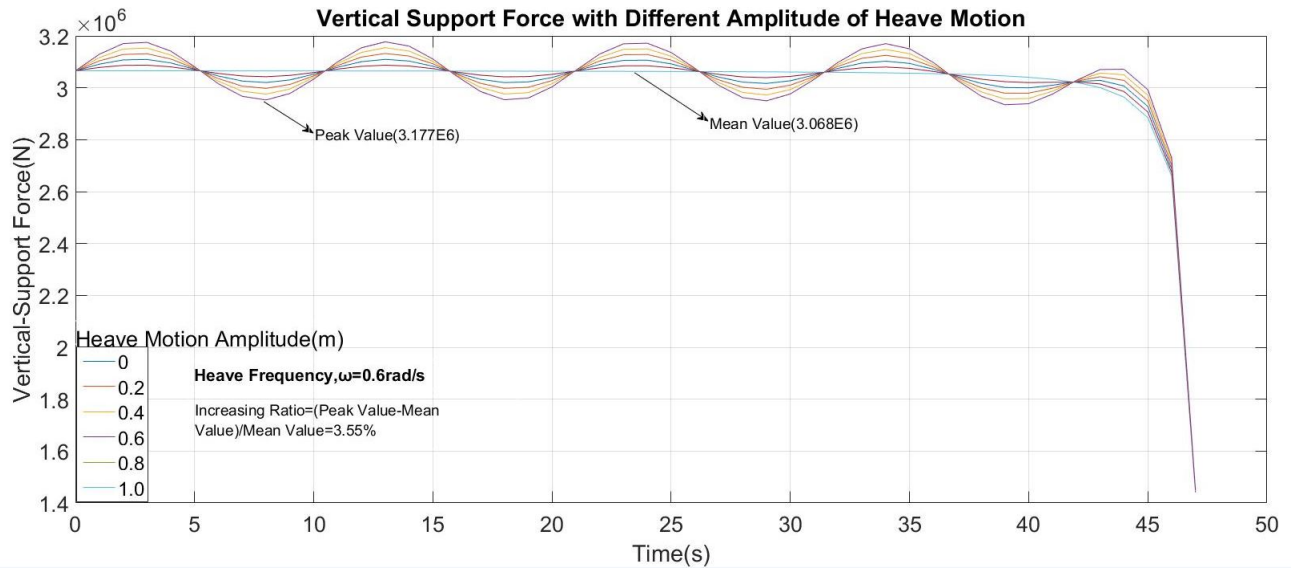


Figure B.6: Time Series of Vertical Support Force under Different Heave Amplitude

## B.4 Result under Different Heave Frequency

Figures B.7 and B.8

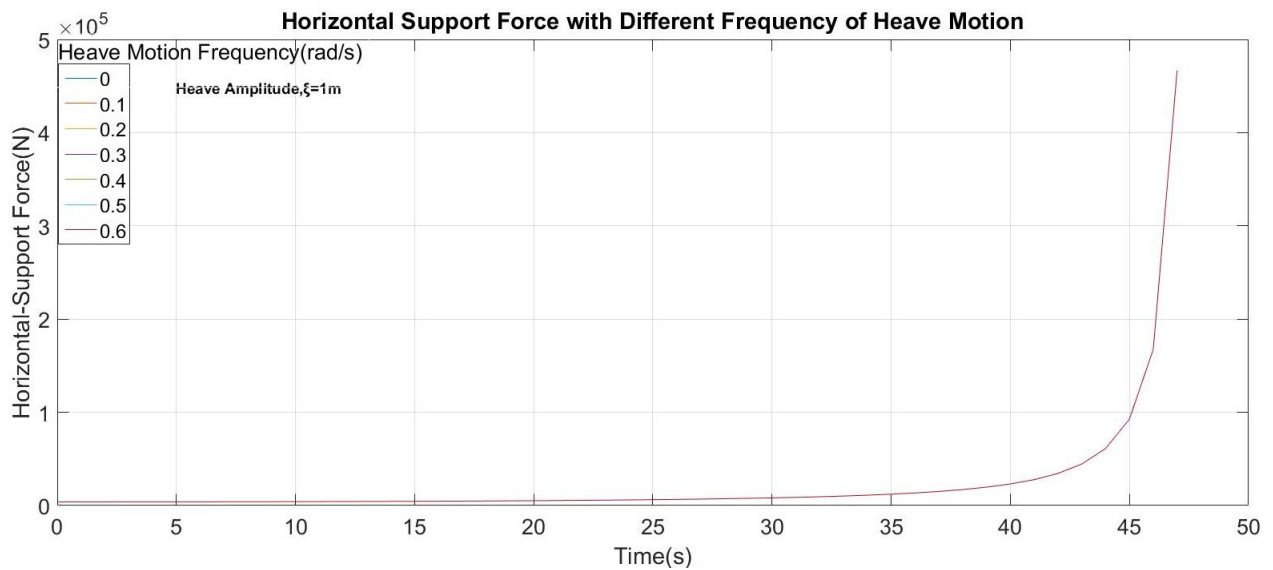


Figure B.7: Time Series of Horizontal Support Force under Different Heave Frequency

## B.5 Different Terms Under Roll Motion

Figure B.9

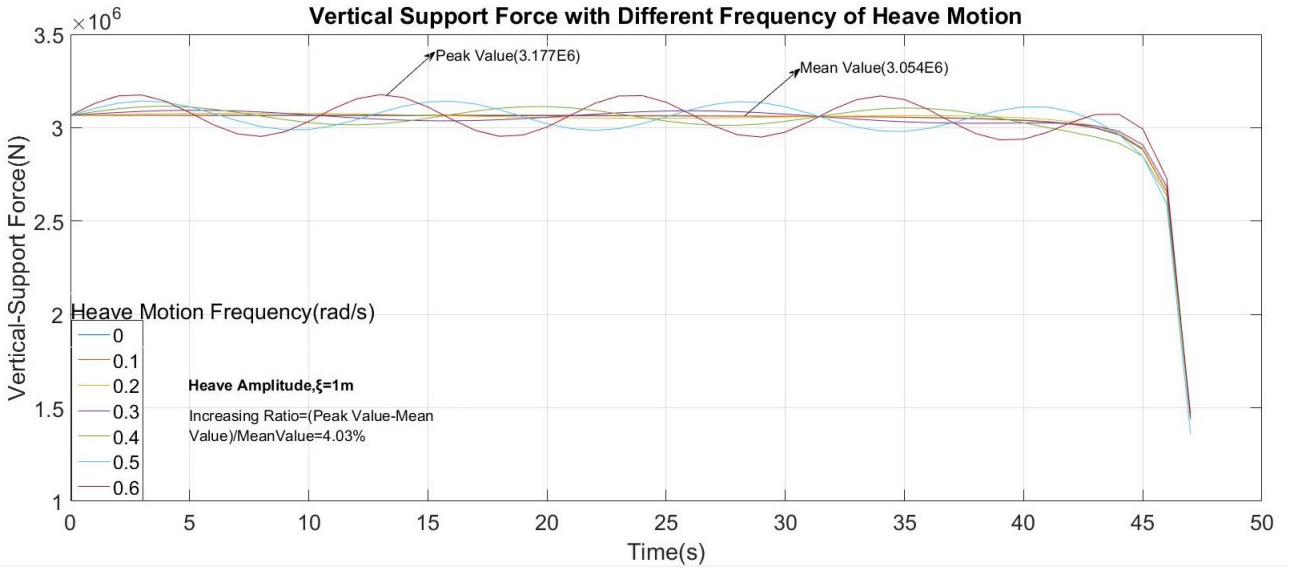


Figure B.8: Time Series of Vertical Support Force under Different Heave Frequency

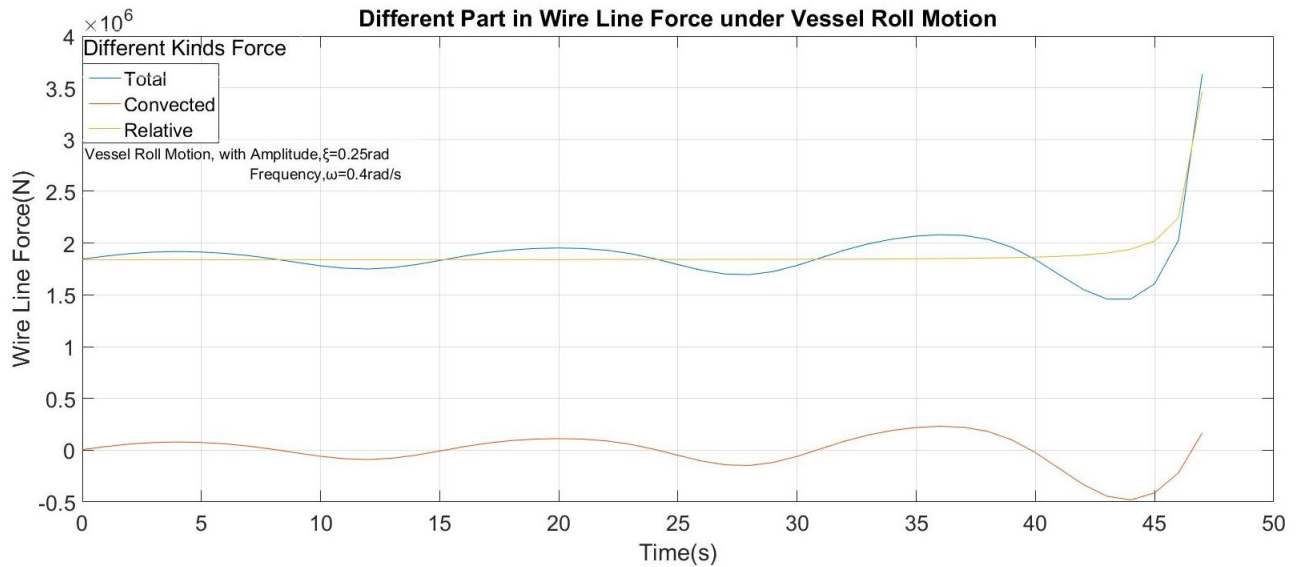


Figure B.9: Time Series of Vertical Support Force under Different Heave Frequency

## B.6 Result under Different Roll Frequency

Figure B.10

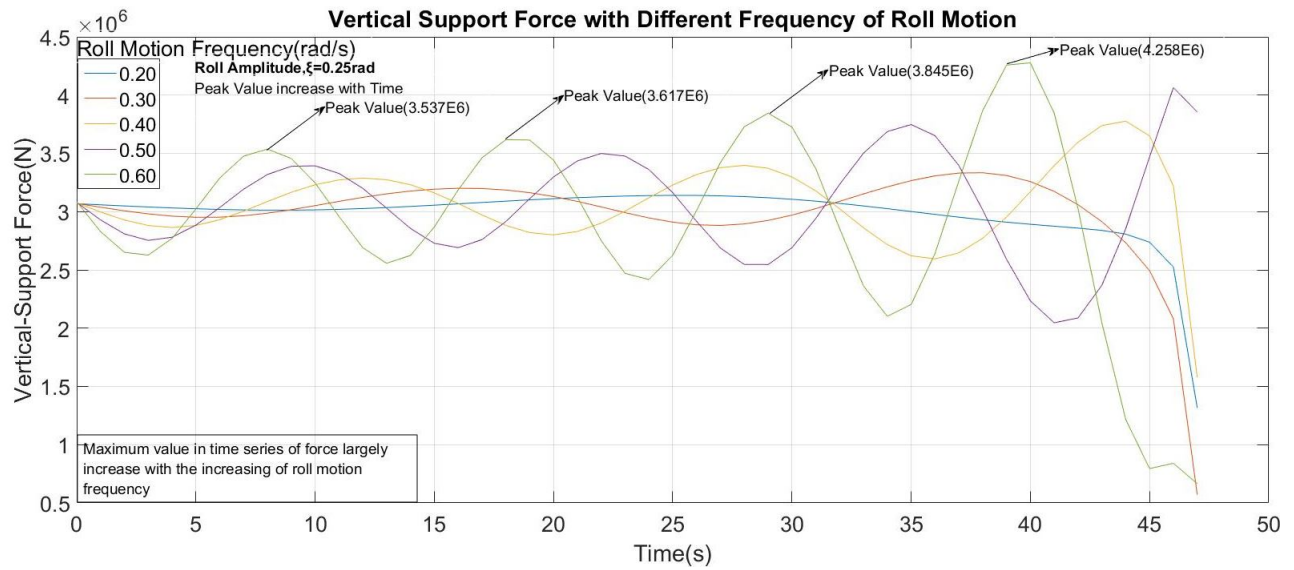


Figure B.10: Time Series of Vertical Support Force under Different Roll Frequency

## B.7 Result in Different Hs and Tp

Figures B.11 and B.12

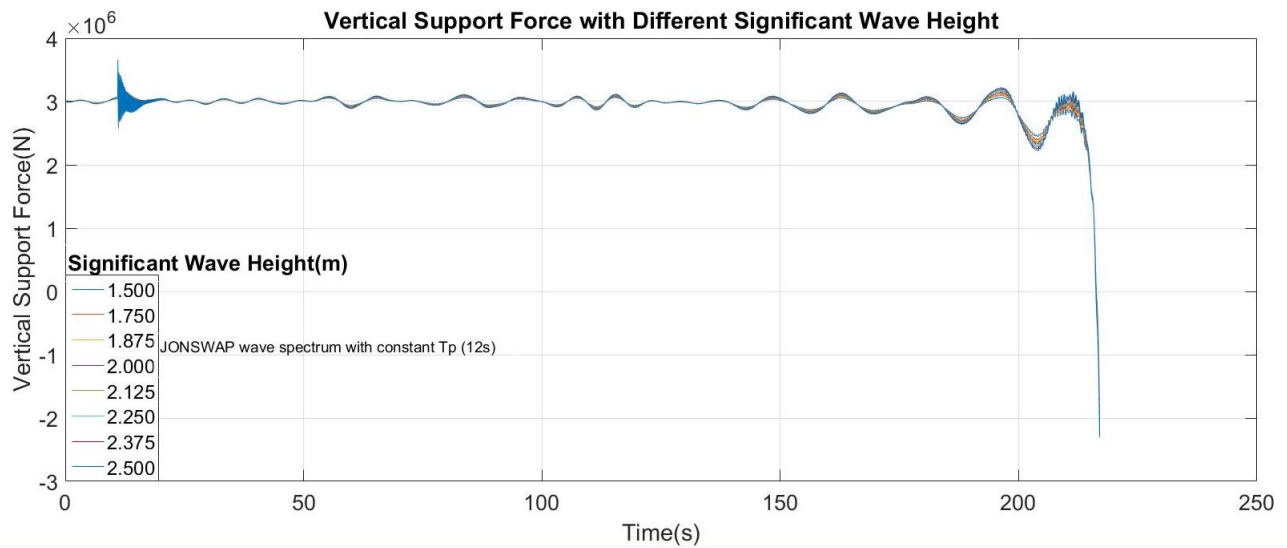


Figure B.11: Time Series of Vertical Support Force with Different Significant Wave Height

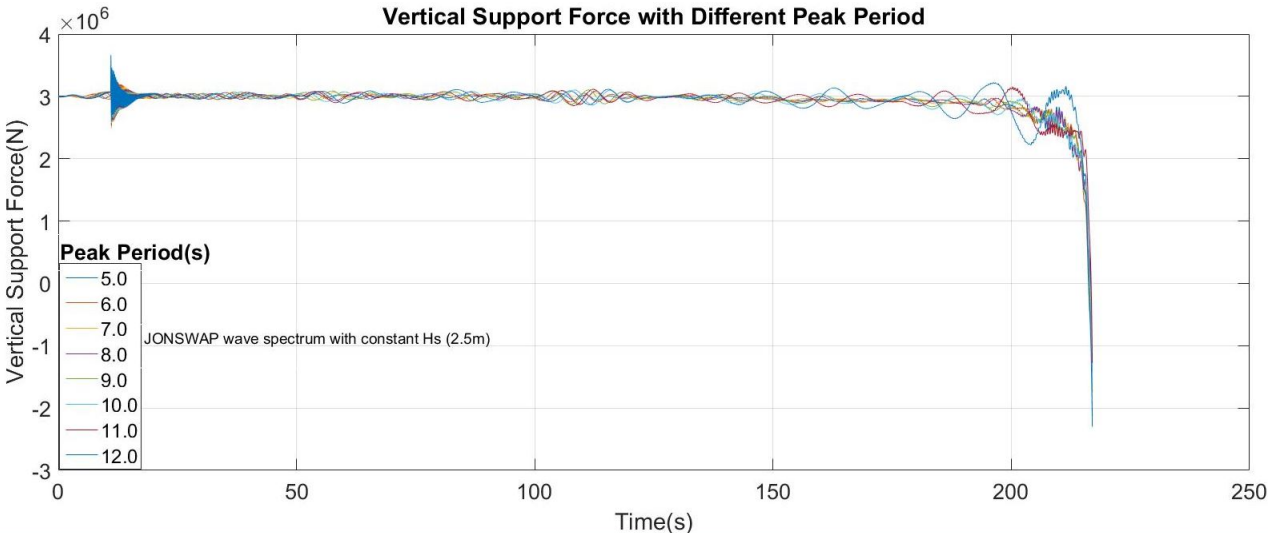


Figure B.12: Time Series of Vertical Support Force with Different Peak Period

# Appendix C

## Matlab Code in Theoretical Analysis

Part of Matlab code used in theoretical analysis would be shown here.

### C.1 Code for Crane Bottom Velocity-First Part

```
clear all  
clc  
v=0.2;  
dt=1;    % time step  
t1=fix((49^2-25^2)/v^2)^0.5);  
omegal=zeros(t1,1); %velocity of crane bottom in 'rad'  
omegald=zeros(t1,1); %velocity of crane bottom in 'degree'  
theta=zeros(t1+1,1); %angule of crane bottom  
omega2=zeros(t1,1); %velocity of crane clined column in 'rad'  
omega2d=zeros(t1,1); %velocity of crane clined column in 'degree'  
alpha=zeros(t1,1); %angule of crane clined column  
for i=1:dt:t1  
    dx=49-(49^2-(v*i)^2)^0.5; %delta x  
    omegal(i)=abs(-1/(1+(1-dx/24)^2)/24*v^2*i*(49^2-(v*i)^2)^(-0.5));  
    omegald(i)=omegal(i)/2/pi*360;  
    a=omegal(i)*dt;
```

```

theta(i+1)=a+theta(i);
omega2(i)=1/((1-1/8/(cos(theta(i+1))^2))^0.5)/2/2^0.5/((cos(theta(i+1)
)) ^2)*sin(theta(i+1))*omega1(i)*(-1);
omega2d(i)=omega2(i)/2/pi*360;
b=omega2d(i)*dt;
alpha(i+1)=b+alpha(i);

```

**end**

## C.2 Code for Crane Bottom Velocity-Second Part

```

clc
clear all
v=0.2;
dt=1;    % time step
t2=fix((49-(49^2-25^2)^0.5)/v);
e=t2/dt;
omega1=zeros(e,1); %velocity of crane bottom in 'rad'
omega1d=zeros(e,1); %velocity of crane bottom in 'degree'
theta=zeros(e,1); %angle of crane bottom
omega2=zeros(e,1); %velocity of crane clined column in 'rad'
omega2d=zeros(e,1); %velocity of crane clined column in 'degree'
alpha=zeros(e,1); %angle of crane clined column
for i=1:1:e
    t=i*dt;
    c=(49^2-25^2)^0.5;
    dx=25-(49^2-(c+v*t)^2)^0.5;    %delta x
    omega1(i)=1/(1+(dx/24)^2)/24*(49^2-(c+v*t)^2)^(-0.5)/2*(2*c*v+2*v^2*t)
    ;
    omega1d(i)=omega1(i)/pi*180;

```

```

a=omegal(i)*dt;
theta(i+1)=a+theta(i);
omega2(i)=1/((1-1/8/(cos(theta(i+1))^2))^0.5)/2/2^0.5/((cos(theta(i+1)
    ))^2)*sin(theta(i+1))*omegal(i);
omega2d(i)=omega2(i)/2/pi*360;
b=omega2d(i)*dt;
alpha(i+1)=b+alpha(i);

```

**end**

### **C.3 Code for Concerned Forces under Different Frequencies Roll Motion of Crane Vessel**

```

clc
clear all
syms x y r
m=500000;
g=9.81;
xi=0.24;
% omega0=0.2;
v=1;
n=49;
j=5;
d=3;
mesupport=zeros(n,j);
acint=zeros(n,j);
fc=zeros(n,j);
fenm=zeros(n,j);
fetaum=zeros(n,j);
omegal=zeros(n,j);

```

```

epsilon1=zeros(n,j);
atau=zeros(n,j);
an=zeros(n,j);
ftau=zeros(n,j);
fn=zeros(n,j);
costheta=zeros(n,j);
sintheta=zeros(n,j);
fsupportx=zeros(n,j);
fsupporty=zeros(n,j);
fline=zeros(n,j);
c=zeros(n,j);
theta=zeros(n,j);
epsilon=zeros(n,j);
fsupportn=zeros(n,j);
fsupporttau=zeros(n,j);
k=1;
for omega0=0.2:0.1:0.6
i=1;
for t=0:1:48

theta(i,k)=asin(v*t/48);
omega1(i,k)=omega0*xi*cos(omega0*t);
epsilon1(i,k)=-omega0^2*xi*sin(omega0*t);
r=((x-23.5)^2+(((48-x)*tan(theta(i,k)))+d)^2)^0.5;
y=(48-x)*tan(theta(i,k));
aen0=omega1(i,k)^2*((x-23.5)^2+(((48-x)*tan(theta(i,k)))+d)^2)^0.5;
aetau0=epsilon1(i,k)*((x-23.5)^2+(((48-x)*tan(theta(i,k)))+d)^2)^0.5 ;
e=[48 -48*tan(theta(i,k))];
f=[23.5-x -d-((48-x)*tan(theta(i,k)))];
cosecf=dot(e,f)/(norm(e)*norm(f));

```



```

sinef=sin(acos(cosef));
aetau=aetau0*cosef-aen0*sinef;
aen=aen0*cosef+aetau0*sinef;
l=48-48*cos(theta(i,k));
h=48+12*cos(theta(i,k));
o=48-12*cos(theta(i,k));
fenm(i,k)=int(aen*m/60/cos(theta(i,k)),x,l,h);
fetaum(i,k)=int(aetau*m/60/cos(theta(i,k)),x,l,h);
mesupport(i,k)=int(aetau*m/60/cos(theta(i,k))*(48-x)/cos(theta(i,k)),x
,l,h);
ac=2*omegal(i,k)*v/cos(theta(i,k))^2/48*(48-x);
acint(i,k)=int(ac,x,l,h);
fc(i,k)=int(ac*m/60/cos(theta(i,k)),x,l,h);

epsilon(i,k)=t*v^3/(48^2-(v*t)^2)^1.5;
atau(i,k)=18*t*v^3/(48^2-(v*t)^2)^1.5;
an(i,k)=18*v^2/(48^2-(v*t)^2);
ftau(i,k)=atau(i,k)*m;
fn(i,k)=an(i,k)*m;
costheta(i,k)=((48^2-(v*t)^2))^0.5/48;
sintheta(i,k)=v*t/48;
fsupportx(i,k)=ftau(i,k)*sintheta(i,k)+fn(i,k)*costheta(i,k)-fetaum(i,
k)*sintheta(i,k)-fenm(i,k)*costheta(i,k)-fc(i,k)*costheta(i,k);
fline(i,k)=(m*g*18*costheta(i,k)+(m*3600/12+18^2*m)*epsilon(i,k)-
mesupport(i,k))/48/costheta(i,k);
fsupporty(i,k)=m*g+ftau(i,k)*costheta(i,k)-fline(i,k)-fn(i,k)*
sintheta(i,k)+fenm(i,k)*sintheta(i,k)+fc(i,k)*sintheta(i,k)-fetaum(
i,k)*costheta(i,k);
c(i,k)=t;

```

```

    fsupporttau(i,k)=fsupporty(i,k)*cos(theta(i,k))+fsupportx(i,k)*sin(
        theta(i,k));
    fsupportn(i,k)=fsupportx(i,k)*cos(theta(i,k))-fsupporty(i,k)*sin(theta
        (i,k));
    i=i+1;
end
k=k+1;
end
clear i
figure(1)
for i = 1:size(c,2)
    plot(c(:,i),fsupporty(:,i),'-'),xlabel('Time(s)'),ylabel('Vertical-Support
        _Force(N)');
    grid on
    hold on
end
title('Vertical_Support_Force_with_Different_Frequency_of_Roll_Motion')
set(gca,'FontSize',20);
hlegend=legend('0.20','0.30','0.40','0.50','0.60','Location','West');
tString = sprintf('_____Omega0,rad/s');
hTitle=legendTitle(hlegend,tString,'FontWeight','bold','FontSize',18)
;
clear i
figure(2)
for i = 1:size(c,2)
    plot(c(:,i),fsupportx(:,i),'-'),xlabel('Time(s)'),ylabel('Horizontal-
        Support_Force(N)');
    grid on
    hold on
end

```

```

title ( 'Horizontal_Support_Force_with_Different_Frequency_of_Roll_Motion' )
set(gca, 'FontSize',20);
hlegend=legend( '0.20', '0.30', '0.40', '0.50', '0.60', 'Location', 'West' );
tString = sprintf ( '_____Omega0,rad/s' );
hTitle=legendTitle (hlegend, tString, 'FontWeight', 'bold', 'FontSize',18 )
    ;
clear i
figure(3)
for i = 1:size(c,2)
plot(c(:, i), fline(:, i), '-'), xlabel( 'Time(s)' ), ylabel( 'Wire_Line_Force(N)' )
    ;
grid on
hold on
end
title ( 'Wire_Line_Force_with_Different_Frequency_of_Roll_Motion' )
set(gca, 'FontSize',20);
hlegend=legend( '0.20', '0.30', '0.40', '0.50', '0.60', 'Location', 'West' );
tString = sprintf ( '_____Omega0,rad/s' );
hTitle=legendTitle (hlegend, tString, 'FontWeight', 'bold', 'FontSize',18 )
    ;

```

## C.4 Code for Concerned Forces under Different Lifting Velocities

```

clear all
clc
syms x y t;
n=61;
j=10;
atau=zeros(n, j);

```

```

an=zeros(n,j);
ftau=zeros(n,j);
fn=zeros(n,j);
fsupportx=zeros(n,j);
fsupporty=zeros(n,j);
fline=zeros(n,j);
c=zeros(n,j);
fnm=zeros(n,j);
ftaum=zeros(n,j);
fsupportxm=zeros(n,j);
flinem=zeros(n,j);
omega=zeros(n,j);
sintheta=zeros(n,j);
epsilon=zeros(n,j);
m=500000;
g=9.81;

k=1;
for v=0.1:0.1:1
i=1;
for thet=0:1:60
theta=thet/180*pi;
omega(i,k)=v/cos(theta)/48;
epsilon(i,k)=v^2*sin(theta)/48^2/cos(theta)^3;
atau(i,k)=18*epsilon(i,k);
an(i,k)=omega(i,k)^2*18;
ftau(i,k)=atau(i,k)*m;
fn(i,k)=an(i,k)*m;
fnm(i,k)=fn(i,k)-500000*9.81*sin(theta);
ftaum(i,k)=ftau(i)+500000*9.81*cos(theta);

```

```

fsupportx(i,k)=ftau(i,k)*sin(theta)+fn(i,k)*cos(theta);
fline(i,k)=(m*60^2/12*epsilon(i,k)+18*cos(theta)*(m*g+ftau(i,k)*cos(theta)-fn(i,k)*sin(theta))+fsupportx(i,k)*18*sin(theta))/(30*cos(theta)+18*cos(theta));
fsupporty(i,k)=m*g+ftau(i,k)*cos(theta)-fn(i,k)*sin(theta)-fline(i,k);
c(i,k)=theta;

    i=i+1;
end
k=k+1;
end

clear i
figure(1)
for i = 1:size(c,2)
plot(c(:,i),fsupporty(:,i),'-'),xlabel('Theta(degree)'),ylabel('Vertical-Support_Force(N)');
grid on
hold on
end
title('Vertical_Support_Force_with_Different_Vertical_Velocity_')
set(gca,'FontSize',20);
legend('0.1','0.2','0.3','0.4','0.5','0.6','0.7','0.8','0.9','1.0','Location','West');

clear i
figure(2)
for i = 1:size(c,2)

```

```

plot(c(:, i), fsupportx(:, i), '-'), xlabel('Theta(degree)'), ylabel('Horizontal
    -Support_Force(N)');
grid on
hold on
end
title('Horizontal_Support_Force_with_Different_Vertical_Velocity_')
set(gca, 'FontSize', 20);
legend('0.1', '0.2', '0.3', '0.4', '0.5', '0.6', '0.7', '0.8', '0.9', '1.0', '
    Location', 'West');

clear i
figure(3)
for i = 1: size(c, 2)
plot(c(:, i), fline(:, i), '-'), xlabel('Theta(degree)'), ylabel('Wire_Line_
    Force(N)');
grid on
hold on
end
title('Wire_Line_Force_with_Different_Vertical_Velocity_')
set(gca, 'FontSize', 20);
legend('0.1', '0.2', '0.3', '0.4', '0.5', '0.6', '0.7', '0.8', '0.9', '1.0', '
    Location', 'West');

```

# Appendix D

## SIMA Code for Model Setting

```
' *****  
_SYSTEM_DESCRIPTION_SIMO  
' *****
```

```
' lenuni_timuni_masuni_grav_____rhow_____rhoa_wakivi_ airkivi  
_M_____S_____Mg_____9.806650000e+00_1.025000000e+00_/_/_/_/_/  
' depth          dirslo slope  
2.500000000e+01 0          0
```

```
' *****  
_ENVIRONMENT_DATA_SPECIFICATION  
' *****
```

```
' _____  
_IRREGULAR_WAVE_SPECIFICATION  
' _____
```

```
' chirwa
```

```

_envi6d
'iwasp1 iwadr1
  22      0
'
-----
_WAVE_SPECTRUM_WIND
'
-----
'siwahe_____tpeak
_2.500000000e+00_1.200000000e+01
'
-----
WAVE DIRECTION PARAMETERS
'
-----
'wadir1          expo1 ndir1
  9.000000000e+01 /      11
'
*****
_BODY_DATA_SPECIFICATION
'
*****
vessel

'ibdtyp_imptyp
_1_____0
'
-----
BODY LOCATION DATA
'
-----
'xglob          yglob          zglob          phi          theta
          psi
  0.000000000e+00 0.000000000e+00 0.000000000e+00 0.000000000e+00
          0.000000000e+00 0.000000000e+00
'
-----

```



\_\_BODY\_MASS\_DATA

---

Imported from

+ by linli on IIMT-LINLI-W - 10-May-2015 15:25:50

'xcog\_\_\_\_\_ycog\_\_\_\_\_zcog

\_\_0.000000000e+00\_\_0.000000000e+00\_\_7.246094000e+00

---

MASS COEFFICIENTS

---

'rm                    rixx                    riyx                    riyy                    rizx

                      rizy                    rizz

5.118539200e+04 1.682900000e+07 0.000000000e+00 1.045800000e+08

0.000000000e+00 0.000000000e+00 1.018900000e+08

---

\_\_ADDED\_MASS\_INFINITE

---

'AM

\_\_1221.04631616\_\_4.19812715054\_\_1748.84971366\_\_-24.4766484840\_\_333504.896367\_\_

120.117697573

\_\_-0.320773425469\_\_14612.8381234\_\_-73.1838714824\_\_-83971.5908839\_\_

-124.822814693\_\_135151.213257

\_\_1707.35446062\_\_-51.0957123167\_\_106295.677570\_\_864.436220110\_\_667526.747692\_\_

-489.838623538

\_\_5.78700358341\_\_-84617.1633719\_\_972.858729557\_\_3328623.02496\_\_3162.36642273\_\_

1082990.82710

\_\_332201.979018\_\_653.475070581\_\_691524.000781\_\_-2206.40898030\_\_137740244.194\_\_

26230.8057126

\_\_23.0967254356\_\_136000.588185\_\_229.401755181\_\_1076018.63789\_\_10106.7640082\_\_

30722682.7691

---

BODY COMPONENTS

' \_\_\_\_\_  
' \_\_\_\_\_

COUPLING POINT

' \_\_\_\_\_

'chcopo chppt xcpl                   ycpl                   zcpl  
**fix**    FIXE   -5.000000000e+01  -2.400000000e+01  5.785000000e+01

' \_\_\_\_\_

\_COUPLING\_WINCH

' \_\_\_\_\_

'chcowi\_chwico

\_winch\_NRUN

'wacm                   wvelm                   druma                   druml                   nrun  
1.000000000e-01  1.000000000e+00  1.000000000e+02  1.000000000e+02  1

'tstart\_\_\_\_\_tstop\_\_\_\_\_runvel

\_1.000000000e+01\_3.000000000e+02\_-1.000000000e-01

' \_\_\_\_\_

HYDROSTATIC STIFFNESS DATA

' \_\_\_\_\_

'istmod

1

' \_\_\_\_\_

\_STIFFNESS\_REFERENCE

' \_\_\_\_\_

'xref\_\_\_\_\_yref\_\_\_\_\_zref\_\_\_\_\_rphi\_\_\_\_\_rtheta\_\_\_\_\_  
\_\_\_\_\_rpsi

```

_0.000000000e+00_0.000000000e+00_0.000000000e+00_0.000000000e+00_
  0.000000000e+00_0.000000000e+00
,
-----
LINEAR STIFFNESS MATRIX
,
-----
'KMAT
0.0000000000 0.0000000000 0.0000000000 0.0000000000 0.0000000000
  0.0000000000
0.0000000000 0.0000000000 0.0000000000 0.0000000000 0.0000000000
  0.0000000000
0.0000000000 0.0000000000 63865.9233531 0.664222007437 213721.717107
  0.0000000000
0.0000000000 0.0000000000 0.664222007437 2618880.10214 -8.78756916479
  -26149.6994562
0.0000000000 0.0000000000 213721.717107 -8.78756916479 124103744.149
  -3.85520324181
0.0000000000 0.0000000000 0.0000000000 -26149.6994562 -3.85520324181
  0.0000000000
,
-----
_LINEAR_DAMPING
,
-----
Sum of damping from Wamit and Retardation function calculati

'LD
_200.000000000_0.0000000000_0.0000000000_0.0000000000_1450.00000000_
  0.0000000000
_0.0000000000_673.000000000_0.0000000000_-4879.25000000_0.0000000000_
  0.0000000000
_0.0000000000_0.0000000000_10000.0000000_0.0000000000_0.0000000000_
  0.0000000000

```

```

_0.0000000000_-4879.25000000_0.0000000000_298374.562500_0.0000000000_
  0.0000000000

```

```

_1450.00000000_0.0000000000_0.0000000000_0.0000000000_137512.500000_
  0.0000000000

```

```

_0.0000000000_0.0000000000_0.0000000000_0.0000000000_0.0000000000_
  3200000.00000

```

```

'*****

```

FIRST ORDER MOTION TRANSFER FUNCTION

```

'*****

```

```

Imported_from_'F:\0_MP_lower_weather_window\WADAM_HLV_MP_25m_freqD\

```

```

  HLV_only\HLV_only_no_offbody\HLV_noK\WAMIT_5S.4

```

```

+ by linli on IIMT-LINLI-W - 05-Nov-2015 14:33:22

```

```

'ndir_nfreq_imosym_itypin

```

```

_13_60_1_2

```

```

'-----

```

WAVE DIRECTIONS MOTION TRANSFER FUNCTION

```

'-----

```

```

'idir dir

```

```

1 0.000000000e+00

```

```

2 1.500000000e+01

```

```

3 3.000000000e+01

```

```

4 4.500000000e+01

```

```

5 6.000000000e+01

```

```

6 7.500000000e+01

```

```

7 9.000000000e+01

```

```

8 1.050000000e+02

```

```

9 1.200000000e+02

```

```

10 1.350000000e+02

```

```

11 1.500000000e+02

```

```

12 1.650000000e+02

```

13 1.800000000e+02

' \_\_\_\_\_  
 ' \*\*\*\*\*  
 POSITIONING SYSTEM DATA  
 ' \*\*\*\*\*

' \_\_\_\_\_  
 CATENARY SYSTEM DATA

' \_\_\_\_\_  
 LINE DATA

'iline lichar imeth iwirun icpro

1 1 3 0 1

'xbdy\_\_\_\_\_ybdy\_\_\_\_\_zbdy

\_8.483400000e+01\_-1.578000000e+01\_4.800000000e+00

'xglb yglb xwinch

5.892160000e+02 5.011650000e+02 0.000000000e+00

'ifmopo\_ftime\_\_\_\_\_btens

\_0\_\_\_\_\_0.000000000e+00\_0.000000000e+00

' \_\_\_\_\_  
 LINE DATA

'iline lichar imeth iwirun icpro

2 1 3 0 1

'xbdy\_\_\_\_\_ybdy\_\_\_\_\_zbdy

\_8.483400000e+01\_-1.578000000e+01\_4.800000000e+00

'xglb yglb xwinch

5.892160000e+02 -5.011650000e+02 0.000000000e+00

```

'ifmopo_ftime_____btens
_0_____0.000000000e+00_0.000000000e+00
'
-----
LINE DATA
'
-----
'iline lichar imeth iwirun icpro
3      1      3      0      1
'xbdy_____ybdy_____zbdy
_7.846400000e+01_1.755000000e+01_4.800000000e+00
'xglb          yglb          xwinch
3.525360000e+02 6.616650000e+02 0.000000000e+00
'ifmopo_ftime_____btens
_0_____0.000000000e+00_0.000000000e+00
'
-----
LINE DATA
'
-----
'iline lichar imeth iwirun icpro
4      1      3      0      1
'xbdy_____ybdy_____zbdy
_7.846400000e+01_-1.755000000e+01_4.800000000e+00
'xglb          yglb          xwinch
3.525360000e+02 -6.616650000e+02 0.000000000e+00
'ifmopo_ftime_____btens
_0_____0.000000000e+00_0.000000000e+00
'
-----
LINE DATA
'
-----
'iline lichar imeth iwirun icpro
5      1      3      0      1
'xbdy_____ybdy_____zbdy

```

└-7.915600000e+01└1.960000000e+01└4.800000000e+00

'xglb                   yglb                   xwinch

  -3.532280000e+02 6.637150000e+02 0.000000000e+00

'ifmopo\_ftime\_\_\_\_\_btens

└0\_\_\_\_\_0.000000000e+00└0.000000000e+00

'

LINE DATA

'

'iline lichar imeth iwirun icpro

6    1       3       0       1

'xbdy\_\_\_\_\_ybdy\_\_\_\_\_zbdy

└-7.915600000e+01└-1.960000000e+01└4.800000000e+00

'xglb                   yglb                   xwinch

  -3.532280000e+02 -6.637150000e+02 0.000000000e+00

'ifmopo\_ftime\_\_\_\_\_btens

└0\_\_\_\_\_0.000000000e+00└0.000000000e+00

'

LINE DATA

'

'iline lichar imeth iwirun icpro

7    1       3       0       1

'xbdy\_\_\_\_\_ybdy\_\_\_\_\_zbdy

└-7.915600000e+01└1.750000000e+01└4.800000000e+00

'xglb                   yglb                   xwinch

  -5.835380000e+02 5.028850000e+02 0.000000000e+00

'ifmopo\_ftime\_\_\_\_\_btens

└0\_\_\_\_\_0.000000000e+00└0.000000000e+00

'

LINE DATA

'

```

'iline lichar imeth iwirun icpro
  8      1      3      0      1
'xbdy_____ybdy_____zbdy
_-7.915600000e+01_-1.750000000e+01_4.800000000e+00
'xglb          yglb          xwinch
 -5.835380000e+02 -5.028850000e+02 0.000000000e+00
'ifmopo_ftime_____btens
_0_____0.000000000e+00_0.000000000e+00
'
-----
LINE CHARACTERISTICS DATA
'
'lichar linpty npth nptv vmin          vmax
  1      2      30   9   -4.000000000e+00 4.000000000e+00
'nseg_ibotco_slope_____zglb_____tmax_____thmin
_3_____0_____0.000000000e+00_-2.500000000e+01_1.051000000e+04_0.000000000e
+00
'iseg ieltyp nel ibuoy sleng          fric          nea itynea
  1   0      30   0      3.000000000e+02 0.000000000e+00 0   1
  2   0      30   0      3.000000000e+02 0.000000000e+00 0   1
  3   0      10   0      1.000000000e+02 0.000000000e+00 0   1
'iseg_dia_____emod_____emfact_____uwia_____
  wafac_____cdn_____cdl
_1_____6.048365000e-02_1.000000000e+08_1.000000000e+00_1.520550000e-01_
  5.900000000e-01_0.000000000e+00_0.000000000e+00
_2_____6.048365000e-02_1.000000000e+08_1.000000000e+00_1.520550000e-01_
  5.900000000e-01_0.000000000e+00_0.000000000e+00
_3_____6.048365000e-02_1.000000000e+08_1.000000000e+00_1.520550000e-01_
  5.900000000e-01_0.000000000e+00_0.000000000e+00
'
*****
BODY DATA SPECIFICATION

```



```

'*****
monopile

'ibdtyp imptyp
1      0
'-----
_BODY_LOCATION_DATA
'-----
'xglob_____yglob_____zglob_____phi_____theta_____
  _____psi
_-5.00000000e+01_0.00000000e+00_2.85000000e+00_0.00000000e+00_
  0.00000000e+00_0.00000000e+00
'-----
BODY MASS DATA
'-----

'xcog          ycog          zcog
0.00000000e+00 6.00000000e+00 0.00000000e+00
'-----
_MASS_COEFFICIENTS
'-----
'm_____rixx_____riyx_____riyy_____rizz_____
  _____rizy_____rizz
_5.00000000e+02_1.51020000e+05_0.00000000e+00_2.03000000e+05_
  0.00000000e+00_0.00000000e+00_1.51020000e+05
'*****
GRAVI FORC INCL

```

```

'*****
'*****
BODY DATA SPECIFICATION
'*****

cran9c

'ibdtyp imptyp
4      3
'chmaster
_vessel
'xapl          yapl          zapl
0.000000000e+00 0.000000000e+00 0.000000000e+00
'xapm_____ yapm_____ zapm
_-7.400000000e+01_-0.000000000e+00_-0.000000000e+00
'chmod
PSI
'posini_____ posmin_____ posmax_____ vmax_____ amax
_-4.500000000e+01_-4.500000000e+01_4.500000000e+01_1.000000000e+01_
1.100000000e+02
'cast
NRUN
'nrun_seqtype
_244_2
'tstart          tstop          vesq          aseq
1.000000000e+01 1.100000000e+01 9.740000000e-04 1.000000000e+02
1.100000000e+01 1.200000000e+01 1.950000000e-03 1.000000000e+02
1.200000000e+01 1.300000000e+01 2.920000000e-03 1.000000000e+02

```

```

2.520000000e+02 2.530000000e+02 2.740117173e+00 1.000000000e+02
2.530000000e+02 2.540000000e+02 5.217998621e+00 1.000000000e+02
' *****
_BODY_DATA_SPECIFICATION
' *****

cran9d

'ibdtyp_imptyp
_4_____3
'chmaster
cran9c
'xapl_____yapl_____zapl
_0.000000000e+00_0.000000000e+00_0.000000000e+00
'xapm          yapm          zapm
0.000000000e+00 0.000000000e+00 1.000000000e+01
'chmod
_THETA
'posini          posmin          posmax          vmax          amax
0.000000000e+00 0.000000000e+00 0.000000000e+00 0.000000000e+00
0.000000000e+00
'cast
_NONE
' *****
BODY DATA SPECIFICATION
' *****

cran62

```

```

'ibdtyp imptyp
  4      3
'chmaster
  _cran9c
'xapl          yapl          zapl
  0.000000000e+00 0.000000000e+00 0.000000000e+00
'xapm_____ yapm_____ zapm
  _0.000000000e+00_0.000000000e+00_3.660000000e+01
'chmod
  THETA
'posini_____posmin_____posmax_____vmax_____amax
  _3.000000000e+01_1.000000000e+01_6.000000000e+01_1.000000000e+01_
    1.100000000e+02
'cast
  NRUN
'nrun_seqtype
  _244_2
'tstart          tstop          vesq          aseq
  1.000000000e+01 1.100000000e+01 -6.260000000e-09 1.000000000e+02
  1.100000000e+01 1.200000000e+01 -3.760000000e-08 1.000000000e+02

  2.520000000e+02 2.530000000e+02 1.250573652e+00 1.000000000e+02
  2.530000000e+02 2.540000000e+02 3.201846712e+00 1.000000000e+02
',
  _____
  _BODY_COMPONENTS

```

```

'
'
'
'_COUPLING_POINT
'

'chcopo_____chppt_xcpl_____ycpl_____zcpl
_winch_point_FIXE__0.000000000e+00_0.000000000e+00_0.000000000e+00
'

COUPLING WINCH
'

'chcowi chwico
winch1 NRUN
'wacm_____wvelm_____druma_____druml_____nrun
_1.000000000e+04_1.000000000e+00_1.000000000e+03_1.000000000e+03_1
'tstart          tstop          runvel
1.100000000e+01 2.540000000e+02 -2.000000000e-01
'

'_BODY_COMPONENTS
'
'

'_COUPLING_POINT
'

'chcopo_____chppt_xcpl_____ycpl_____zcpl
_guidePoint_GUID__0.000000000e+00_0.000000000e+00_6.788000000e+01
'dguid          dv1          dv2          dv3
1.000000000e-02 0.000000000e+00 0.000000000e+00 -1.000000000e+00
'
'*****

```

\_COUPLING\_DATA

'\*\*\*\*\*

simp4e

'-----

\_SIMPLE\_WIRE\_COUPLING

'-----

'cpl\_name1

\_winch\_point

'@Name2=monopile

'chbdy2\_xbdy2\_ybdy2\_zbdy2

\_monopile\_0.00000000e+00\_-2.40000000e+01\_0.00000000e+00

'nguide

1

'chgupo\_iactive

\_guidePoint\_1

'ea rlen flexc dampsw irest

ehla

8.00000000e+37 1.60400000e+02 1.33000000e-06 1.60000000e+05 0 0

'ifmoco\_ftime\_btens

\_0\_0.00000000e+00\_0.00000000e+00

'\*\*\*\*\*

COUPLING DATA

'\*\*\*\*\*

docked

'-----

DOCKING CONE COUPLING

```

'-----
'chbdy1  xbdy1          ybdy1          zbdy1
  monopile 2.850000000e+00 2.500000000e+01 0.000000000e+00
'chbdy2_xbdy2_____ybdy2_____zbdy2
_vessel_-4.500000000e+01_-2.500000000e+01_-2.850000000e+00
'npt exp          intpoc vemic          ehla
  4  1.000000000e+00 1          0.000000000e+00 0
'naxpts
_2
'radmax
  5.000000000e-01
'dv1_____dv2_____dv3
_-1.000000000e+00_0.000000000e+00_0.000000000e+00
'iaxpt axpt
  1  0.000000000e+00
  2  1.000000000e+01
'dist_____force_____damp
_0.000000000e+00_0.000000000e+00_0.000000000e+00
_5.000000000e-03_0.000000000e+00_1.000000000e-01
_1.000000000e-02_2.500000000e+01_2.500000000e+00
_5.000000000e-02_5.002500000e+03_3.335000000e+02
'dist          force          damp
  0.000000000e+00 0.000000000e+00 0.000000000e+00
  5.000000000e-03 0.000000000e+00 1.000000000e-01
  1.000000000e-02 2.500000000e+01 2.500000000e+00
  5.000000000e-02 5.002500000e+03 3.335000000e+02
'ifmoco_ftime_____btens
_0_____0.000000000e+00_1.000000000e+03
'*****
COUPLING DATA

```

```

'*****
dockee

'
-----
DOCKING CONE COUPLING
-----
'chbdy1  xbdy1          ybdy1          zbdy1
monopile -2.850000000e+00 2.500000000e+01 0.000000000e+00
'chbdy2_xbdy2_____ybdy2_____zbdy2
_vessel_-5.500000000e+01_2.500000000e+01_2.850000000e+00
'npt exp          intpoc vemic          ehla
4  1.000000000e+00 1          0.000000000e+00 0
'naxpts
_2
'radmax
5.000000000e-01
'dv1_____dv2_____dv3
_1.000000000e+00_0.000000000e+00_0.000000000e+00
'iaxpt axpt
1  0.000000000e+00
2  1.000000000e+01
'dist_____force_____damp
_0.000000000e+00_0.000000000e+00_0.000000000e+00
_5.000000000e-03_0.000000000e+00_1.000000000e-01
_1.000000000e-02_2.500000000e+01_2.500000000e+00
_5.000000000e-02_5.002500000e+03_3.335000000e+02
'dist          force          damp
0.000000000e+00 0.000000000e+00 0.000000000e+00
5.000000000e-03 0.000000000e+00 1.000000000e-01

```



```

1.000000000e-02 2.500000000e+01 2.500000000e+00
5.000000000e-02 5.002500000e+03 3.335000000e+02
'ifmoco_ftime_____btens
_0_____0.000000000e+00_1.000000000e+03
'*****
COUPLING DATA
'*****
'chcpl
poinef

'_____
_FENDER_COUPLING
'_____
'npt_ifric_dynfric_____stafric_____stiffric_____exp_____
_intpo_vemin_____ehla
_3_____1_____1.000000000e+00_1.500000000e+00_1.000000000e-03_1.000000000e+00
_1_____0.000000000e+00_0
'chbdy1 xbdy1 ybdy1 zbdy1
monopile 2.850000000e+00 2.500000000e+01 0.000000000e+00
'chbdy2_xbdy2_____ybdy2_____zbdy2_____xn_____
yn_____zn
_vessel_-4.715000000e+01_2.500000000e+01_2.850000000e+00_-1.000000000e+00_
0.000000000e+00_0.000000000e+00
'dvlx dvly dvlz r11 r12
0.000000000e+00 0.000000000e+00 1.000000000e+00 2.000000000e+01
8.000000000e+01
'dist_____aforce_____damp
_0.000000000e+00_0.000000000e+00_0.000000000e+00
_-1.000000000e+00_1.000000000e+05_1.000000000e-03

```

```

_-2.000000000e+00_1.000000000e+05_2.000000000e-03
'*****
COUPLING DATA
'*****
'chcpl
  poin0a

'
_FENDER_COUPLING
'
'npt_ifric_dynfric_____stafric_____stiffric_____exp_____
  _intpo_vemin_____ehla
_3_____1_____1.000000000e+00_1.500000000e+00_1.000000000e-03_1.000000000e+00
  _1_____0.000000000e+00_0
'chbdy1  xbdy1          ybdy1          zbdy1
  monopile -2.850000000e+00 2.500000000e+01 0.000000000e+00
'chbdy2_xbdy2_____ybdy2_____zbdy2_____xn_____
  yn_____zn
_vessel_-5.285000000e+01_2.500000000e+01_2.850000000e+00_1.000000000e+00_
  0.000000000e+00_0.000000000e+00
'dvlx          dvly          dvlz          r11          r12
  0.000000000e+00 0.000000000e+00 1.000000000e+00 2.000000000e+01
  8.000000000e+01
'dist_____aforce_____damp
_0.000000000e+00_0.000000000e+00_0.000000000e+00
_-1.000000000e+00_1.000000000e+05_1.000000000e-03
_-2.000000000e+00_1.000000000e+05_2.000000000e-03
'*****
END

```

, \* \* \* \* \*